UNIVERSITÀ DELLA CALABRIA

UNIVERSITA' DELLA CALABRIA

Dipartimento di Fisica

Dottorato di Ricerca in

SCIENZE E TECNOLOGIE FISICHE, CHIMICHE E DEI MATERIALI

CICLO

XXIX

IMPROVING OILFIELD PERFORMANCE ENABLING HORIZONTAL DRILLING TECHNIQUES: DEVELOPMENT AND OPTIMIZATION OF STANDARD AND SPECIAL MEASURES FOR A REAL CASE STUDY

Settore Scientifico Disciplinare: INGEGNERIA DELLE INFRASTRUTTURE E DEL TERRITORIO (ICAR/02)

Tematica di Ricerca INGEGNERIA DEL PETROLIO ED AMBIENTALE

Tutors: Prof. Raffaele **Romagnoli**

Prof. Vincenzo **Carbone**

Dottorando: Dott. Amer Abdulhakim Mohammed **Al-Taie**

Abstract

Drilling technique is a crucial issue to pay attention to. Drilling a horizontal well has a great interest to the oil and gas industry since nowadays it provides attractive means for improving both production rate and yet the recovery efficiency. The great improvements in drilling technology make it possible to drill horizontally no matter how complex are the trajectories and how deep it is suppose to reach.

This study aims at presenting the optimal design aspects of a horizontal well. Design aspects include the selection of bit and casing sizes, detection of setting depths and drilling fluid density, casing, hydraulics, well profile, and construction of drill string simulator.

When many vertical wells exist, an oil field named (Z14 field) should be designated to have a short radius horizontal well able to increasing the productivity and to promote the developing of the field itself.

A single build profile with build rate 90 deg/100ft is constructed based on geological data. A drill string simulator composed of soft-string model and buckling tendency is constructed to predict torque and drag of string for six operating conditions. These conditions are pick-up, slack-off, sliding, pick-up with rotation, slack-off with rotation and drilling with rotation. Results of loads analysis showed that the suggested drill string can be used without exceeding torsional, tensile and buckling strengths. Analysis of single build profile showed that the torque and drag while drilling horizontal well could be minimized by drilling with low build rate, employing lighter pipe, and improving the lubricating capability with oil base mud (low friction forces).

A finite element model was constructed to predict inclination tendency for multistabilizer rotary BHA in three dimensions, static condition. The bottom hole assembly was idealized with beam element capable of resisting axial forces, bending moments about the two principal axes, and twisting moments about its centroidal axis. Bit and stabilizer were treated as contact point and restricted from movement in all directions. Each element is loaded with gravity and normal contact forces. Model validation showed closer agreement between the model and Jiazhi's method (analytic) for slick, single, and two stabilizers BHA, compared to Akgun results. Predictions with finite element model showed that for building assembly, the weight on bit had small effect on bit side force especially in high angle wells. Also inclination tendency

(building, dropping) would depend on position of the stabilizer, diameter of drillcollar behind the bit, and number of stabilizers.

Sintesi

Quello della tecnica di perforazione è un argomento che, per la sua importanza, merita attenzione.

L' industria petrolifera nutre un grande interesse per la perforazione orizzontale in quanto oggigiorno essa costituisce una tecnica attraente per migliorare sia la produzione che l'efficienza di recupero. I grandi miglioramenti nella tecnologia di perforazione hanno reso possibile le perforazioni orizzontali, a prescindere dalla complessità delle traiettorie e dalla profondità che si vuole raggiungere.

Questo studio ha l'obiettivo di delineare gli aspetti ottimali di progettazione di un pozzo orizzontale. Gli aspetti di progettazione includono la selezione delle dimensioni della punta del trapano e dell'involucro, la rilevazione delle profondità di impostazione e della densità del fluido di perforazione, l'involucro, l'idraulica, il profilato e la costruzione del simulatore delle stringhe di perforazione.

In presenza di molti pozzi verticali, un campo petrolifero chiamato (campo Z14) dovrebbe essere progettato in modo tale da avere un pozzo orizzontale a raggio corto in grado di aumentare la produttività e favorire lo sviluppo del campo. Un unico profilo di costruzione con tasso di costruzione 90 deg / 100ft è costruito sulla base di dati geologici. Un simulatore di stringa di perforazione, composto da un modello soft-string e dalla tendenza al'instabilità, è costruito per prevedere la coppia e la resistenza aerodinamica della stringa per sei condizioni operative. Queste condizioni sono il pick-up, lo slack-off, lo scorrimento, il pick-up con rotazione, lo slack-off con la rotazione e la perforazione con la rotazione. I risultati dell'analisi dei carichi hanno dimostrato che la stringa del trapano suggerita può essere usata senza superare le tensioni torsionali, la resistenza alla trazione e l'affilatura. L'analisi del profilo di costruzione singola ha dimostrato che la coppia e la resistenza aerodinamica nella perforazione orizzontale potrebbero essere ridotte al minimo mediante foratura con basse velocità di costruzione, impiegando tubi più leggeri e migliorando la capacità di lubrificazione con fango a base di olio (forze di attrito ridotto).

Un modello a elemento finito è stato costruito per prevedere la tendenza all'inclinazione per il rotante multistabilizzatore BHA in tre dimensioni, in condizione statica. Il BHA è stato progettato con elemento a fascio in grado di resistere alle forze assiali, ai momenti di flessione attorno ai due assi principali e ai momenti di torsione attorno al suo asse centroidale. La punta del trapano e lo stabilizzatore sono stati trattati come punto di contatto e limitati dal movimento in tutte le direzioni. Ogni elemento è stato caricato con gravità e forze di contatto normali. La convalida dei modelli ha dimostrato che il modello è in linea con il metodo di Jiazhi (analitico) per gli affilati, singoli e due stabilizzatori BHA, più di quanto lo siano i risultati di Akgun. Le previsioni con il modello a elemento finito hanno dimostrato che per l'assemblaggio, il peso sulla punta del trapano aveva un piccolo effetto sulla forza laterale della punta del trapano, specialmente nei pozzetti ad alto angolo. Anche la tendenza all'inclinazione (costruzione, caduta) dipende dalla posizione dello stabilizzatore, dal diametro del collare dietro la punta del trapano e dal numero di stabilizzatori.

Table of Contents

Chapter Four
Design Aspects

Chapter Five
Results and Discussion

Chapter six

Conclusions and Recommendations

List of Tables

List of Figures

Symbols	Description	Unit
A_s	cross section area of pipe	in^2
A_n	area of bit nozzles	in^2
A	area of the beam	in^2
A_1A_2	azimuth at station 1and station 2	degree
a,a_1,a_2,a_3	coefficients of shape function	
BUR	build up rate of angle	deg/100ft
B_c	buoyancy correction factor	
C	dog-leg angle	degree
C_{max}	maximum permissible dog-leg	deg/100ft
DLS	dog-leg severity	deg/100ft
D_i	inside diameter of pipe	in
D_o	outside diameter of pipe	in
D_h	hole diameter	in
Db	bit diameter	in
Ds1	diameter of 1^{st} stabilizer	in
Ds2	diameter of 2^{nd} stabilizer	in
Dc	diameter of drill collar	in
E	modulus of elastcity	psi
E_b	bending strain energy	lb_f-ft
E_p	potential energy	lb_f-ft
E_t	total energy	lbf-ft
E_1	surface connection constant	
F_N	net normal force	lb
F_f	friction slide force	lb
F_{cir}	sinusoidal buckling force	lb

F^*	r helical buckling force	lb
F_b	bending force	lb
F_B	bit side force	lb
$\vec{F}$	nodal force vector	
F_x,F_y,F_z	forces acting along x,y,z axes	lb
F_w	weight force	lb
F_n	normal contact force	lb/ft
g	gravity acceleration	ft/sec^2
G	shear modulus	psi
H1	horizontal displacement of build section	ft
H2	horizontal displacement of tangent section	ft
H3	horizontal displacement of second build section	ft
I_1,I_2	inclination at station 1and 2	degree
I	moment of inertia of pipe	in^4
I_z,I_y	moment of inertia of pipe about axes z and y	in^4
J	polar moment of inertia	in^4
K	consistency index	$lb.s/100ft^2$
L1	length of build section	ft
L2	length of tangent section	ft
L3	length of second build section	ft
L	length of pipe	ft
L_j	half the distance between tool joints	in
L_T	tangency length	ft
L_1	distance from bit to first stabilizer	ft
L_2	distance between first and second stabilizer	ft
M1	bending moment about first stabilizer	lb.ft
M2	bending moment about second stabilizer	lb.ft
M_x,M_y,M_z	bending moment about x,y,z axes	lb.ft
n	flow behavior index	

N1,N2,N3,N4	interpolation functions	
PV	plastic viscosity	cp
P_1	surface connection pressure losses	psi
P_2	pipe pressure losses	psi
P_3	annulus pressure losses	psi
P_{bit}	pressure losses across bit	psi
P_c	compressive load on drillcollar	lb_f
P_{c1}	compressive load on first section	lb_f
P_{c2}	compressive load on second section	lb_f
Q	flow rate	gpm
Q_1	weight of collar from bit to the stabilizer	lb_f/ft
Q2	weight of collar from stabilizer to the tangency point	lb_f/ft
R	radius of curvature	ft
R1	radius of upper build section	ft
R3	radius of lower build section	ft
r	radial clearance between pipe and the hole	in
$\vec{s}$	nodal displacement vector	
$\vec{s}^T$	transpose of nodal displacement vector	
T	axial tension	lb_f
T_b	buoyed weight below dog-leg	lb
TOB	torque at bit	ft-lb_f
V1	vertical height of upper build section	ft
V2	vertical height of tangent section	ft
V3	vertical height of lower build section	ft
v'	average drilling fluid density	ft/m
V_n	nozzles velocity	ft/sec
V_1,V_2	vertical displacements	in
V	total volume of element	in^3
W	buoyed weight of pipe	lb

WOB	weight on bit	lb_f
W_e	external work	lb_f-ft
W_c	weight of pipe in air	lb/ft
X	transcendental function	
ΔT	change of axial tension	lb_f
Y_p	yield point of drilling fluid	$lb/100ft^2$
ΔM	change of torsion	ft-lb_f
$\Delta_x,\Delta_y,\Delta_z$	nodal displacements in x,y,z axes	in

Greek Symbols	**Description**	**Unit**
Θ	inclination angle	degree
Φ	azimuth angle	degree
f	friction factor	
θ_{300}	dial reading at 300 rpm	$lb/100ft^2$
θ_{600}	dial reading at 600 rpm	$lb/100ft^2$
ρ	drilling fluiddensity	ppg
υ	poisson's ratio	
θ_1,θ_2	rotational displacements	radian
σ_b	bending stress	psi
σ_t	buoyed tensile stress	psi

Chapter One
Introduction

1.1. General:

Recent technology advances have contributed to a significant increase in the use and scale of directional drilling. Perhaps the technologies with the highest impact have been steerable mud motors, measurement-while-drilling (LWD) tools, and logging-while-drilling (LWD) tools. These tools in combination have provided the ability to follow complex, 3D well profiles without changing bottom hole assemblies (BHA), and to measure where the bit has drilled without having to run a wireline to survey or log. Equally important engineering models have provided the fundamental tools for evaluating drillstrings, hydraulics, BHA, and the drilled formations themselves. These advances have enabled the drilling of extended-reach , horizontal, and multiple-target well profiles once thought impractical, uneconomical , or impossible.[1]

1.2. Definition of Horizontal Well:

A horizontal well may be defined as a well which is drilled to an inclination of 90 degree, and maintains this inclination for a significant distance. Owing to the need for special equipment and the longer drilling times that must be expected , horizontal wells are considerably more expensive than conventional deviated well.[2]

Today, oil industry recognized three types of horizontal wells. These are long, medium and, short radius wells. Figure (1-1) gives a summary of the features and tools for each type[3].

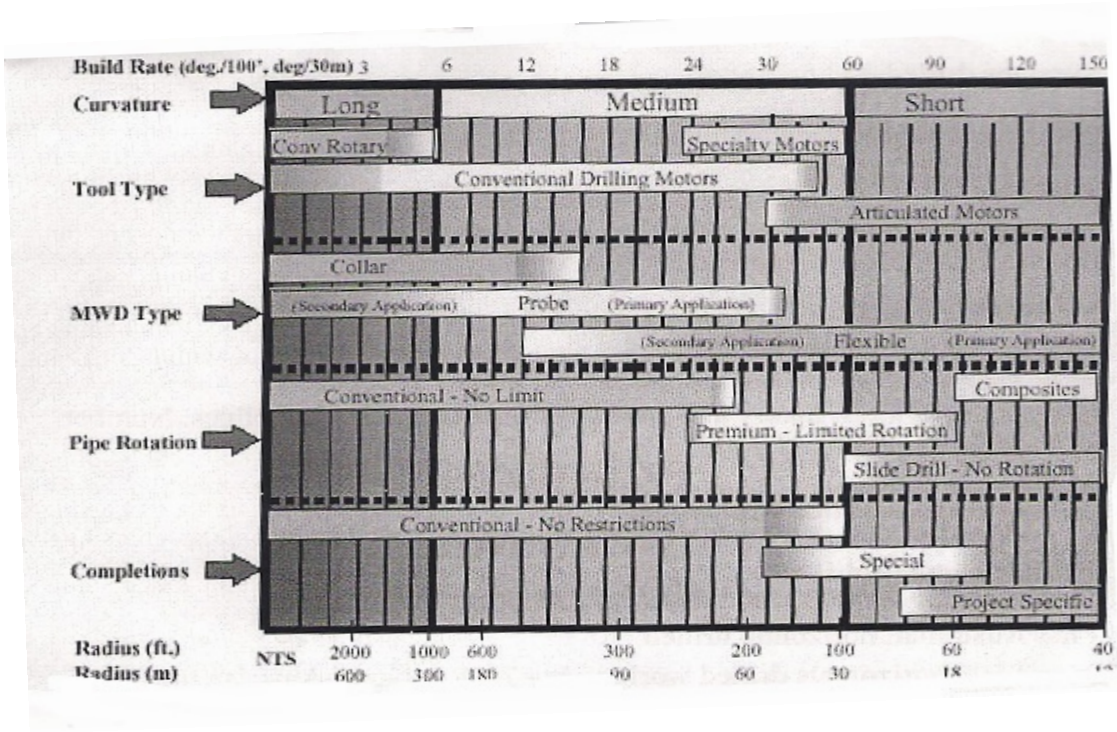

Figure 1-1: Features and Types of Horizontal Wells[3].

1.3. Multilateral Wells:

Multilateral wells are a development issued from horizontal drilling. A multilateral well is a well that has two or more drainage holes (or secondary laterals or branches or arms or legs) drilled from a primary wellbore (or trunk or main bore or mother bore or backbore). Both trunk and branches can be horizontal, vertical or deviated.

A multilateral well could be dual opposite well which has two laterals opposed at 180 degree emerging from the same wellbore as shown in Figure(1-2).This configuration is suggested when the pressure drop becomes detrimental while fluids flow in a horizontal well.

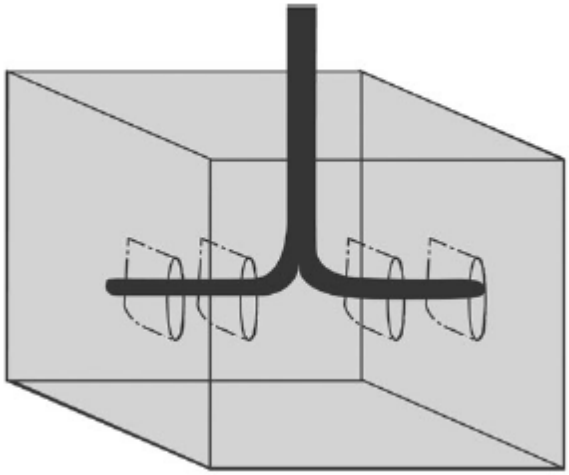

Figure 1-2: Dual Opposite Laterals [1].

Another configuration of lateral is called stacked lateral well as it seen in figure (1-3). This well has two or more laterals departing from the same wellbore at different depths. This configuration is suited for drainage several layers which may or may not communicated. In thick formations with low-mobility crudes (such as heavy oil), stacked multilaterals can be constructed[1].

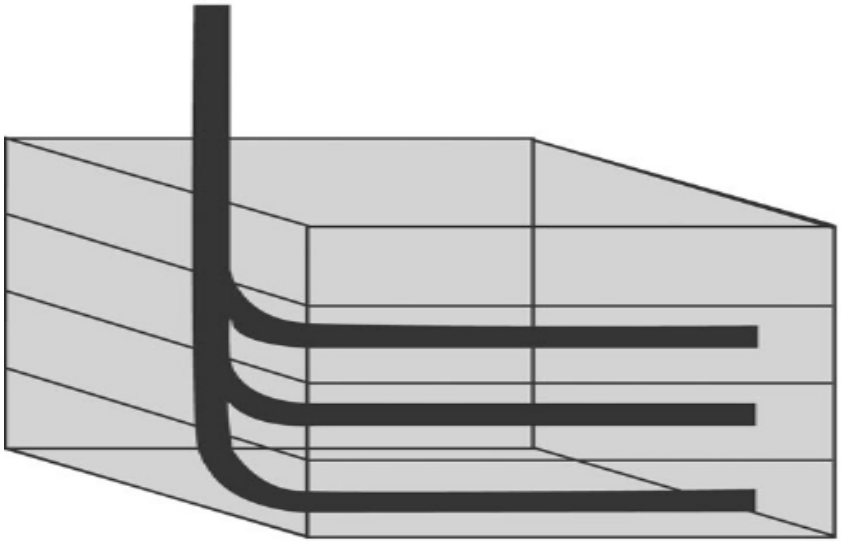

Figure 1-3: Stacked Lateral Well[1].

A multibranch well is lateral well drilled from a horizontal lateral in the horizontal plane. Figure (1-4) shows multibranch well called fishbone which have several horizontal laterals starting from the main horizontal well.(3)

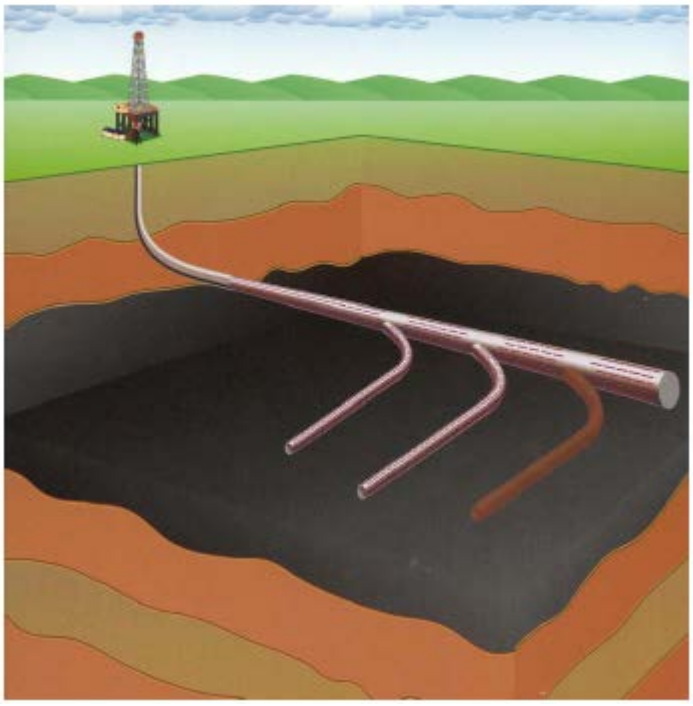

Figure 1-4: Fishbone Multibranch Well(4).

1.4. Causes of Horizontal Drilling:

There are several causes to drill a horizontal well rather than a vertical well which are:

1.4.1. Increased Production Rate From Single Well:

The greater contact area of the well bore through the producing zone allows a much longer completion interval, which means more of the formation contributing directly to the production, and higher flow rates

can be expected. Horizontal wells are therefore suited to relatively thin beds that cover a large area, or to formations where permeability is to low. Also, horizontal well can be used as an alternative to hydraulic fracturing as a means of improving production rates from tight formations, and to improve water injection as a means of improving oil recovery from the reservoir.

1.4.2. Reducing in Coning Problems:

When a vertical well is drilled through a relatively thin pay zone overlying an aquifer, there is tendency for the water to be drawn up into perforated interval and leads to increased water cut in the producing wells. A horizontal well can be alleviating this problem, since it can be placed away from both gas- and water bearing zones. Owing to the longer length of the completion, the drawdown in the reservoir pressure around the wellbore will also be reduced, giving greater oil recovery before the onset of coning problems as shown in Figure (1-5).

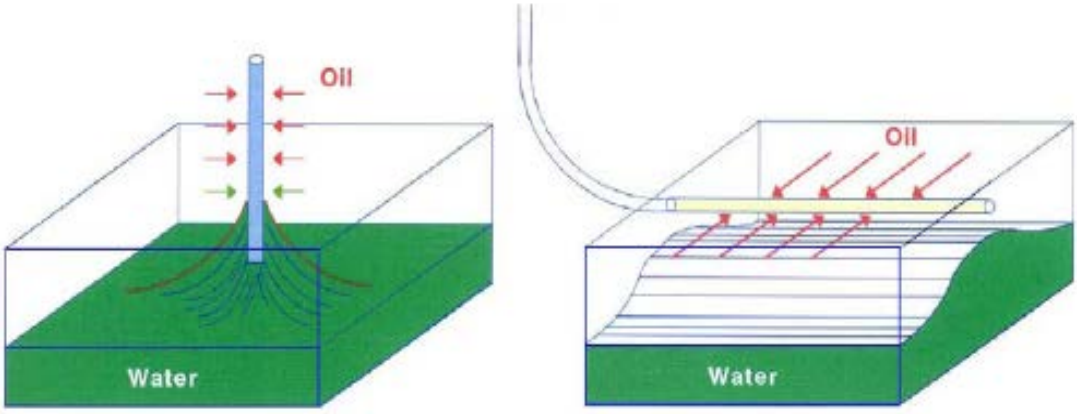

Figure 1-5: Reducing Water Conning With Horizontal Well[4].

1.4.3. Intersection of Vertical Fractures:

Many reservoirs contain fractures that are vertical or near-vertical at depths greater than 2000-3000 ft. Although the matrix of the rock may be fairly impermeable, the oil may still be able to flow a long the fractures. It has been found that in some reservoirs (e.g. fractured reservoir) the most efficient way of producing the oil is to drill highly deviated or horizontal wells to intersect as many fractures as possible. If the orientation of the fractures is known, a horizontal well can be planned to intersect the fractures at right-angle. Figure (1-6) shows horizontal well intersected fractured reservoir.

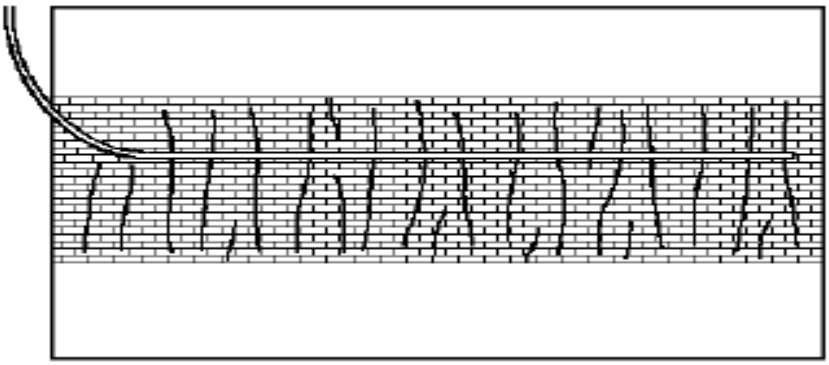

Figure 1-6: Fracture Reservoir[5]

1.4.4. Enhanced Oil Recovery:

Large deposits of highly viscous oil occur in many parts of the world. Since these reservoirs cannot be exploited by conventional means, injection of steam or polymers to improve the mobility of the oil. In this case a horizontal well is drilled near the base of the deposit to act as producing well, and number of vertical injection wells are drilled above the horizontal well. The viscosity of the oil in the vicinity of the steam

injectors was reduced, and it drained down-wards under gravity towards the horizontal producing well.

1.4.5. Development of Non-Producing Resources:

Coal seams in certain areas of the world contain large volumes of methane gas. The gas has to be drained off before the coal can be extracted, since a concentration of 5-15% methane in air forms an explosive mixture. To remove the methane, a small – diameter horizontal well can be drilled through the coal seam.(2)

1.5. Horizontal Well Planning:

Horizontal well planning involves so many steps and constraints. Each of these factors must be considered separately to improve the drilling efficiency and minimize the overall cost for horizontal drilling.

The first step in the planning is to define the horizontal target accurately. Information such as target coordinates entry point into the reservoir, length of horizontal drain, azimuth range of target, vertical depth and, dip of target is usually needed. Most of reservoirs have marker zone which can be used as starting point for the final build up section before entering the reservoir.

The second step is selection of completion that is compatible with reservoir conditions such as thickness, GOC, OWC, and fluid mobility. Future workover requirements must be considered.

The third step involved detection of hole sizes, casing sizes and, setting depths of casing string. A certain data of pore and fracture pressures with depth are required in this step. Casing program should be designed to case problem zones before drilling the lateral section.

The fourth step in the horizontal well design is to design the well profile. This process included determination depth of kick off point,

selection of angle build up rate and, if necessary including tangent section. Reviewing offset drilling data to identify potential drilling problem will help in modifying the well design, well profile and, casing program to reduce the potential for these problems.

The fifth step includes design of drilling fluid program. Hole cleaning, hole stability and, formation damage are most important factors in designing process. In addition, drilling fluids must provide a low friction factor to reduce torque and drag (oil mud, polymer).

Drillstring design is the next step in the planning process. This process involves detection of size, weights and, lengths of drill pipe and collars. Also, torque and drag modeling of drillstring, buckling load of drillstring are detected in each section of hole. A safety factor must be considered to prevent drillstring failure.

Design the hydraulic program is the seventh step in the planning. Calculations are made to select bit nozzle sizes. Hydraulic program should design to ensure adequate hole cleaning and optimum performance of the down hole motors.

The last step in the horizontal well planning is selection of bottom hole assembly. Selected bottom hole assembly should provided the planned build up rate and could be used in drilling more than one section of planned well. Rotary bottom hole assembly and steerable motor assembly are usually used in drilling horizontal wells. Figure (1-7) is diagram shows the steps of planning process.[6]

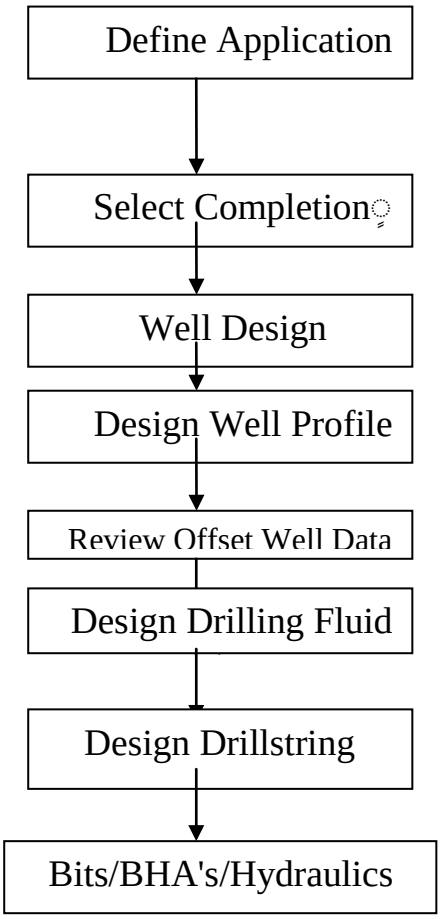

Figure 1-7: Steps of Planning Horizontal Well[6].

1.6. Field Description:

Ajell field is located about 30 km to the North Eest of Tikrit city,North Iraq .The reservoir structure consists of the main (southern) dome and North West dome.The main reservoir is a thick carbonate with minor anhydrite consist of six units of Miocene age.Table (1-1) depicts lithology description of the field[7].

In 1996 HORWELL Company examined for N.O.C the possibility to apply horizontal well technology on the field to increase its productivity. Five main formations were selected to perform the study, which are T12-T15, Jeribe, Dhiban, Euphrates, and Favreina. Due to the

proximity of gas and/or water contacts in some critical areas and low permeability in other, the company suggested three locations for horizontal drilling which are Jeribe, Euphrates, and Favreina. With aid of analytical calculation and correlation issued from basic numerical simulation, high horizontal well productivity indexes were obtained ranged from 6 up to 14 for replacement ratio from 2.75 to 6.5.[8]

Table 1-1: Lithology Description of the Z14 Field[7].

Age	Formation		Thickness(m)	Lithology Description	Top of Formation
Upper miocene	Upper Fars		143.16	Sandston,siltstone,marl	surface
Medium Miocene	Lower Fars	Upper Red Beds	120	Sandstone,Siltstone, Anhydrite,Marl	-143.16
		Seepage Beds	31,5	Anhydrite,Marl,Siltstone,limstone	-263.16
		Saltfereous Beds	202.	Anhydrite,salt,Marl Limestone,siltstone	-294.66
		Transition Beds	106	Anhyrite,Dolomtic limstone	-407.16
Lower Miocene	Jeribe		25	Dolomitic limestone, limstone	-603.16
	Dhiban		32.5	Anhydrite,Dolomitic limstone	-628.16
	Eurphrates		30.3	Dolomtic limestone,Anhydrite, Marl	-660.66
oligocene	Oligocene		97.4	Dolmitic	-691

	Rock		limestone,Anhydrite, Marl	
Eiocene	Jaddala	46,2	Limestone	-788.46

1.7. The Objective of the Study:

The main objective of this study is to design all drilling aspects of a horizontal well. These aspects included the following items:

1.7.1. Detection of bit sizes used to drill the hole ,casing sizes that could be used for casing program and casing setting depths based on pore and fracture pressures data of given field.

1.7.2. Design of different horizontal well profiles (short, medium and, long) based on geological data.

1.7.3. Construction the loads diagram of each horizontal well profile under different operating conditions using soft-string model. Six different operating conditions were considered for drag calculation (pick-up, slack-off, sliding, pick-up with rotation, slack-off with rotation and, drilling with rotation) and also for torque calculation for a given drillstring dimensions.

1.7.4. Detection the critical buckling loads of drillstring for each horizontal well profile.

1.7.5. Design of hydraulic program of the well based on critical annular velocity for Bingham plastic and power law drilling fluids.

1.7.6. Analyzing the effect of build up rate, types of drilling fluids, and drillstring weight on well load diagram.

1.7.7. Modeling of rotary bottom-hole assembly with finite element method in three dimensions, static condition to predicate their inclination tendency under different drilling parameters.

Chapter Two

Literature Review

2.1. Introduction:

It is well known that the design of horizontal wells required good understanding to the mechanical aspects of drillstring components. Thus extensive researches have been made to know how the high well angle affected on behavior of drillstring under different operating conditions. In this chapter, most of the published work about each aspect of drillstring design in high angle and horizontal wells will be presented.

2.2. Drillstring Mechanics:

In directional wells, deviation of wellbore from the vertical cause an increase in contact forces between drillstring and wellbore. As result frictional forces would increase and cause an increase in torsional and tensile loads.

The mechanical properties that have noticeable effect on the designing high angle and horizontal wells are:

2.2.1. Torque and Drag

2.2.2. Buckling

2.2.3. Bending

2.2.1. Torque and Drag:

Drag forces or drag develops during tripping operations (running in and running out), while the torque is produce when the drillstring is rotating. Knowledge of torque and drag will enable the selection of an

optimum well profile and optimum size and weight of the drillstring and its components.

Dellinger et.al (1980)[9] mentioned that the axial drillstring drag could be reduced if the drill string was rotated. They analyzed velocity vector of drillstring to circumferential velocity (Vc) (caused by rotation) and axial velocity (Va) (pipe tripping). The resultant velocity (Vr) which a sum of (Vc) and (Vr) has a fixed quantity. So, when the rotation of drill string increased, it increases the circumferential component and decreases axial friction as shown in fig.(2-1).

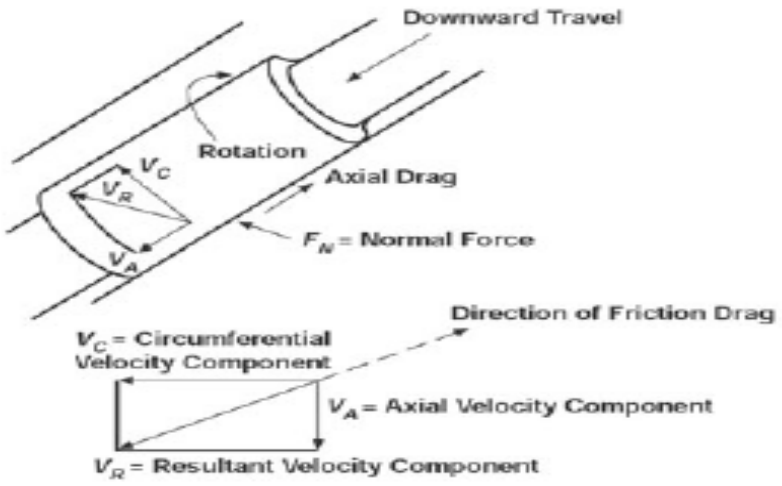

Figure 2-1: Effect of Drillstring Rotation on Axial Friction[9].

Johancsik et.al (1983)[10] developed mathematical model to predict drillstring torque and drag in the directional wells under different operating conditions. They consider the sliding friction between the drill string and the wall of the hole is the primary source of torque and drag. Also, they mentioned that the realistic friction coefficients could be determined from field data with this model. For water base mud systems,they assigned typical friction factors rang from 0.25-0.4.

Cobert et.al (1984)[11] incorporated artificial directional survey data for wells that are being planned by creating smooth survey to hit a specific target. They adding to it a uniform sinusoidal dog legs obtained from regression analysis to give realistic survey as follows:

SWA=2.795-0.000147*kop-0.334*Rob+0.13*Rod (2-1)

Where:

SWA: sine wave amplitude, deg.

Kop: depth of kick-off point,ft.

Rob: rate of angle build –up, deg./100 ft .

Rod: rate of drop- off angle deg./100 ft.

Sheppard et.al (1987)[12] showed that the deviated well with an under section trajectory (i.e., a trajectory lying below the conventional tangent section and constantly building to target) could exhibited lower drag and torque. Tension and drag profiles were constructed from the following equations:

$$\frac{\partial \sigma_e}{\partial s} = W_b \cos\theta(s) \mp k\left\{\left[\sigma_e \frac{\partial \theta}{\partial s} + W_b \sin\theta(s)\right]^2 + \left[\sigma_e \frac{\partial \beta}{\partial s}\sin\theta(s)\right]^2\right\}^{1/2} \quad (2\text{-}2)$$

$$F(S) = k\left\{\left[\sigma_e(s) \frac{\partial \theta}{\partial s} + W_b \sin\theta(s)\right]^2 + \left[\sigma_e(s) \frac{\partial \beta}{\partial s}\sin\theta(s)\right]^2\right\}^{1/2} \quad (2\text{-}3)$$

In addition to reduction in drag, undersection well can also exhibited increase in the side force in the drill collar. This increase lead to greater danger of sticking in the bottom hole assembly.

H.S.HO (1988)[13] discussed the shortcomings of the "soft-string" model which has been widely used in the drilling industry. He mentioned that the model ignored the effects of drillstring stiffness, stabilizer placement, and bore hole clearance. He presented improved drilling program that combined BHA analysis with an improved soft-string model. Results of stiffened torque- drag model showed that the stiffness was important in the collar section and negligible for other sections of drill string.

Wu et.al(1991)[14] presented a new mathematical model for calculating torque and drag in the horizontal and extended reach wells. He defined (α) as the transition angle, at which the contact force (N) equal zero. At angle above (α) the contact force would negative (pipe contact upside of wellbore) and, when angle below (α) the contact force would be positive (pipe contact lowside of wellbore).

Zifeng et.al(1993)[15] established steady tension-torque model for drill string in the horizontal wells. The model take into account the effect of drillstring motion ,well trajectory, and the viscous and structural strength of drilling fluid .It was used to calculate friction factor between wellbore and drillstring, WOB while drilling by down hole motor and, predicated the maximum allowable length of the horizontal section.

2.2.2. Buckling:

In vertical wells, buckling can not be avoided except at very low weights on bit. As the hole angle increases, bottom hole assembly lies on the lower side of the well which provide supporting and making it more stable to the buckling.

Lubinski and Woods (1953)[16] conducted experimental study to determine the onset of the helical buckling in inclined wells. They mentioned that for given values of drill collar weight and compressive load, there is a value of (Φ/r) below which helical buckling may occurred, and above it cannot occurred. Their experimental results were fitted to give the following equation:

$$F_{cir} = 2.85*(EI)^{0.504}(\rho\ A\ g)^{0.496}\ (\sin\Phi/r)^{0.511} \qquad (2\text{-}4)$$

Pasaly and Bogy (1964)[17] analyzed the stability of circular rod lying on the low side of horizontal hole. Their analysis was simplified to yield the following expression for predicting the onset of buckling (critical compressive load):

$$F_{cir} = \frac{(1-\nu)^2 EI}{(1+\nu)(1-2\nu)} \frac{\Pi^2}{L^2}\left(n^2 + \frac{L^2 \rho A g}{n^2 \Pi^4 EIr} \right) \qquad (2\text{-}5)$$

Dawson and Pasaly (1984)[18] simplified the analysis of Pasaly and Bogy of rod stabilizing to obtain the following equation.

$$F_{cir} = 2\left(\frac{EI\rho Ag \sin\theta}{r} \right)^{0.5} \qquad (2\text{-}6)$$

They stated that in high-angle wells, theforce of gravity pulls the drillstring against the low side of the hole. This in turn would stabilize the string and made drill pipe to carry axial compressive loads without buckling, which reduce the torque and drag. Fig.(2-2) shows the stability analysis of 5 in drill pipe .

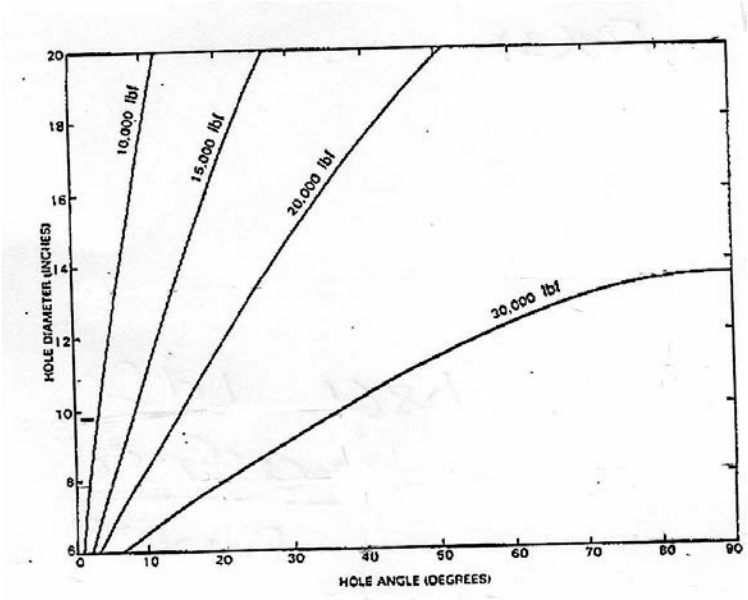

Figure 2-2: Critical Buckling Loads for 5 in, 19.5lb/ft. Drillpipe[18].

Cheatham et.al (1984)[19] approached the helical buckling problem by applying the principle of virtual work to the deviation of the column from its straight, buckled configuration. Based on simple lab experiments they stated that the force-pitch equation could be applied during unloading condition.

Kwon (1986)[20] used beam-column equation to developed a new solution to helical buckling of pipe. His solution give helical shapes of the buckled pipe with varying helix pitch a long the length of the pipe. The results were in term of length change of buckled pipe, bending moments and bending stresses. Also he derived new formula for computing tool clearance in helically buckled pipe.

Mitchell (1988)[21] developed more general approach that replaced the virtual work relations with the full set of beam-column equations constrained to be contact with the casing. His solution has good accuracy except near the neutral point which has a new

definition derived from contact –force criterion. Also, he showed that the Lubinski solution was a special case of his new analytic solution, and gives an approximate solution to the tapered-string buckling problem.

Chen et.al (1990)[22] described new theoretical results for predicating the buckling behavior of pipe in horizontal holes. They presented equations for computing forces required to initiate sinsoudle and helical buckling. A simple experimental tests were conducted to confirm the theoretical results.

Schuh (1991)[23] extended Pasaly-Dawson equation to determine critical buckling force in vertically , laterally curved and inclined boreholes. He adjusted the geometry to account for the shape of the buckled pipe in the curved borehole. He concluded that the Pasaly-Dawson buckling equation was more accurate than Cheatham, Chen and Lin equation. Also, he presented method for computing the bending stress of buckled pipe with tool joint and, if deflection of the pipe at mid span would touch the wall of the hole.

Mitchell (1995)[24] solved the differential equation of helical buckling to show the effect of hole deviation on buckling stability. Also, he developed stability criteria for transition from lateral buckling to helical buckling. He considered that the results of lubinski and woods were not valid for deviated or horizontal wells.

Stefan et.al (1995)[25] presented a new equations for predicting critical buckling force in inclined and horizontal wellbore. The new equations take into account the influence of torque and well bore inclination angle. Results showed that the torque caused reduction in

the predicted critical buckling load. The reduction was normally small but depending on the value of torque and wellbore inclination could exceed 10% as shown in Fig. (2-3).

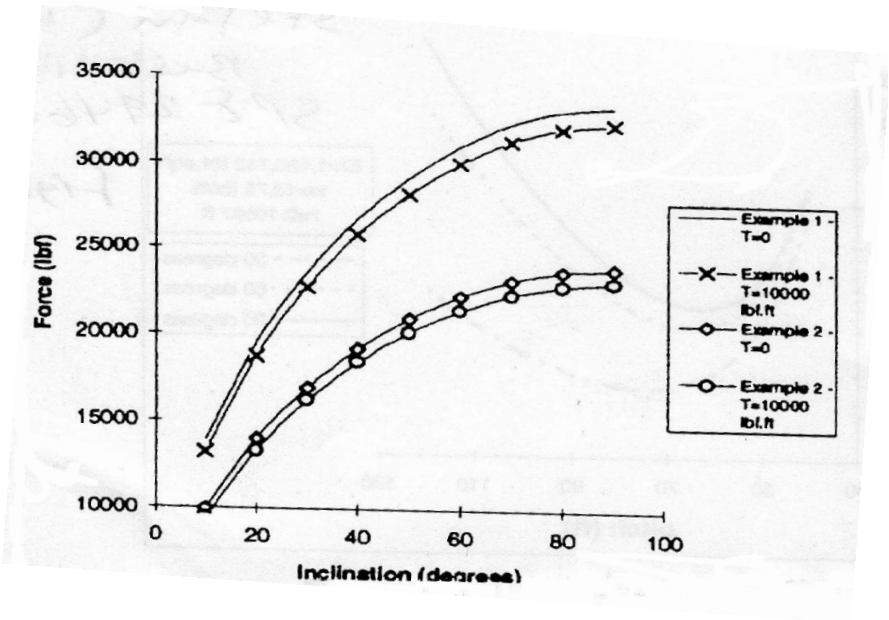

Figure 2-3: Effect of Torque on Critical Buckling Load[25].

X.He et.al (1995)[26] used Kyllingstad's theory of buckling to developed theoretical models. These models reflected the effects of torque on helical buckling, normal contact force, and pitch of helix in curved wellbore. They stated that the pipe buckling lead to increase in torque, drag and contact force. While the torque affected the buckling by reducing the critical buckling compress ional force.

Mitchell (1996)[27] presented a set of correlations to the numerical solution of the buckling differential equation for deviated wells. His calculation included buckling length changing, tubing contact forces, bending stress, and dog-leg angle. Fig (2-4) showed the significant impact of hole deviation on buckling tubing length change.

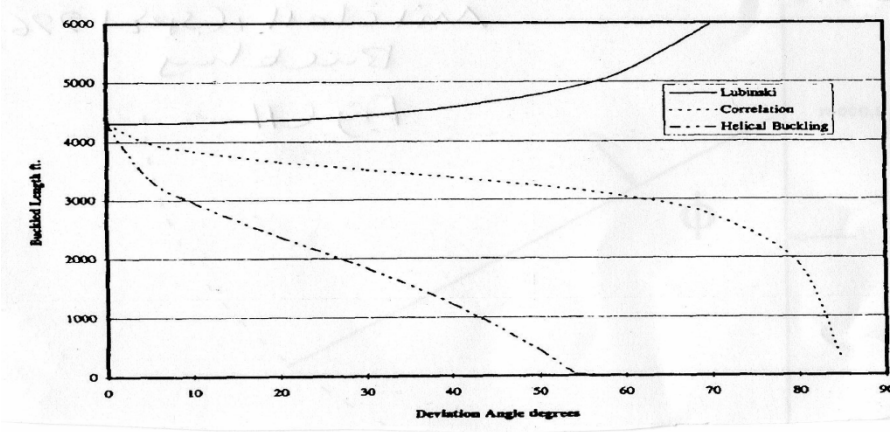

Figure 2-4: Effect of Hole Angle on Buckling Length[27].

Akgun et.al (1996)[28] investigated the effect of borehole parameters on the drill pipe stability in an inclined and curved holes by means of non-liner analysis of finite element method. Drilling parameters such as hole inclination and curvature, pipe size and thickness, hole size, mechanical properties of drill pipe and weight on bit were considered in the study. They concluded that large pipe size could withstand higher (WOB) before it buckles and, critical buckling load becomes less sensitive to change in pipe (OD) at higher hole curvatures. In addition the bending stress was affected by (DLS) and hole clearance but remains unchanged when changing inclination.

Jiang(1997)[29] derived new equations for calculating buckling loads and length of drill string under axial compressive and torsional loads in vertical, horizontal and, curved wellbores. He concluded that the torsional loads would reduce the buckling limit and have minimal effect on buckling length as shown in Fig(2-5).

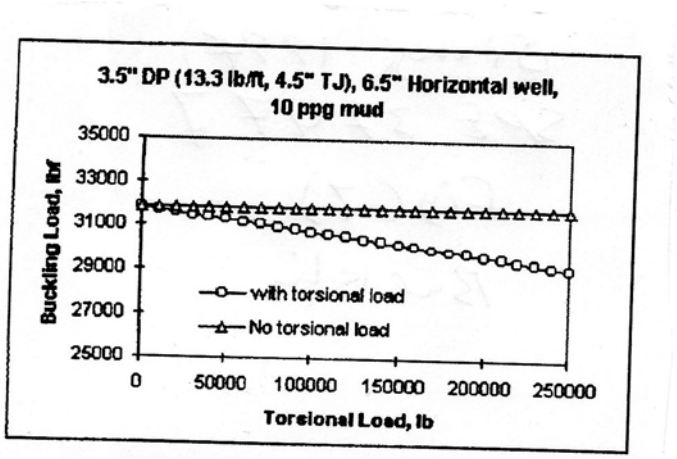

Figure 2-5: Effect of Torsional Load on Buckling Tendency[29].

2.2.3. Bending:

In high angle and horizontal wells, change the inclination angle or direction per certain distance known as dog-leg severity. This change cause additional tensile load and lead to the drill pipe fatigue.

Lubinski (1961)[30] published an equation for determining maximum permissible change of hole angle to insure a trouble-free hole, using a minimum amount of surveys. Calculation of pipe fatigue was made for gradual and long dog-legs and for abrupt dog-leg cases. Results of analysis showed that when drillpipe subjected to high tension, the smaller hole curvature which the pipe may withstand without fatigue failure as shown in fig(2-6).

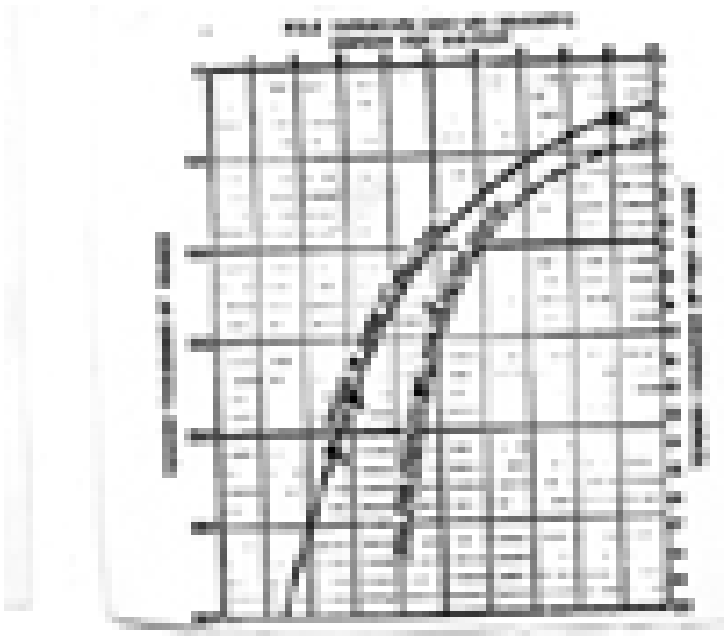

Figure 2-6: Effect of Tension on Dog-Leg Severity[30].

Hansford and Lubinski (1966)[31] provided curves for determining cumulative fatigue damage in curved wellbore for either steel or aluminum drill pipe going through dog-legs. They showed that the rate of pipe fatigue damage increased with the severity of dog-leg and, the tension in the drill pipe at the dog-leg. Also, aluminum pipe suffered much less fatigue damage than steel pipe

Paslay and Cernoky (1991)[32] extended the analysis of lubinski of pipe fatigue to the case of axial compressive loads. They presented sets of dimensionless curves for bending stress calculation for both tensile and compressive axial loads. All the results in term of a new factor called bending stress magnification (BSM), which was the ratio of the maximum absolute value of the curvature in pipe body divided by the curvature of the hole.

Jaing (1997)[33] presented an analysis of drill pipe bending and fatigue in rotary drilling horizontal wells. He considered in his calculation wellbore curvature, axial compressive load, drill pipe weight, and contact of drill pipe to the wellbore. He concluded that maximum drill pipe bending stress and fatigue damage could be reduced if there was contact between wellbore and drill pipe as shown in fig (2-7).

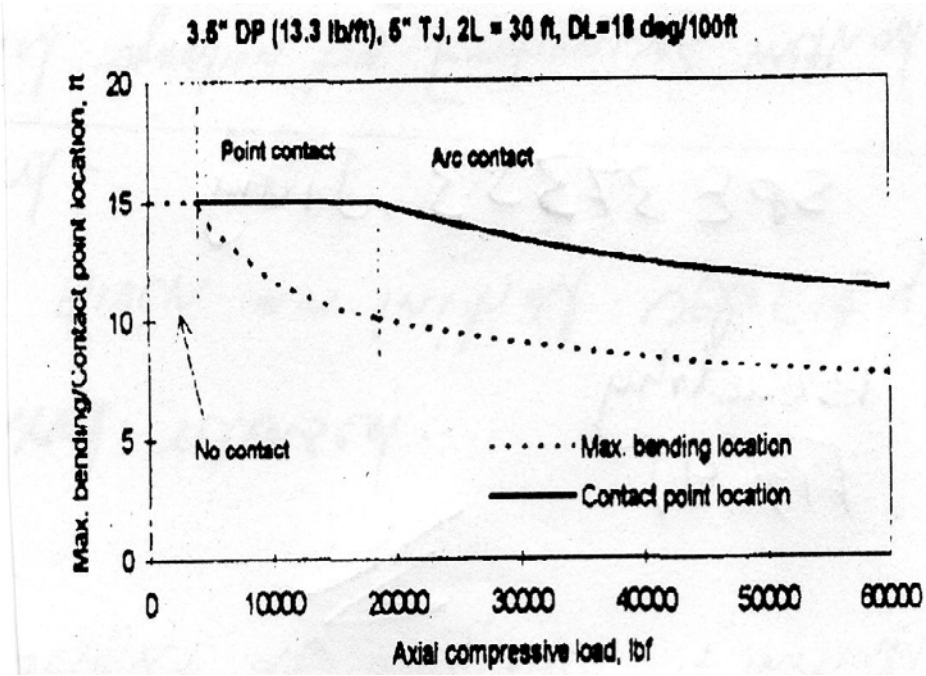

Figure2-7: Drillpipe Stationary and first Contact Locations [33].

2.3. Bottom Hole Assembly Modeling:

Bottom hole assembly is a part of drillstring. It is responsible for directing of wellbore. Since the pioneering work by Lubinski et al[34]., the drilling industry has gradually come to accept and appreciate the importance of analysis of BHA, which is now regarded as important in controlling the deviation tendencies of well trajectory, especially in directional and horizontal wells.

Murphey et.al (1966)[35] summarized theories that advanced to explained causes of hole deviation. They introduced a new correlation of physical variables to indicate how factors such as, drill collar stiffness, clearance and bit weight influenced bore hole deviation. Also, they proposed a method for predicting the rate of change of hole angle when drilling conditions were changed.

Walker (1973)[36] presented mathematical analysis of bottom hole assembly to detect optimum location of stabilizer in order to maximize their effectiveness. His mathematical model consider drilling parameter such as hole size, collar size, hole angle, bit weight, stabilize size and location, and mud weight.

Fischer (1974)[37] analyzed static deformation of bottom hole assembly and drillstring in two-dimension curved boreholes. His model was based on finite difference method which operates directly on the differential equations of bending of structural model. A computer program called (SCHADS) was built to predicted locations of contact points, contact forces, the force and moment within the drillstring, and the resultant force which the bit exerts on the formation being drilled.

K. Millheim (1977)[38] pointed out that hole curvature variation (inclination and azimuth) have significant effect on analyzing bottom hole assemblies .He used finite element program in the predicting bottom hole assemblies response for both cases of constant and variable inclination. Figure (2-8) shows computer analysis of two typical bottom hole assemblies with two curvatures, slight and

moderate inclination. A significant difference in the values of side force at the bit for the two cases at eight various depths.

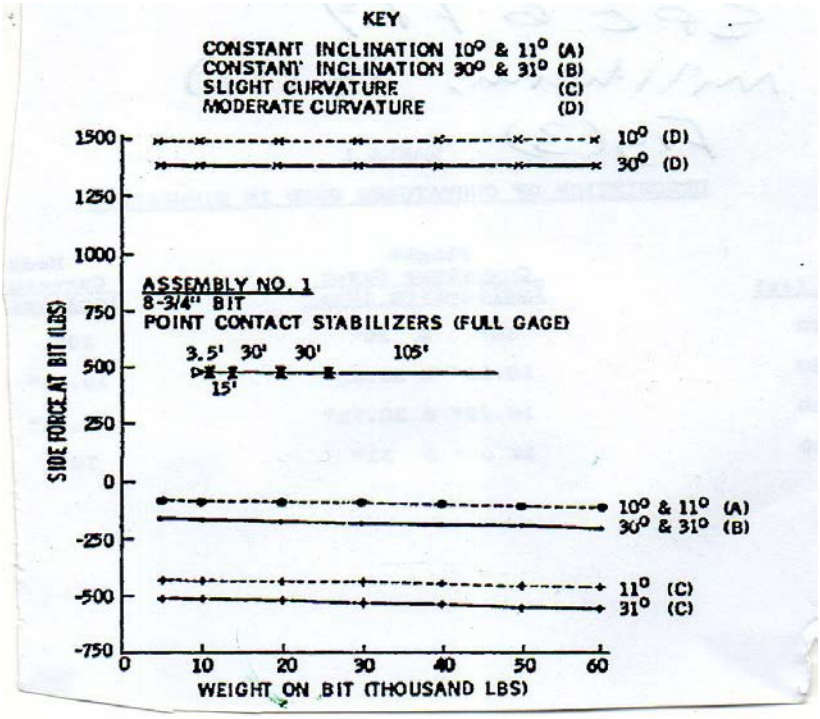

Figure2-8: BHA Analysis For Curvature and Non Curvature Cases[38].

K.Millheim (1978)[39] analyzed the complex behavior of bottom hole assembly in static condition ,two dimension by using finite element method. The method was considered the changes in geometry, loading, material properties, and the boundary conditions. Reaction forces at the bit were used to find the dropping or building tendency of various assemblies. The drill collar was modeled as straight beam with 6 degree of freedom and special gap element that gave excellent results. Also second modeled involved curved beam element with nonlinear elastic foundation when analyzing curved borehole assemblies.

Cheatham and Ho (1981)[40] developed a linear mathematical model to predict the resulting drilling direction for a bit drilling in

anisotropic rock. The rock drillability was described by three constants representing the drilling rates in three orthogonal directions, while the bit was described by two constants representing the drilling rate for the bit along the axis of the bit in radial direction when drilling isotropic rock. Model prediction showed that the hole would tend to deviated in radial direction for which the bit force is zero.

Jiazhi (1982)[41] used the beam- column theory and derived a system of equations of three moments to calculate reactive side force at the bit. Various types of pendulum assemblies were treated but his analysis was focused on the pendulum assemblies with two stabilizers.

Barid et.al (1984)[42] developed a finite difference computer program called "GEODYN". The program capable of simulating three-dimension transient dynamic response of polycrystalline diamond compact (PDC) bit interacting with a non-uniform formation. A series of verification problems were conducted to detected the responses of penetration rate, bit torque, side force and, bit motion to the variations in hole size, hole shape, and formation properties. Model predictions showed that the hole size had strong influence while hole shape was most noteworthy .Also, variation of formation hardness was observed to influence the penetration rate, bit torque, and to degree the side force.

Baird et.al (1985)[43] presented a three-dimensional transient dynamic finite difference computer program called"GEODYN2". The program capable of simulating the behavior of a rotating bottom hole assembly interacting with non-uniform formation.

M.Birades and R. Fenoul (1986)[44] described two-dimensional static finite element microcomputer called(ORPHEE). The program capable of quantitatively predicting the inclination behavior of bottom hole assembly by determining their equilibrium curvature. Comparison with the field data showed that, the model predictions could be more accurate if the penetration rate was considered in the computing equilibrium curvature of BHA.

Bertt et.al(1986)[45] combined the results of a finite difference BHA analysis ,including this with bent sub and down hole motor with bit penetration models to get analytical model for predicting inclination behavior of rotary drilling bottom hole assembly in three dimension. A comparison of the model results with field data are good in areas where formation affects are benign, while in areas of significant formation directional affects are poor. Figure (2-9) shows a sample of comparison.

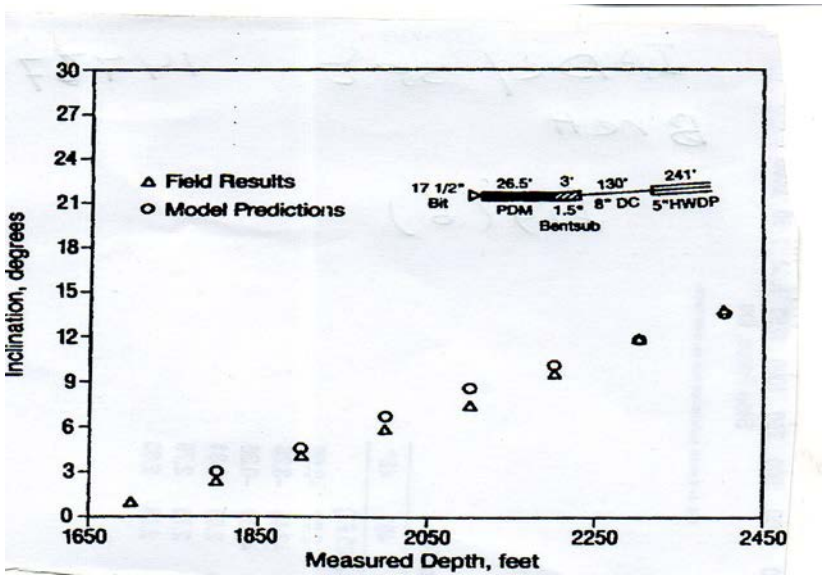

Figure 2-9: Predicted and Actual Field Inclination [45].

Rafie et.al (1986)[46] discussed three- dimensional directional drilling computer named" DIDRIL". The computer program was used

to analyze building, dropping, and holding assemblies in straight, 2-D curved, 3-D curved boreholes based on finite difference technique. They investigated effects of WOB, TOB, and borehole curvature on the build /drop and walk trends of the assemblies. Investigation results showed that the borehole curvature has strong effect on the bit side force as shown in fig (2-10).

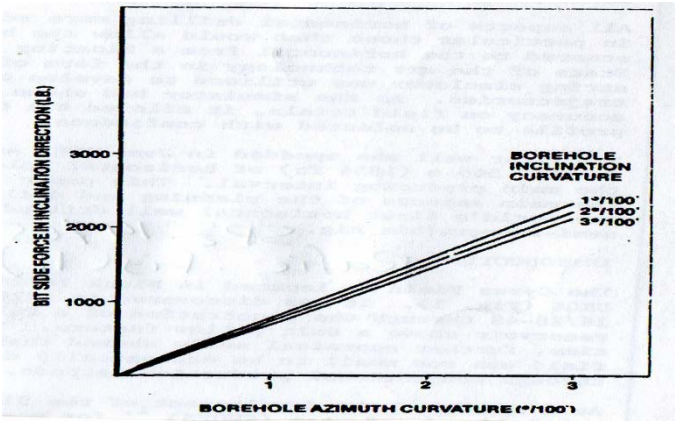

Figure 2-10: Effect of Curvature on Bit Side Force in Azimuth Direction [46].

Birades(1986)[47] discussed a three-dimensional mathematical model to compute static equilibrium of bottom hole assembly, taking into account friction force at the contact points between wellbore and bottom hole assembly. He distinguished two types of side force which are inclination side force and azimuth side force. His analysis showed that hole enlargement causes a decrease of inclination side force for different assemblies as shown in fig. (2-11).

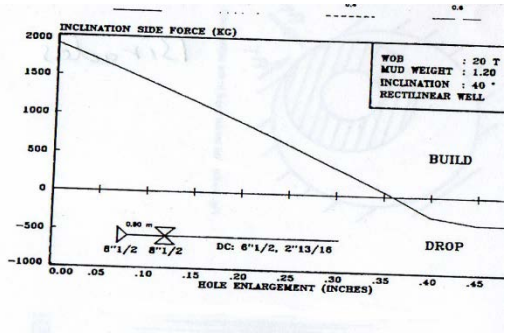

Figure 2-11: Effect of Hole Enlargement on Inclination Bit Side Force[47].

H.S.HO (1986)[48] investigated the effect of non-linear effect on the bit side force in three –dimension model for drillstring deformation under static condition. His formulations were accounted for large deformation effects and simplified by using finite difference method. Model predictions showed that nonlinear effects on bit side force were small as shown in Fig. (2-12).

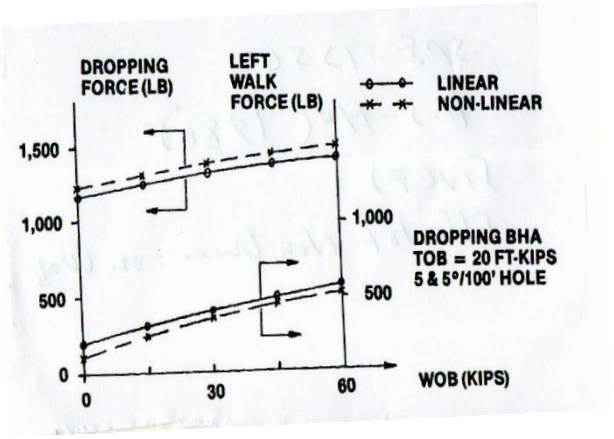

Figure 2-12: Effect of WOB on Dropping and Walk Force For Liner and Non linear Deflection[48].

A.Lubinski and J.S.Williamson (1987)[49] presented two dimension, constant hole curvature , and static mathematical model for predicting BHA performance. They developed computer program

takes into consideration formation characteristics, number of stabilizer, drillcollar size, square collar, motors, and measurement while drilling (MWD).

H.S.Ho(1987)[50] generalized existing 2-dimension model to presented 3-dimension model, taking into account the anisotropic drilling characteristics of both the formation and the bit. The new model capable of predicting the walk tendency, and the build/drop tendency of BHA under different conditions. A significant differences in the predicting walk and build/drop tendencies by his model and other predicting models.

Williamsmet.al(1989)[51] modified three-dimensional finite difference model of a bottom hole assembly to consider the nonlinear behavior of bottom hole assembly that contains bens and eccentric contact points along its length. Model predictions shows the strong influence of bent sub, bent housing, eccentric stabilizer on the bit side force and bit title of bottom hole assembly. Figure (2-13) shows these effects

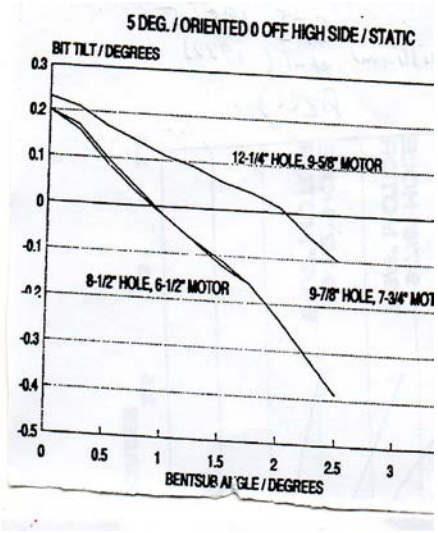

Figure 2-13: Effect of Bent Sub Angle on Bit Tilt[51].

Brakel and Azar(1989)[52] presented three-dimension numerical dynamic model to predict wellbore trajectory in both vertical and horizontal planes. Two bit/rock interaction models one for roller-cone bit and other for polycrystalline-diamond-compact (PDC) bit were incorporated into the model to detect correct boundary condition at the bit/rock interface. Model predictions showed that the both direction tendency (inclination and azimuth) would influence by hole inclination, WOB, rotary speed and, bit/stabilizer clearance.

Zifeng et.al(1994)[53] established three –dimension static mathematical model under large deflection for analyzing bottom hole assembly including steerable down hole motor. Forces and deflections of drillstring were calculated by making use of the method of weight residuals, the weight objective function and the method of optimization. They showed that the stiffness of large deflection model was smaller than that of small deflection, and the building force in large deflection analysis was smaller than that in small deflection analysis as shown in fig. (2-14).

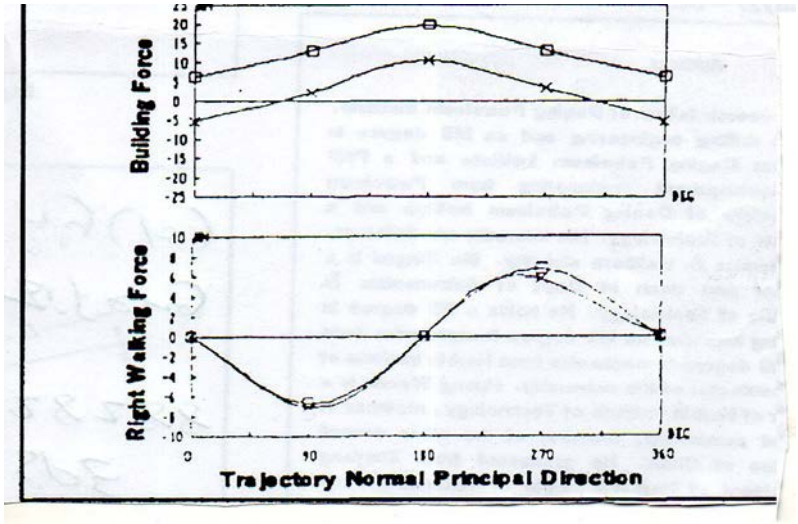

Figure 2-14: Effect of Well Trajectory Normal Principal Direction on Bit Side Force [53].

Mamdouh et.al (1994)[54] proposed a design criteria for selecting and optimization appropriate parameters of steerable bottom hole assembly. These parameters include bend angle, position of top stabilizer and, weight on bit. Analytical model for analyzing bottom hole assembly and field data of four BHA were used in selection method.

Yinao et.al(1995)[55] offered a formula to calculate the building rate of articulated down hole motor assembly(K) for short radius horizontal drilling which was:

$$K= (2/L)*[TAN^{-1}[C_k(R_b+F_a)/P_b]+\theta_b]+K_i \quad (2\text{-}7)$$

Where:

L:distance between near bit bearing point and bottom of bit.

C_k:cutting coefficient related to bit and formation type.

R_b:bit side force.

F_a: formation force decided by WOB.

P_b: weight on bit;

A series of quantitative analysis were conducted to relate the structure of bottom hole assembly, borehole geometry and, operating drilling parameters to bit side force and bit tilt angle..

Mamdouh et.al (1996)[56] proposed steerability concept(S) which was difference between the maximum and minimum side force to WOB ratios .i.e.

$$S= (F_s)_1/(F_a)_{min}- (F_s)_2/(F_a)_{max} \quad (2\text{-}8)$$

Where

F_a=axial force

$(F_s)_1$: side force at minimum F_a.

$(F_s)_2$: side force at maximum F_a.

They used that concept as criteria to design optimum rotary bottom hole assembly configuration (drill collar size and stabilizer positions). The larger range of the side force to WOB obtained for same BHA give the higher steerability, which allowed maximum correction in hole inclination by varying the weight on bit.

Akgun(2004)[57] proposed static, two-dimension, finite element model for predicting bit side force and tilt angle of rotary bottom hole assembly in horizontal wells. Results showed that at hole inclination near 90 deg , bit side force dose not changed when changing WOB , and both analytical and numerical methods give similar values of tangency length and bit side force. While for two stabilizer assembly, a significant deviation between two methods at WOB equals 60000 lb due to additional pipe-hole contact points.

Chapter Three
Theoretical Background

3.1. Introduction:

The drilling and utilization of horizontal wells is one of the most active and existing areas of development in petroleum production technology. The purpose of this chapter is to define all design concepts of horizontal well.

3.2. Horizontal Well:

A horizontal well may be defined as directional well which is drilled to an inclination of 90 deg and maintains this inclination for significant distance. Figure (3-1) shows a typical Horizontal well diagram which consist of the following sections [58]:

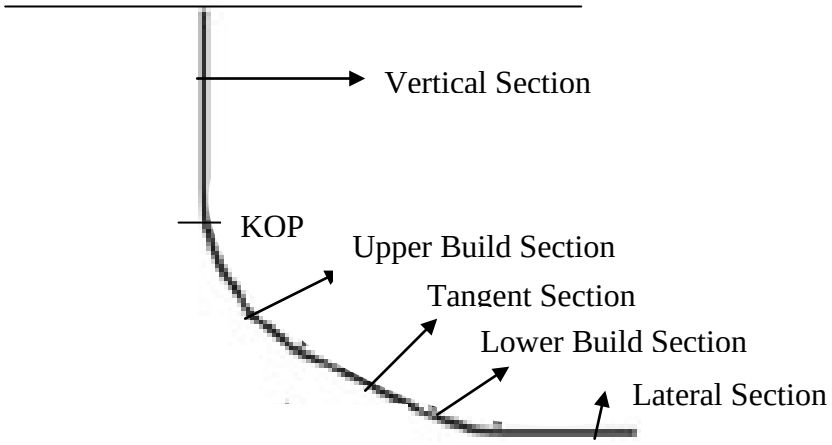

Figure 3-1: Typical Horizontal Well.

3.2.1. Vertical Section:

It is the vertical distance from the surface to the kick-off point. It has zero inclination angle from the vertical.

3.2.2. Upper Build Section:

It is starting of building hole angle from zero to the desired angle detected previously.

3.2.3. Tangent Section:

It is portion of the well profile design that has constant inclination angle starting from upper build section. It included increasing horizontal displacement to reach the target entry point, correct for target entry TVD uncertainties, and correct for imperfect directional performance.

3.2.4. Lower Build Section:

It is a build angle section extended from tangent angle section to the horizon. Usually this section is drilled in marker zone that is close to reservoir.

3.2.5. Lateral Section:

It is the Length of horizontal section in the pay zone. It depends on type of horizontal well profile. Productivity and drainage area are proportional with this length.

3.3. Types of Horizontal Wells

In the oil industry, there are three categories of horizontal wells. This classification is based on the rate of angle build up in the well trajectory from vertical to horizontal. Figure (3-2) summarized these type and their features.

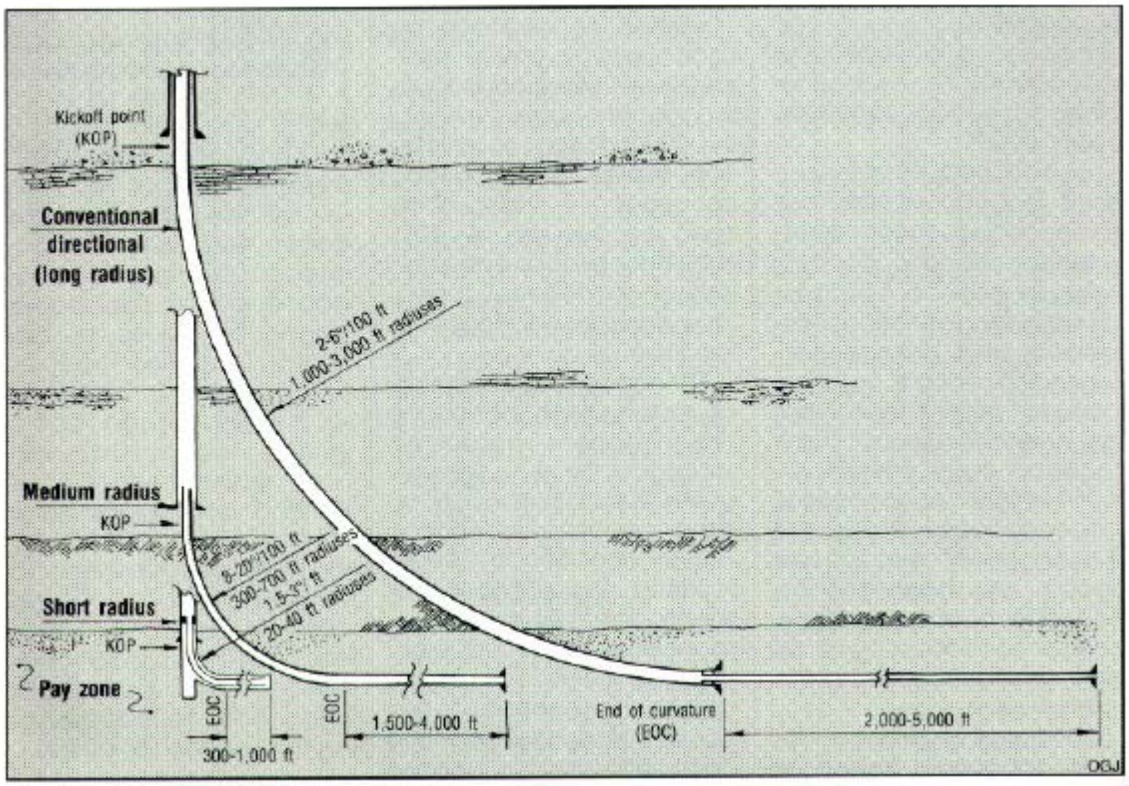

Figure 3-2: Types of Horizontal Wells [4].

3.3.1. Long Radius Well:

A long radius horizontal well is characterized by build rates of 2-6 deg./ 30m(100 ft), which is needed vertical depth between (1000- 3000 ft)(290-900 m) to turn the well from vertical to horizontal. The amount of vertical depth required is a function of the build rate and, any tangent which is included in the well profile. Thus, this profile is well suited for application where a long horizontal is required, especially offshore.

Long radius wells may be drilled with a combination of conventional directional drilling assemblies. The wells are kicked off with downhole motor assemblies. This assembly could be a slick motor with a bent sub, but is usually a steerable motor assembly. If a steerable motor assembly is used to drill the build section, it is usually used to drill the tangent section

as well. If a bent sub assembly is used to kick the well off, the tangent section is often is drilled with rotary bottom hole assembly[6].

3.3.1.1. Advantages of Long Radius Wells:

Long horizontal wells have the following advantages:

1- Lower dog-leg severity.

2- Long lateral section.

3- Adaptation of conventional directional drilling techniques and equipments.

4- Greater amount of rotary drilling which allows improved drilling performance.

5- Fewer restrictions on hole/equipments sizes.

6-wider range of completion options [6].

3.3.2. Medium Radius Wells:

A medium radius horizontal well is characterized by build up rate of 6-35 deg/30 m(100 ft), which is needed a vertical depth between(50- 300 m)(160- 1000 ft) to turn the well from vertical to horizontal. While the drilled lateral section may be reached up to 2500 m (8000 ft) long.

The definition of medium radius wells will vary with the hole size. Table (3-1) shows approximate guidelines for medium –radius well.

Table 3-1: Medium Radius Well Guidelines [1]

Hole size (in.)	Build Rate (°/100ft)	Radius (ft)
6 to 6 3/4	12 to 25	478 to 229
8 1/2	10 to 18	573 to 318
12 1/4	8 to 14	716 to 409

These wells are drilled with specialized down hole motors and conventional drillstring components. Double bend assemblies are designed to build angles at rates up to 35 deg. /30 m (100 ft) in the oriented mode (non rotating) mode. This profile is common for land based application and for reentry horizontal drilling[6].

In practical terms, a well is medium radius if the bottom hole assembly cannot be rotated through the build section at all times. At the upper end of medium radius, drilling the maximum build rate is limited by the bending and torsional limits of API tubulars[1].

3.3.2.1. Advantages of Medium Radius Wells:

Medium radius horizontal wells have the following advantages:

1- Conventional drilling equipments could be used.

2- Less hole restrictions on hole sizes.

3- Wider range of completion options.

4- Multiple laterals possible from single well[6].

3.3.3. Short Radius Wells:

A short radius horizontal well is characterized by build up rate of 5-10 deg/m (1.5- 3deg/ft), which equates to radius of 6.1-12.2 m (20-40 ft). Most wells drilled with this system have been less than 3000 m (10000 ft) TVD and with lateral reaches of 90-120 m (300-400 ft),although up to 350 m(900 ft) has been obtained. As usual, hole size will affect the radius of curvature that can drilled. Table (3-2) contains guidelines for short –radius wells[6].

Table 3-2: Short Radius Well Guidelines[1]

Hole Size (in.)	Build Rate (°/100 ft)	Radius (ft)
8 1/2	48 to 88	120 to 65
6 to 6 3/4	57 to 115	100 to 50
4 3/4	64 to 143	90 to 40
3 3/4	72 to 191	80 to 30

Short radius wells are drilled with specialized articulated motors to affect high build angles. Frequently, short radius wells are drilled by re-entering existing wells, and the radius of the well is simply defined by the distance from the existing casing seat to the pay zone[1].

3.3.3.1. Advatages of Short Radius Well:

Short radius horizontal wells have the following advantages:

1-short curved section.

2-Kick of point is closer to the reservoir.

3-Multiple lateral possible from single well.

4-Minimum measured depth.

5-Easy reentry of existing wells[6].

3.4. Drillstring Mechanics of Horizontal Wells:

The analysis of forces acting on the drillstring in the horizontal wells under different operating conditions is of great interest. The drillers and companies have devised computer programs for their analysis to detect the worst conditions during drilling operation. The basic mechanical loads for the horizontal drilling are:

3.4.1. Torque and Drag:

Torque and drag is a broad term which refers to the effects of the geometry and other aspects of the drill hole may have on the turning and pulling of the drillstring[58].

In directional and horizontal wells, friction between the drillstring and the wall of hole has great effect on the weight on bit. In build and horizontal section, the drill pipe lies on the bottom of the hole and its weight does no thing to drive the bit forward. Thus, its weight multiplied by the coefficient of friction results in a force that decrease the weight on bit. That is, drag is produce when the drillstring is moving and the torque is produced when the drill string is rotating[3].

Torque and drag calculations are very important in the designing horizontal wells. Models of torque and drag calculation can be used for various purposes, including:

- Evaluating and optimizing wellpaths to minimize torque and drag.
- Providing normal force loads for inputs into other programs, such as casing wear models.
- Identifying depth or reach capabilities or limitations, both for drilling and running casing/tubing.
- Matching the strength of drill string components to the loads (axial, torsional or lateral) in the wellbore.
- Identifying the hoisting and torque requirements of the drill rig [1].

3.4.1.1. Operating Conditions

While planning horizontal well, the torque-drag modeling should included the operating conditions with worst –case friction factors to ensure that the drillstring can be advanced, rotated, slide if oriented

drilling is necessary, and pulled out of the hole. The most known operating conditions of drillstring during drilling horizontal well are:

3.4.1.1.A. Rotating off-Bottom:

Which represented the weight of drillstring whiles the string off bottom and rotated. Usually the rotary speed above 35 rpm.

3.4.1.1.B. Slack-off Without Rotation:

Represents the drillstring weight while lowering the string in the hole at normal working speed.

3.4.1.1.C. Pick-up without Rotation:

Represents the weight of drillstring while pulling the string out of hole at normal working speed.

3.4.1.1.D. Drilling:

Represents the surface tension of drillstring when weight on bit is applied for drilling[58].

The results from torque/drag are usually expressed graphically with torque and/or drillstring tension on one axis and measured depth on the other. Figure (3-3) shows typical loads diagram with respect to measured depth for different operating parameters[1].

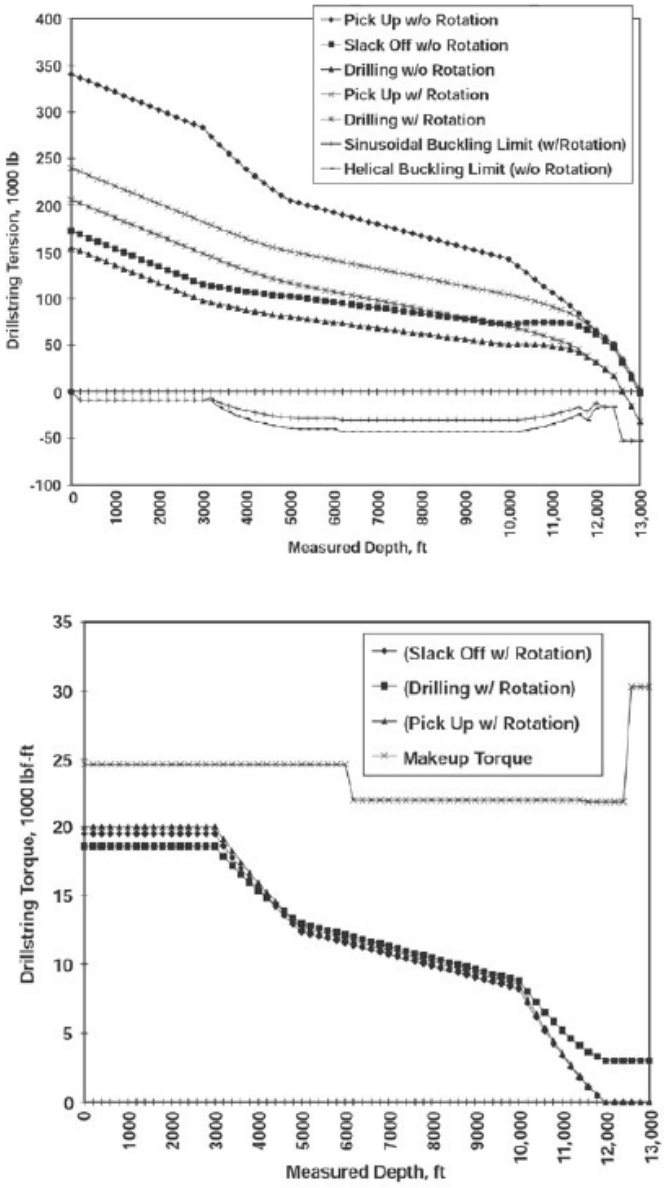

Figure 3-3: Torque and Drag Analysis[1]

3.4.2. Buckling:

During drilling horizontal well,slack-off operation exerted axial load on the drillstring and some time caused it to buckle. The severity of buckling increased with additional applied load and reached to degree where little WOB available at the bit. This case is associated with use of steerable bottom hole assembly and causing reduction in horizontal reach

capability. Thus it is very significant to detect the onset and degree of buckling in the drillstring.

Dawson & Pasaly (1984)[18] showed that conventional drillpipe will buckle with low axial loads in near vertical wells. When the angle hole increased, the gravity force will pulls the drillstring against the low side of hole (stabilized) and allows drillpipe to carry axial compressive loads without buckling. Figure (3-4) shows compressive load capabilities of several commonly used sizes of drillpipe in deviated well as function of hole angle. It is clear that when hole angle increased, more compressive load could be transmit by drillpipe without buckling. Also these compressive capabilities could be enhanced when drilling wells with small diameters or increasing outside diameter of the pipe.

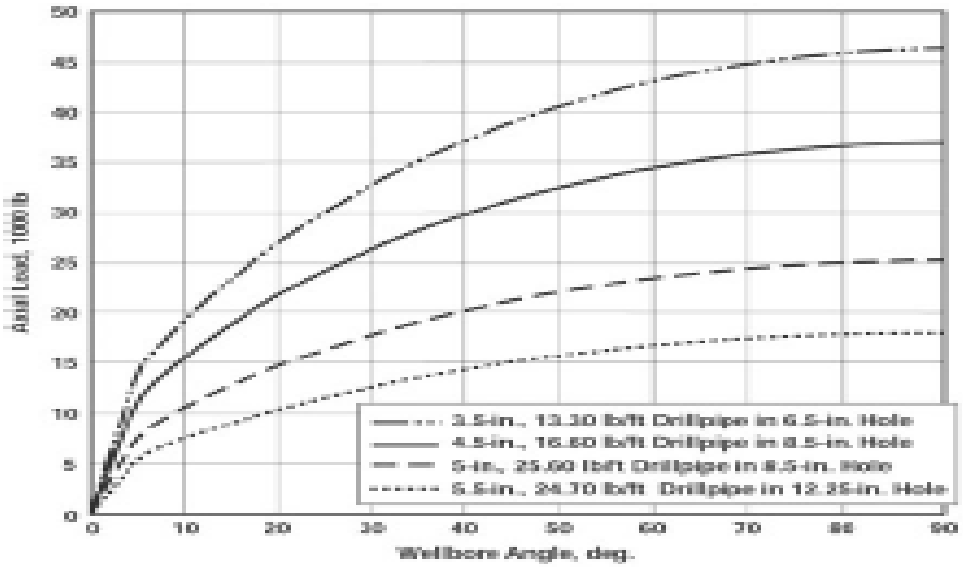

Figure 3-4: Effect of Hole Angle on Compressive Capability of Pipe[1]

In directional and horizontal wells drillstring can be buckled into two modes which are sinusoidal and helical buckling as shown in fig (3-5). Theoretical analysis of pipe buckling shows that the axial compressive force required to buckle into a sinusoidal configuration depend on pipe

stiffness, weight and, hole size. As the axial force is increased, the buckling mode changes from sinusoidal to helical buckling. Most of experimental models confirm the results of the theoretical analyses[22].

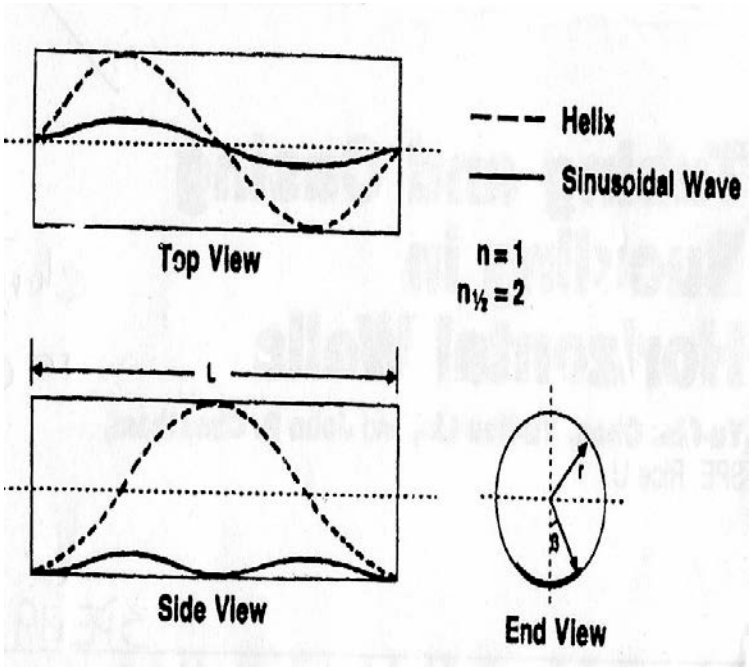

Figure 3-5: Sinusoidal and Helical Buckling Configuration[22].

3.4.3. Bending:

In directional and horizontal wells, the effect of wellbore curvature on axial stress in the drillstring must be considered in the drillstring design. When string is forced to bend, the axial tension on the convex side of the bend can be increased greatly[59].

3.4.3.1. Dog-leg Severity:

The curvature of a directional and horizontal wells generally is expressed in terms of dog-leg severity, which is defined as the change in hole inclination and /or hole direction over a specific interval (100 ft or 30 m).

The bending of pipe near a dog-leg produces compression in the fibres of the joint at point A in Fig. (3-6) and produce tension at point B. At point A the resultant tensile stress (weight carried + induced compressive stress of compression) is less than that at point B(weight carried+ induced tensile stress). Hence, as the pipe is rotated, the stress at the periphery of the pipe in the dog-leg areas varies between a maximum at B and a minimum at A. The repeated change in the magnitude of stress results in fatigue failure of pipe[60].

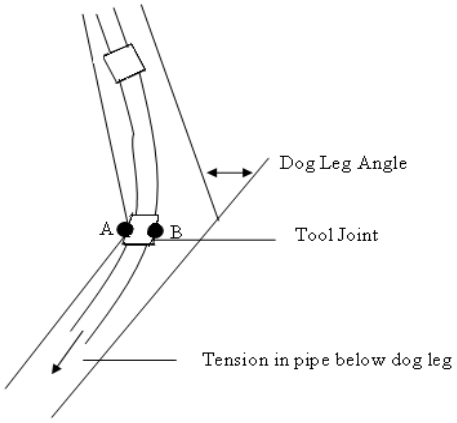

Figure 3-6: Dog-Leg[60].

Lubinski (1961)[30] has shown that the greater the tension to which drillpipe is subjected , the smaller the dog –leg severity (or hole curvature) which the pipe may be withstand without fatigue failure occurring. The maximum permissible dog-leg severity in deg/100 ft , C_{max}, without pipe fatigue can be determined from :

$$C_{\max} = \frac{137510}{ED_o}\sigma_b \frac{\tanh(KL_j)}{KL_j} \qquad (3\text{-}1)$$

$$K = \sqrt{\frac{T_b}{EI}} \qquad (3\text{-}2)$$

Where:

E: Young's modulus=30000000 psi for steel.

D_o: outside diameter of pipe, in.

L_j: half distance between tool joints, in.

I: moment of inertia of pipe, in^4.

T_b: buoyant weight suspended below the dog-leg, lb.

σ_b; maximum bending stress, psi.

The maximum bending stress, σ_b, for each Grade of drill pipe is determined as follows:

For Grade E:

$$\sigma_b = 19500 - \frac{10\sigma_t}{67} - \frac{0.6(\sigma_t - 33500)^2}{(670)^2} \quad (3\text{-}3)$$

Equation (3-44) is valid for σ_t values up to 67000 psi.

For grade S-135:

$$\sigma_b = 20000\left(1 - \frac{\sigma_t}{145000}\right) \quad (3\text{-}4)$$

Equation (3-45) is valid for σ_t up to values of 133400 psi where:

$$\sigma_t = \frac{T_b}{A_s} \quad (3\text{-}5)$$

σ_t=buoyed tensile stress, psi.

A_s: cross sectional area of drillpipe, in^2.

Lubinski constructed fatigue curves of gradual dog-leg for two types of drillpipe (S-135, E) and different sizes. These curves could be used as guidelines for maximum tension of drillpipe that could be tolerated in the dog-leg portion. Figure (3-7) shows fatigues curves for drillpipe type S-135.

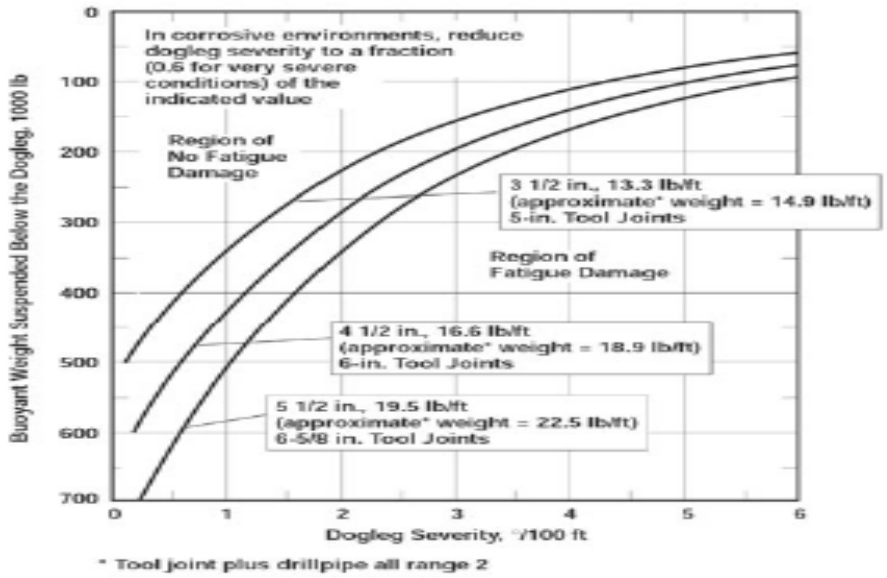

Figure 3-7: Dog-leg severity Limits for S-135 Drillpipe[1]

3.5. Bottom Hole Assembly(BHA):

A bottom hole assembly is the portion of the drillstring that affects the trajectory of the bit and, consequently, of wellbore. It construction could be simple ,having only a drill bit, collars, and drill pipe, or it may be complicated, having a drill bit, stabilizer, magnetic collar, telemetry unit, shock sub, collars, reamers, jars, crossover subs, heavy weight drill pipe, and regular drill pipe[59].

3.5.1. Functions of BHA:

The functions of a bottom hole assembly are as listed in the following:

1- Control direction and inclination in directional and horizontal wells.
2- Protect the drill pipe in the drillstring from excessive bending and torsional loads.
3- Reduce severities of dog-legs, keyseats, and ledges.

4- As tool in fishing, testing, and workover operations.

5- Increase drill bit performance.

6- Reduce rough drilling, (rig and drill string vibrations)[58].

3.5.2. Types of Bottom Hole Assembly:

There are two types of bottom hole assembly that could be used in the drilling of high angle and horizontal wells. These are:

3.5.2.1. Rotary Bottom Hole Assembly:

This type of bottom hole assembly was used in earlier days of directional drilling and some times in the present. Usually, this type is used in the drilling tangent sections where the directional objective is to drill straight ahead. Rotary assemblies are most commonly used where formation tendencies are predictable and rig economics allowed to use.

In rotary assembly, the weight of the collar gives it a tendency to sag or flex to the low side of the hole; collar stiffness and length and stabilizer diameter and placement are engineered as a means of controlling the amount of flexure to give the desired hold, drop, or build tendency. Rotary assembly has only single directional tendency (build or drop), thus it has limited ability to vary the directional tendency. Its limited ability comes from primarily from varying WOB which is used to tune that tendency[1].

Basically there are three type of rotary BHA as shown in Figure(3-8), these are:

3.5.2.1. A.Pendulum(Dropping)BHA:

The pendulum BHA is used to drop angle especially on high angle wells where it is usually very easy to drop angle. This BHA relies on the principle that the force of gravity can be used to deflect the hole back to vertical. The force of gravity is related to the length of

drillcollars between the bit and first point of tangency between the hole. This length is called the active length and can be resolved into two forces: one perpendicular to the axis of the wellbore (side force) and one acts along the hole.

Increasing the active length of drillcollars causes the side force to increase more rapidly then the along hole component. The side force is the force that brings about the deflection of the hole back to the vertical. Some pendulum assemblies may also use an under gauge near-bit stabilizer to moderate the drop rate[3].

3.5.2.1. B.Fulcrum(Building)BHA:

This BHA is used to build angle (or increase hole inclination), by utilizing a near bit stabilizer to act as a pivot or fulcrum of a lever. The lever is the length of drillcollars from their point of contact with the low side of the hole and top of the stabilizer. The drill bit is pressed to the high side of the hole causing angle to be built as drilling ahead progresses. Since the drillcollars bend more as more WOB is applied, the rate of angle build will also increase with WOB[3].

2.5.2.1.C. Packed(Hold) BHA:

This BHA is used to hold or maintain inclination and direction and are typically used to drill tangent section of a well. The packed BHA relies on the principle that two contact points will contact and follow a sharp curve, while three points will follow a straight line. Packed BHA have several full gauge stabilizers in the lowest portion of the BHA, typically three or four stabilizers. This makes the BHA stiff and hence it tends to maintain hole angle and direction[3].

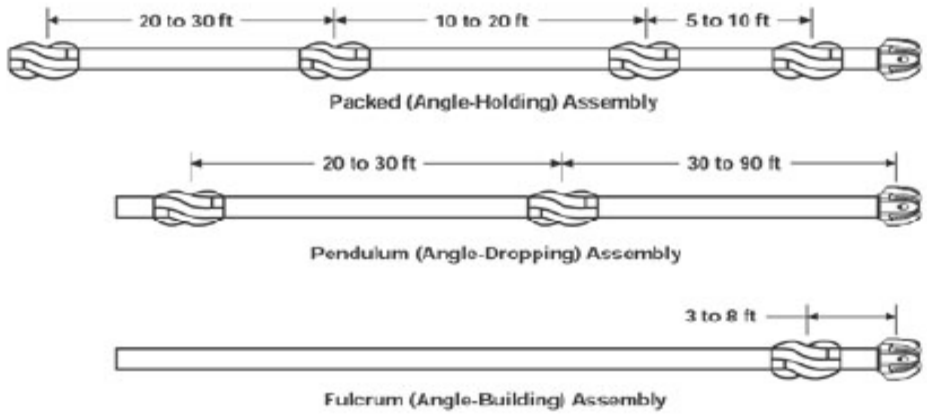

Figure 3-8: Types of Rotary Bottom Hole Assemblies[1].

3.5.2.2. Steerable Bottom Hole Assembly:

In the late 1980s, the petroleum industry introduced the steerable motor as the most advancement in the trajectory control. Figure (3-9) presents typical steerable motor configuration.

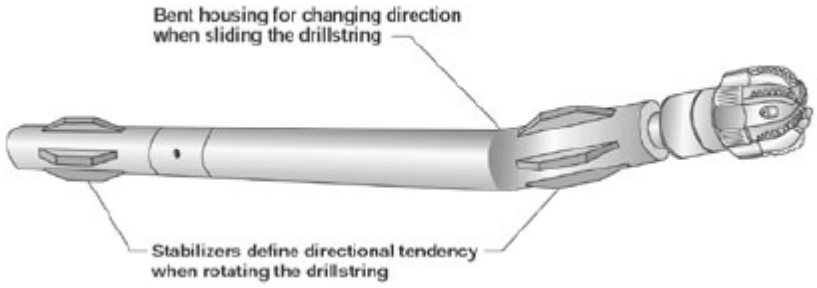

Figure 3-9: Typical Steerable Motor Configuration [1].

The steerable motor is positive displacement motor (PDM) configured with bend in the connecting rod housing (bent housing). In this configuration the PDM operates with two mode which are sliding (oriented) and rotary mode as shown in Fig. (3-10). In the sliding mode, the steerable motor is oriented by slowly rotating the drillstring with aid of MWD signals to determine toolface or bend orientation.

Once the desired downhole toolface orientation is achieved, the drillstring is then slid (i.e.,advanced without rotating),maintaining the desired toolface. The rotation required to drive the bit is generated entirely by the PDM. The combination of stabilizers and bent housing generates a side force on the bit, causing it to drill in the direction of toolface.

In the rotary mode, the drillstring is rotated and the effect of the bend is negated, at least as far as changing direction is concerned. When rotated , the steerable motor behaves directionally like rotary assembly and set up to drill straight ahead although they can be configured to build or drop while rotating(1).

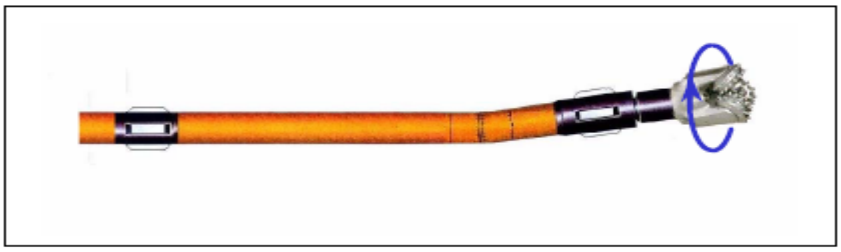

Sliding mode

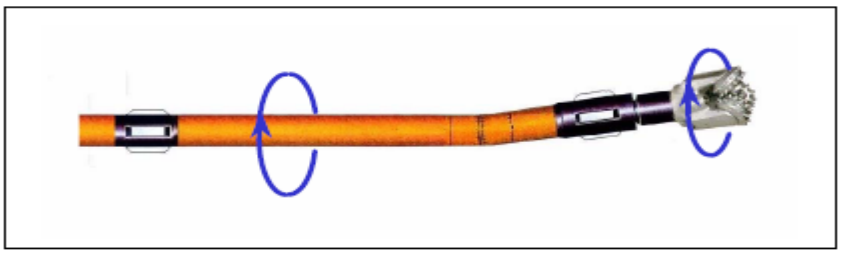

Rotary mode

Figure 3-10: Sliding and Rotating Mode, Steerable Bottom Hole Assembly(4).

3.5.3. Stiffness:

Each component of BHA have shape, dimensions, and physical properties. Dimensions included inside and outside diameters while physical properties included density and elastic modulus of the material.

The product of moment of inertia and modulus of elasticity is called the stiffness of material,i.e;

Stiffness coefficient=E*I

$$Stiffness coefficient = \frac{E\pi\left(OD^4 - ID^4\right)}{64} \tag{3-6}$$

The stiffness coefficient can be used as an indicator of relative rigidity. Figure (3-11) shows stiffness of various drillstring and BHA components as function of outside and inside diameter.

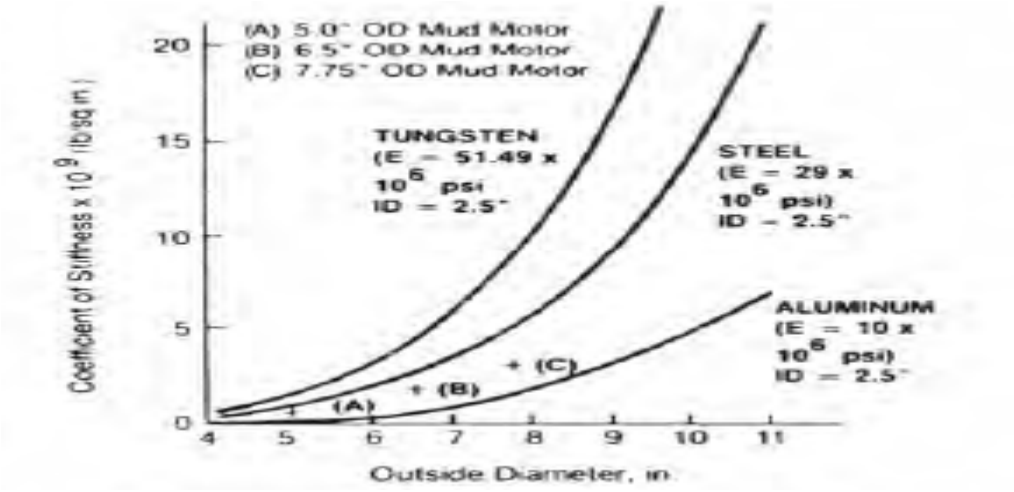

Figure 3-11: Drillcollar Stiffness [61].

3.5.4. Bit Tilt:

Bit tilt may be defined as the angle between the axis of drillstring and axis of the bit. Adjustability of the tilt angle is a feature of modern

motors. This adjustment is made on the rig floor to suit the plane for the hole to be drilled. With low setting of tilt angle a particular motor may be steerable, whereas with high angle, it may be only be able to operate in non-rotatable, sliding fashion. Build sections are usually drilled with sliding mode, while hold sections such as horizontal sections are drilled with rotation mode[62].

3.5.5. Relation Between Bit Tilt and Build Rate :

The bit tilt angle (Θ) required to achieve a given hole curvature radius (R) can be estimated from the geometry shown in Figure (3-12). It is assumed there are two stabilizers and the bit, and that these lie on a circle having the radius of curvature (R). The two sections of the assembly L1 and L_2 are titled with respect to each other by angle Θ. The relation between build rate and geometric parameters may be written as follows:

$$\theta = \frac{ArcBC}{R} = \frac{(L_1 + L_2)}{2R} \tag{3-7}$$

$$R = \frac{(L + L_{21})}{2\theta} \tag{3-8}$$

$$BUR = \frac{200\theta}{(L + L_{21})} \tag{3-9}$$

Where:

BUR: build angle rate, deg/100 ft.

Θ: bend angle, deg.

L_1: distance from bit to first stabilizer, ft.

L_2: distance from first stabilizer to second stabilizer, ft[4].

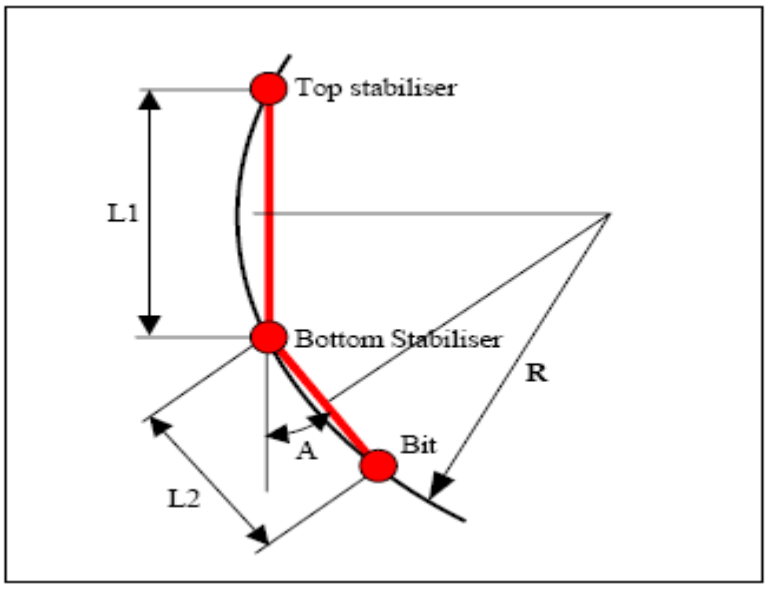

Figure 3-12: Bent Housing Geometric Efficiency[4]

3.5.6. Maximum Length of Bottom Hole Assembly:

Short-radius horizontal wells are usually drilled with high angle build rates. These high build rates possessed high bending stress and side forces on bottom hole assembly components and sometimes caused faulier. Thus, BHA components must be shorted (articulated) to pass through build section without interference. As shown in Figure (3-13), articulation are knuckle joints or hinge points that transmit axial loads and torque, but not bending[1].

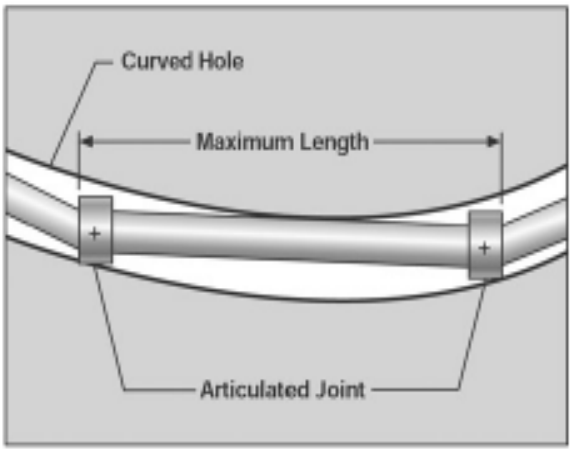

Figure 3-13: Articulation of Short Radius Well BHA[1].

The maximum length of(L) BHA components can be determined from the following relation:

$$L = 2\sqrt{24R(D_h - D_p) + (D_h - D_p)^2} \quad (3\text{-}10)$$

As shown in the Figure (3-14), the maximum length of BHA is function of build rate and clearance between the tool and the diameter of the hole. a long sections of BHA could be used when reducing build rates or using small pipe sizes[4].

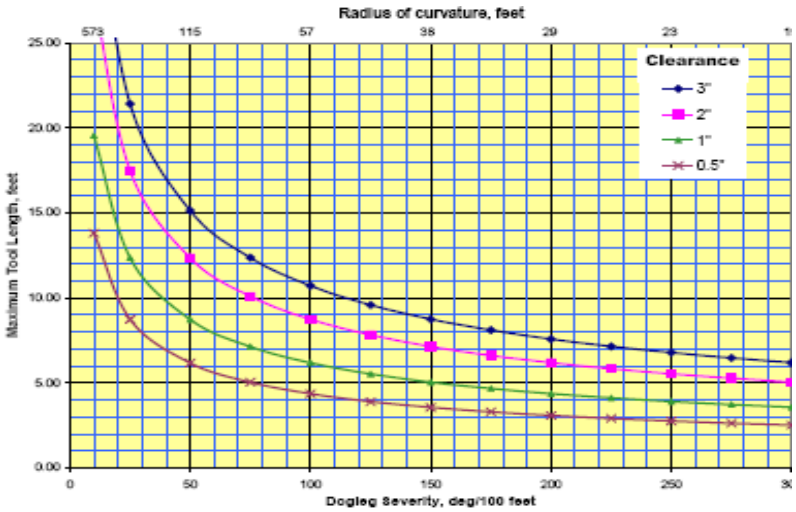

Figure 3-14: Maximum Tool Length Versus Dog-Leg Severity [4].

3.5.7. Bit Side Force(F_B):

Bit side force may define as the resultant force at the bit between pendulum force and bending force. As shown in figure (3-15), the ultimate direction of the hole will dictated by mechanical forces of drillstring and formation reaction. The mechanical forces included pendulum force (F_p) and bending force (F_b).

When the axial weight is applied on elastic drillstring, the string will bend and contact the hole at point called" tangency point". Thus , the

pendulum force(F_p) which arises due to gravity and hole inclination, is depend on the active length between the bit and tangency point. This force try to deviated the hole to the right (reduce the inclination).

The second component of mechanical forces is the axial load(WOB) applied on the bit. The lateral component of axial load (positive bending force,F_b) is responsible for hole deviation and tended to deviate the hole to the left. This force could be determined after assessing the bending moments over the active portion of the BHA. Active portion refers to all parts below the main tangency point.

The final hole inclination will depend on the difference between (F_p) and (F_b) (i.e.; on the bit side force). If the (F_B) is positive, the bottom hole assembly will have building angle tendency. While if F_B is negative, the bottom hole assembly will have dropping angle tendency. In case of zero F_B, the bottom hole assembly have holding angle tendency[(60)].

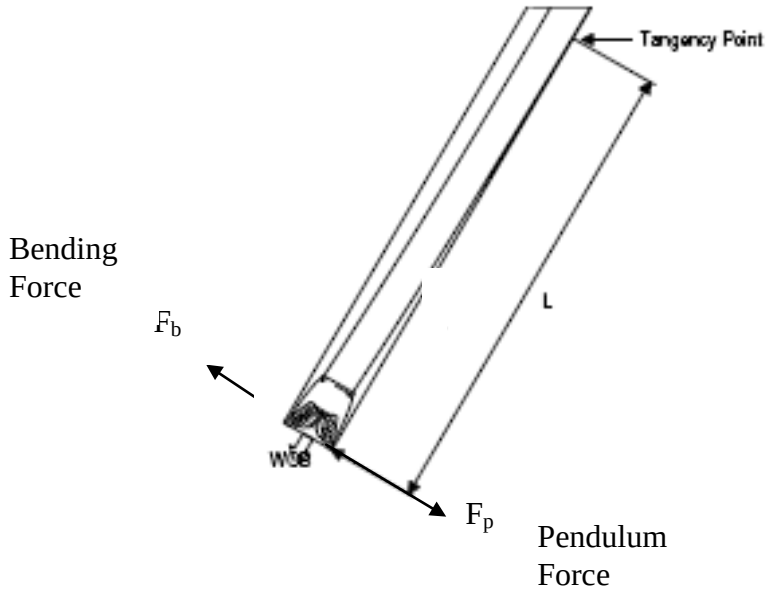

Figure 3-15: Effect of Mechanical Factors on Hole Deviation[(60)].

Basically, there are three mathematical methods available for detection bit side force. These are:

3.5.7.1.Analytical Method(Jiazhi's Method):

Based on Timoshenko's method" Three Moment Equations", Jiazhi derived a set of equations for computing bit side force in two dimensions, static mode. These equations are derived depending on how many stabilizers are attached such as slick BHA, single-stabilizer BHA, and two-stabilizer BHA. In all cases, the essence of the technique is to determine the point of contact between the pipe and wall of the hole (Tangency point). The tangency point of each BHA is found applying weight on bit and used trial and error approach. Once the tangency point is determined, the bending moments and bit side force can be calculated.

Practically, this BHA analysis technique becomes more tedious as number of stabilizers increase. Also, the deflection of BHA to the side of borehole can not determined with this technique. In addition, if more contact points developed due to increased WOB between bit and first stabilizer or between two stabilizers, the method will not be applicable[(57)].

3.5.7.2. Finite Difference Method:

This is a well –established numerical method suitable for solving any types of differential equations. The governing equations for the bottom hole assembly displacements and bit side force are converted into systems of matrix equations by proper differencing of the various derivatives.

The main disadvantage of this method is that it requires small grid intervals in order to obtain accurate solutions, which result in a larger matrix size. In addition, the governing differential equations and boundary conditions have complexities which make it troublesome [(53)].

3.5.7.3. Finite Element Method:

The finite element method (FEM), sometimes referred to as *finite element analysis* (FEA), is a computational technique used to obtain approximate solutions of boundary value problems in engineering. Simply stated, a boundary value problem is a mathematical problem in which one or more dependent variables must satisfy a differential equation everywhere within a known domain of independent variables and satisfy specific conditions on the boundary of the domain [(63)].

The most widely used form of finite element analysis is the matrix displacement method. In this method the structure is idealized into an assembly of discrete structural elements. A displacement form (displacement function) solution is assumed to approximate the displacements for each element owning to applied force. The complete solution is then obtained by combining these individual approximate displacements in a manner which satisfies the displacement compatibility and force equilibrium at junctions of these elements [(64)].

The advantages of this method are it is physically based, adapts to complex matrix geometry variations, and generally allows large element size than the finite difference method [(53)].

Chapter Four

Design Aspects

4.1. Introduction:

The following aspects are considered in design of horizontal well:

4.1.1. Selection of bits and casing sizes.

4.1.2. Detection of setting depths and drilling fluid densities.

4.1.3. Design of horizontal well profile.

4.1.4. Design of drillstring simulator (torque, drag, and buckling)

4.1.5. Design of hydraulic program.

4.1.6. Calculation of bit side force of rotary BHA (Analytical and numerical methods).

4.2. Selection of Bit and Casing Sizes:

The size of bit and casing string is controlled by necessary ID of the production casing and the number of intermediate casing strings required to reach the depth_objective. To enable the production casing to be placed in the well, the bit size used to drill the last interval of the well must be slightly larger than the OD of the casing connector. Also, the bit used to drill the lower portion of the well must fit inside the casing string above. This in turn determines the minimum size of the second –deepest casing string.

Table (4-1) provides commonly used bit sizes for drilling hole in which various API casing strings can be placed without getting the casing stack. While Table (4-2) provides ID's and drift diameters for various standard casing sizes and wall thickness. The pipe manufacturer assures that a bit smaller than the drift diameter will pass through every joint of casing bought [59].

Table 4-1: Commonly Used Bit Sizes For Running Casing [59].

Casing Size (OD in)	**Coupling Size** (OD in)	**Bit Sizes** (in)
4 1/2	5	6 , 6 1/8 , 6 1/4
5	5.563	6 1/2, 6 3/4
5 1/2	6.05	7 7/8, 8 3/4
6	6.625	7 7/8, 8 3/4, 8 1/2
6 5/8	7.39	8 1/2, 8 5/8, 8 3/4
7	7.656	8 5/8, 8 3/4, 9 1/2
7 5/8	8.5	9 7/8, 10 5/8, 11
8 5/8	9.625	11, 12 1/4
9 5/8	10.625	12 1/4, 14 3/4
10 3/4	11.75	15
13 3/8	14.375	17 1/2
16	17	20
20	21	24, 26

Table 4-2: Commonly Used Bit Sizes Pass through Casing [59].

Casing Size (O.D., in.)	Weight Per Foot (lbm/ft)	Internal Diameter (in.)	Drift Diameter (in.)	Commonly Used Bit Sizes (in.)
4½	9.5	4.09	3.965	3⅞
	10.5	4.052	3.927	
	11.6	4.000	3.875	
	13.5	3.920	3.795	3¾
5	11.5	4.560	4.435	4¼
	13.0	4.494	4.369	
	15.0	4.408	4.283	
	18.0	4.276	4.151	3⅞
5½	13.0	5.044	4.919	4¾
	14.0	5.012	4.887	
	15.5	4.950	4.825	
	17.0	4.892	4.764	
	20.0	4.778	4.653	4⅝
	23.0	4.670	4.545	4¼
6⅝	17.0	6.135	6.010	6
	20.0	6.049	5.924	5⅝
	24.0	5.921	5.796	
	28.0	5.791	5.666	
	32.0	5.675	5.550	4¾
7	17.00	6.538	6.413	6¼
	20.00	6.456	6.331	
	23.00	6.366	6.241	
	26.00	6.276	6.151	6⅛
	29.00	6.184	6.059	6
	32.00	6.094	5.969	
	35.00	6.006	5.879	
	38.00	5.920	5.795	5⅝
7⅝	20.00	7.125	7.000	6¾
	24.00	7.025	6.900	
	26.40	6.969	6.844	
	29.70	6.875	6.750	
	33.70	6.765	6.640	6½
	39.00	6.625	6.500	
8⅝	24.00	8.097	7.972	7⅞
	28.00	8.017	7.892	
	32.00	7.921	7.796	6¾
	36.00	7.825	7.700	
	40.00	7.725	7.600	
	44.00	7.625	7.500	
	49.00	7.511	7.386	
9⅝	29.30	9.063	8.907	8¾, 8½
	32.30	9.001	8.845	
	36.00	8.921	8.765	
	40.00	8.835	8.679	8⅝, 8½
	43.50	8.755	8.599	
	47.00	8.681	8.525	8½
	53.50	8.535	8.379	7⅞
10¾	32.75	10.192	10.036	9⅞
	40.50	10.050	9.894	
	45.50	9.950	9.794	9⅝
	51.00	9.850	9.694	
	55.00	9.760	9.604	
	60.70	9.660	9.504	8¾, 8½
	65.37	9.560	9.404	8¾, 8½
11¾	38.00	11.154	10.994	11
	42.00	11.084	10.928	10⅝
	47.00	11.000	10.844	
	54.00	10.880	10.724	
	60.00	10.772	10.616	
13⅜	48.00	12.715	12.559	12¼
	54.50	12.615	12.459	
	61.00	12.515	12.359	
	68.00	12.415	12.259	
	72.00	12.347	12.191	11
16	55.00	15.375	15.188	15
	65.00	15.250	15.062	
	75.00	15.125	14.939	14¾
	84.00	15.010	14.822	
	109.00	14.688	14.500	
18⅝	87.50	17.755	17.567	17½
20	94.00	19.124	18.936	17½

4.3. Detection of Setting Depths and Drilling Fluid Densities:

Setting depths of casing strings and densities of drilling fluid can be determined based on the data of pore and fracture pressure. Usually these data are plotted against the depth. A safety margin mud data are generated by adding 200 psi to pore pressure data. Once the setting depth of production casing is being known, an interpolation technique was applied between safety and fracture data to detect densities of drilling fluid and setting depths of casing strings.

A computer program called "bit sizes" was built to select bit and casing sizes, and to detect setting depths and fluid densities.

4.4. Design of Horizontal Well Profile:

The process of design well profile included calculation the dimensions of each section in the profile and kick-off point. Two profiles are considered in the design process which are:

4.4.1. Single Curve Design:

Figure (4-1) depicts the dimensions of single curve profile. The following equations are used to in the design of this profile:

$R = 5730 / BUR$ (4-1)

$V1 = R.(\sin I_2 - \sin I_1)$ (4-2)

$H1 = R.(\cos I_1 - \cos I_2)$ (4-3)

$L1 = 100.(I_2 - I_1)/BUR$ (4-4)

Where:

R: radius of curvature, ft

BUR: build- up rate, deg./100 ft

V1: vertical height of build section, ft

H1: horizontal displacement of build section, ft

L1: length of build-up section, ft

I_1: initial inclination angle, deg

I_2: final inclination angle, deg [3].

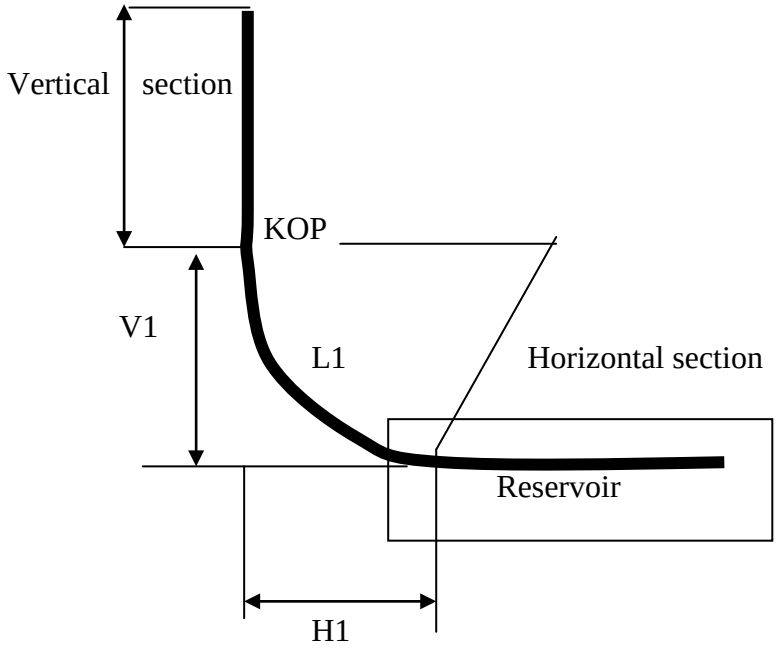

Figure 4-1: Single Curve Design [3].

4.4.2. Double build curve design:

Figure (4-2) depicts the dimension of build-tangent-build well profile. The following equations are used to design this type of well profile:

For upper build section:

$R1=5730/BUR1$ (4-5)

$V1=R.(SinI_2-SinI_1)$ (4-6)

$H1= R1.(CosI_1-CosI_2)$ (4-7)

$L1= 100.(I_2-I_1)/BUR1$ (4-8)

For tangent section:

$V2=L2.CosI_2$ (4-9)

$H2=L2.SinI_2$ (4-10)

For lower build section:

$R3=5730/BUR2$ (4-11)

$V3=R3.(SinI_3- SinI_2)$ (4-12)

$H3=R3.(CosI_2- CosI_3)$ (4-13)

$L3= 100.(I_3-I_2)/BUR2$ (4-14)

Where:

V2: vertical height of tangent,ft.

L2: length of tangent section, ft.

H2: horizontal displacement of tangent section, ft.

I_3: final build angle, usually 90 degrees.

V3: vertical height of second build-up section ,ft.

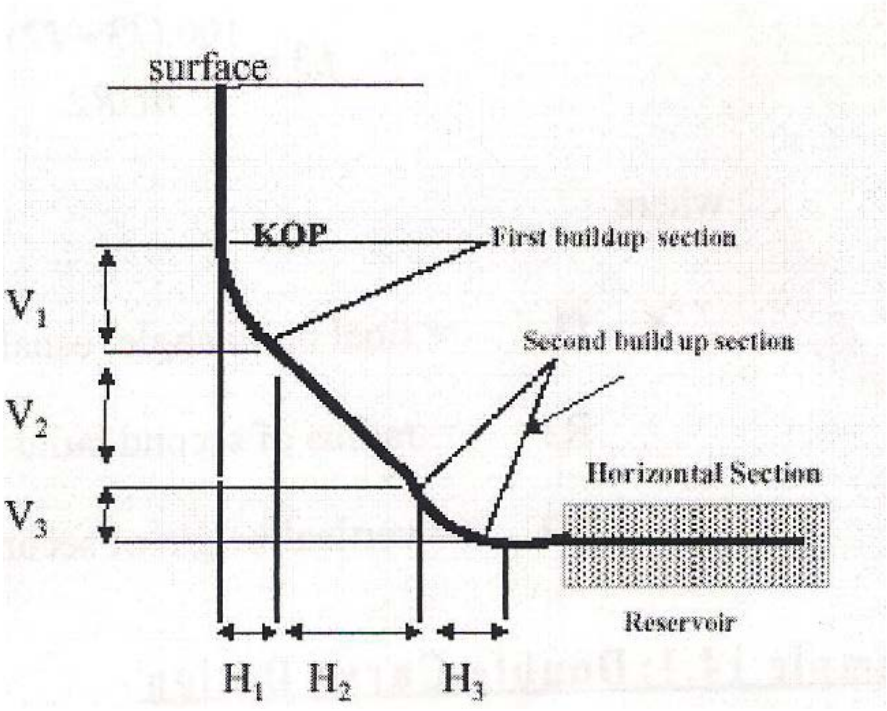

Figure 4-2: Double Curve Design[3].

4.5. Drillstring Simulator:

4.5.1.Torque and Drag:

The most commonly used torque / drag models are based on the "soft string" model developed by johancsisik et al (1983)[10]. The drillstring is modeled as a string or cable that is capable of carrying axial loads but not bending moments. Friction is the product of normal forces and a coefficient of friction. The normal force at each calculation node has two components, the buoyed weight of the pipe in the drilling fluid, and the lateral reaction force resulting from drillstring tension through curved sections of the wellbore. A simplified drillstring element, shown in Fig. (3-5) has net axial forces and normal forces acting upon it. The equations for these forces are:

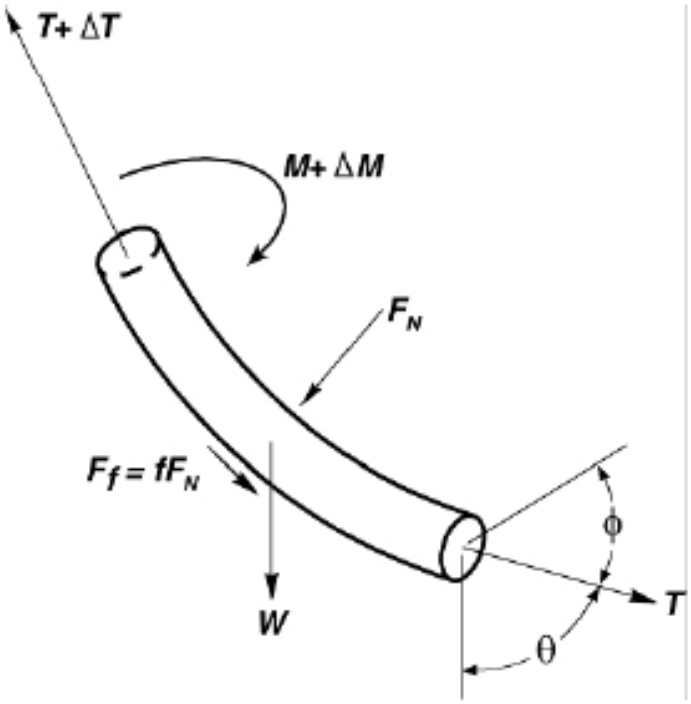

Figure 4-3: Drillstring Element For "Softstring" Torque-Drag Model [1].

$$F_N = [(T\,\Delta\varphi \sin\theta_{AVG})^2 + (T\,\Delta\theta + W \sin\theta_{AVG})^2] \qquad (4\text{-}15)$$

$$\Delta T = W \cos \theta_{AVG} \pm f F_N \quad (4\text{-}16)$$

$$\Delta M = f F_N r \quad (4\text{-}17)$$

$$F_f = f F_N \quad (4\text{-}18)$$

Where:

F_N:is the net normal force, lb_f.

T: axial tension at the lower end of the element, lb_f .

W: buoyed weight of drillstring element, lb_f.

F_f: sliding friction force acting on the element, lb_f.

r: characteristic radius of element, ft.

M: torsion at the lower end of element, ft-lb_f.

Θ: inclination angle at the lower end of element, degree.

Φ: azimuth angle at lower end of element, degree.

f: coefficient of friction.

ΔT: change of axial tension over the length of element, lb_f.

ΔM: change of torsion over the length of element, ft-lb_f.

Δθ: change of inclination angle over the length of element, degree.

ΔΦ: change of azimuth angle over the length of element, degree.

In equation (4-16), the product ($f F_N$) can be positive or negative, depending on whether the drillstring is advancing into the hole or being pulled out of the hole. In case of running into the hole, the sign will be negative and, in case of pulled of the hole the sign is positive.

Friction factors should be derived from analogous case histories. The properties of the drilling fluid used in the baseline wells and the planned well should be similar. However, in the case of new region or experience is unavailable , the ranges in the table (4-3) can be used in the calculations.

Table 4-3: Range of Friction Factors in Casing and Formation[65].

Drilling Fluid	*f* in casing	*f* in formation
Oil-based	0.16 to 0.20	0.17 to 0.25
Water-based	0.25 to 0.35	0.25 to 0.40
Brine	0.30 to 0.40	0.30 to 0.40

4.5.1.1. Operating Conditions:

When soft-string model is used to predict torque and drag of drillstring for different operating conditions, the following boundary conditions at bit are used:

1-Rotating off-Bottom:

WOB=0; TOB=0; f=rotating value

2-Slack-off without Rotation:

WOB=0; TOB=0; f=(-ve)

3- Pick-up without Rotation:

WOB=0; TOB=0; f=(+ve)

4- Drilling:

WOB=value; TOB=value; f=rotary value

5-Sliding:

WOB=value; TOB=TBHA; f=(-ve)

6-Pick-up with Rotation:

WOB=0; TOB=0; f=rotating value

7-Slack-off with Rotation:

WOB=0; TOB=0; f=rotating value

4.5.2. Buckling:

4.5.2.1.Sinusoidal Buckling:

Dawson and Pasalay (1984)[17] performed stability analysis to detect the maximum compressive load that can drill pipe carried without buckling the pipe. They simplified Paslay and Bogy(1964), equation which is:

$$F_{cir} = \frac{(1-\upsilon)^2 EI\pi^2}{(1+\upsilon)(1-\upsilon)L^2}\left(n^2 + \frac{L^4 \rho A_s g}{n^2 \pi^4 EIr}\right) \qquad (4\text{-}19)$$

This equation applies to a rod or pipe in a horizontal hole only. To generalize this equation to inclined holes, multiply the weight- per- length factor, ρAg, by sinθ. Also assume that Poisson's ratio, υ, is approximately 1/3, in which case the loading coefficient in Eq.(4-19), becomes 1.0. These changes give:

$$F_{cir} = EI\frac{\pi^2}{L^2}(n^2 + \frac{L^4 \rho A_s g \sin\phi}{n^2 \pi^4 EIr}) \qquad (4\text{-}20)$$

Equation (4-20), results from an eigen value problem where n is the number of buckles (or the order of buckling) that occur in a pipe length (L). The buckling of long lengths of pipe in inclined holes dos not start with the first order and then proceed to higher orders at increased loads. The first buckle that appears will have some higher order (n>1), depending on the pipe length. The buckle that first occurs is the one whose n gives the lowest value of F_{cirt} as calculated by Eq(4-20).

For fairly long rods, the simplest way to proceed is to ignore the fact that n takes on only integral values and to treat it as a continuous

variable. With that assumption the minimum value of F_{cirt} may be found by setting the derivative equal to zero. Thus:

$$\frac{\partial F_{cir}}{\partial n} = 0 \qquad (4\text{-}21)$$

Which is

$$\frac{\partial^2}{\partial n}\left(\frac{EI\pi^2}{L^2}\right)\left(n^2 + \frac{L^4 \rho A_s g \sin\phi}{n^2 \pi^4 EIr}\right) = 0 \qquad (4\text{-}22)$$

Or

$$2n = \frac{2L^4 \rho g A_s \sin\phi}{n^3 \pi^4 EIr} = 0 \qquad (4\text{-}23)$$

This gives

$$n^2 = \left(\frac{L^4 \rho g A_s \sin\phi}{\pi^4 EIr}\right)^{0.5} \qquad (4\text{-}24)$$

If this value of n^2 is substituted back into Eq(4-24) then considerable simplification results which is:

$$F_{cir} = 2\left(\frac{EI\rho A_s g \sin\phi}{r}\right)^{0.5} \qquad (4\text{-}25)$$

where:

F_{crit}: is the critical buckling force which is the minimum compressive force which results in the pipe buckling, lb_f.

E: Young's modulus, psi

I: moment of inertia of pipe,$in^4 = \pi(D_o^4 - D_i^4)/ 64$

A_s: cross- sectional area of pipe,in^2

g: gravitational force, lb_f .

ρ: weight per cubic inch, lb_m.

θ: hole angle, measured from vertical, deg.

υ: Poisson's ratio.

r: radial clearance between pipe and hole, in =(Dh-Odj)/2

n : order of buckling.

L: length of column, in.

4.5.2.2. Helical Buckling:

As the axial compressive force F is increased above F_{crit} , helical buckling eventually can occur in a horizontal hole. The bending strain energy (E_b) for the helix derived by Cheatham and Pattilo is:

$$E_b = \frac{8\pi^4 EILr^2}{\left(\frac{L}{n}\right)^4} \qquad (4\text{-}26)$$

And the external work (W_e) by force F during buckling is:

$$We = \frac{2FL\pi^2 r^2}{\left(\frac{L}{n}\right)^2} \qquad (4\text{-}27)$$

The change of potential energy (E_p) when the pipe moves from a straight configuration along the low side of the hole into a helix with center of gravity at the center of the hole is:

$$E_p = wLr \qquad (4\text{-}28)$$

Conservation of energy requires that the total energy, Et should be zero or:

$Et=W_e-E_b-E_p=0$ (4-29)

Substituting Eqs.(3-32),(3-33),(3-34)into Eq.(3-35) and solving for F^* yields:

$$F^* = 4EI\left(\frac{n\pi}{L}\right)^2 + \left(\frac{W}{2r}\right)\left(\frac{n\pi}{L}\right)^2 \quad (4\text{-}30)$$

For the minimum value of F^* for long pipe,$\partial F^*/\partial n=0$ yields

$$\left(\frac{n\pi}{L}\right)^2 = \left(\frac{\pi}{P}\right)^2 = \left(\frac{W}{8EIr}\right)^{0.5} \quad (4\text{-}31)$$

Substituting Eq.(4-30) into Eq.(4-31) gives:

$$F^* = 2.83\sqrt{\frac{EIW}{r}} \quad (4\text{-}32)$$

Where

F^*: is the minimum compressive force required to start helical buckling of pipe, lb_f

W: buoyed weight of pipe lb/in = $\rho g A_s$

4.5.3. Bending:

Bending forces arises when the drillpipe is run in highly deviated wells or in wells with severe dog-leg problem. There are many equations that related bending force and dog-leg severity. The simplest relation is the pure beam bending equation which is :

$$F_b = 64 DLS D_o W_c \quad (4\text{-}33)$$

Where:

F_b: bending force, lb_f.

D_o: outside diameter of pipe, in

W_c; weight of pipe in air lb/ft.

DLS: dog –leg severity,deg/ 100ft which can be obtained from the following equations:

$$\text{Cos}(C) = \cos(I_2 - I_1) - \sin I_1 \sin I_2 * (1 - \cos(A_2 - A_1)) \quad (4\text{-}34)$$

$$Dog - LegSeverity(DLS) = \frac{C}{100\,ft} \quad (4\text{-}35)$$

Where:

C: dog-leg angle, degree.

I_1,I_2: inclination angles of hole at station 1 and station 2,degree.

A_1,A_2: azimuth of hole at station 1and station 2,degree[59].

As shown in Fig (4-4), this equation assume that the wall of the pipe is fully contacts the wall of hole which is smooth and circular [57].

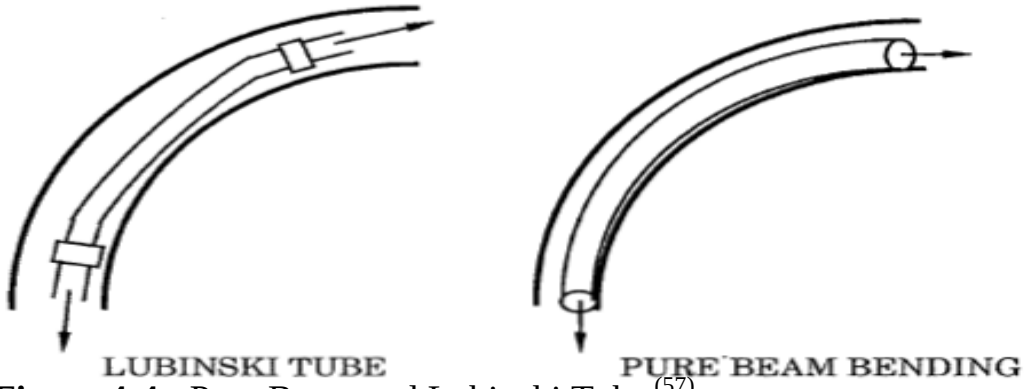

Figure 4-4: Pure Beam and Lubinski Tube [57].

When the drillstring is in contact with the borehole wall only at the connectors, the radius of curvature of the pipe is not constant as shown in Fig(4-4). In this case, the axial stress will be grater than that predicted by Eq.(3-41).Lubinski(1961)[30] applied the classical beam deflection theory to this case and derived the following equation for calculating maximum bending force, F_b:

$$F_b = 64DLSD_o W_c \frac{6KL_j}{\tanh\left(6KL_j\right)} \tag{4-36}$$

$$K = \sqrt{\frac{T_b}{EI}} \tag{4-37}$$

Where

T_b: buoyant weight suspended below the dog-leg,lb.

L_j:Half the distance between tool joints, in.

4.6. Hydraulic Program:

Hydraulic design included determination of pressure losses in the various parts of the circulating system and sizes of bit nozzles. Two models are used in the calculation which is Bingham plastic and power law model. The following are basic equations for each model.

4.6.1.Bingham Plastic Model:

-Plastic viscosity (PV):

$$PV = \theta_{600} - \theta_{300} \tag{4-38}$$

-Yield point (YP):

$$YP = 2\theta_{300} - \theta_{600} \tag{4-39}$$

- Surface connection losses (P_1)

$$P_1 = E_1 \rho^{0.8} Q^{1.8} (PV)^{0.2} \tag{4-40}$$

-Pipe flow (laminar flow):

$$v^{-} = \frac{24.5Q}{D_i^{\,2}} \tag{4-41}$$

$$P_2 = \frac{LPVv^{-}}{90000 D_i^{\,2}} + \frac{LYp}{225 D_i} \tag{4-42}$$

-Pipe flow (Turblent flow):

$$P_2 = \frac{8.91*10^{-5} \rho^{0.8} Q^{1.8} (PV)^{0.2} L}{D_i^{\,4.8}} \tag{4-43}$$

-Annular flow (laminar flow):

$$v^{-} = \frac{24.5Q}{D_h^{\ 2} - D_o^{\ 2}} \tag{4-44}$$

$$P_3 = \frac{LPVv^{-}}{60000(D_h - D_o)} + \frac{LYP}{200(D_h - Do)} \tag{4-45}$$

-Annular flow (turbulent flow):

$$P_3 = \frac{8.91*10^{-5}\rho^{0.8}Q^{1.8}(PV)^{0.2}L}{(D_h - Do)^3(D_h + Do)^{1.8\,h}} \tag{4-46}$$

-Pressure across the Bit:

$$P_{bit}=P_{standpipe}-(P_{dp}+P_{dc}+P_{adp}+P_{adc}) \tag{4-47}$$

-Nozzle velocity (V_n):

$$V_n = 33.36\sqrt{\frac{P_{bit}}{\rho}} \tag{4-48}$$

-Total area of nozzles (A_n):

$$A_n = 0.32\frac{Q}{V_n} \tag{4-49}$$

-Nozzles sizes in multiples of 32(d_n):

$$d_n = 32\sqrt{\frac{4A_n}{3\pi}} \tag{4-50}$$

4.6.2. Power law model:

-Flow behavior index, n:

$$n = 3.32\log\left(\frac{\theta_{600}}{\theta_{300}}\right) \tag{4-51}$$

-Consistency index, K:

$$K = \frac{\theta_{300}}{(511)^n} \tag{4-52}$$

- Surface connection losses (P_1)

$$P_1 = E_1 Q^{1.8} \rho^{0.8} (PV)^{0.2} \tag{4-53}$$

-Pipe flow (laminar flow):

$$P_2 = \frac{KL}{300 D_i}\left[\frac{1.6v^-}{D_i}\frac{(3n+1)}{4n}\right]^n \tag{4-54}$$

-Pipe flow(Turbulent flow):

$$P_2 = \frac{8.91*10^{-5}\rho^{0.8}Q^{1.8}(PV)^{0.2}L}{D_i^{4.8}} \tag{4-55}$$

-Annular flow (laminar flow):

$$P_3 = \frac{KL}{300(D_h - D_o)}\left[\frac{2.4v^-}{D_h - D_o}\frac{(2n+1)}{3n}\right]^n \tag{4-56}$$

-Annular flow (turbulent flow):

$$P_3 = \frac{8.91*10^{-5}\rho^{0.8}Q^{1.8}(PV)^{0.2}L}{(D_h - D_o)^3 (D_h + D_o)^{1.8\,h}} \tag{4-57}$$

4.7.Hole Cleaning:

B.Tarr( ) combined the critical velocity of slurry in horizontal annulus with slip velocity in vertical hole to calculate the critical velocity without settling of cutting. He presents the following equation:

$V_{ft}=V_s\cos(\theta)+V_2\sin(\theta)$ (4-58)

Where

V_{ft}: full transport annular velocity ,ft/m.

V_s: slip velocity of cutting, ft/m.

V_2: critical transport velocity of solid in horizontal annulus, ft/m.

$$V_2 = 44\left[\left(\frac{Sw-mw}{mw}\right)*g^3*\left(\frac{H-D}{12}\right)^3\right]^{1/6} \quad (4\text{-}59)$$

Where

Sw: cutting density, ppg.

mw: mud density, ppg.

H: hole diameter ,in.

g :gravity acceleration,ft/sec^2.

The slip velocity for transitional flow can be calculated from the following equation:

$$V_s = 175\frac{d_p(sw-mw)^{0.667}}{mw^{0.333}\mu_e{}^{0.333}} \quad (4\text{-}60)$$

Where

V_s: particle slip velocity, ft/m.

D_p: Particle diameter, in.

$\mu_{e:}$ effective viscosity,cp.

While the slip velocity for turbulent flow can be calculated from the equation:

$$V_s = 113.4\left[\frac{Dp(sw-mw)}{1.5mw}\right]^{0.5}$$

In field design,the largest value of two flow is taken for worst case.

4.8. Bit Side Force Calculation:

The bit side force for rotary bottom hole which is detected the inclination tendency of the assembly was calculated with the following methods:

4.8.1 Analytical Method(Jiazhi's Method):

4.8.1.1. Slick BHA:

Figure (4-5) depicts slick BHA (bit+drillcollar) without applied axial weight(a) and with applied axial weight (b). For case (a),F_B can be determined from the following equation:

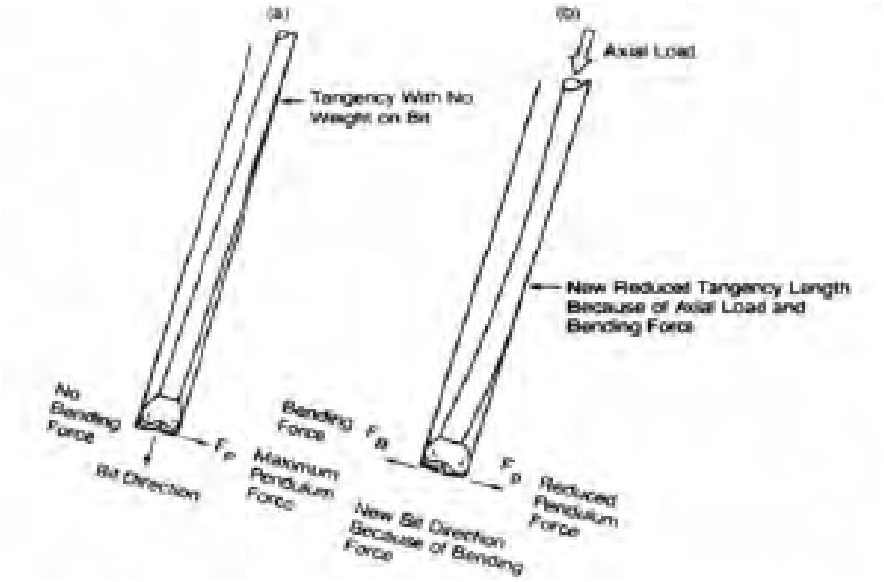

Figure 4-5: Slick BHA (a) without WOB (b) with WOB [58].

$$F_B = -0.5 * W_c * B_c * L_T * \sin(\alpha) \quad (4\text{-}62)$$

Where:

F_B: bit side force , lb_f

W_c: weight of pipe in air, lb_m/ft.

L_T: length of BHA between the bit and first point of tangency, ft.

B_c: buoyancy correction factor, dimensionless.

$B_c=(1- W_m/W_c)$

Where

W_m: weight of drilling fluid ,lb/ft^3.

α: inclination angle, deg.

If the axial weight on bit is applied as in case (b), a positive bending force must be considered. Jiazhi[40] present the following equation to calculate bit side force:

$$F_B= -0.5*W_c*B_c*L_T*\sin(\alpha)+ (WOB- 0.5*W_c*B_c*L_T*\cos(\alpha))*\ell/L_T \quad (4\text{-}63)$$

Where:

WOB: weight on bit, lb_f.

ℓ : clearance radius of drillcollar, ft.

ℓ= 0.5*(db-ddc)

db:bit diameter ,in

ddc: outside diameter of collar, in.

For Jiashi's solution one must guess the tangency length L_T. the guess should be compared with the calculated tangency length from the following equation:

$$L_T^{\,4} = \frac{24EI\ell}{W_c B_c \sin(\alpha) X} \quad (4\text{-}64)$$

Where X is a transcendental function given by following Equation:

$$X = \frac{3(\tan u - u)}{u^3} \quad (4\text{-}65)$$

Where u is in radian and given by:

$$u = \frac{L_T}{2}\left(\frac{P_c}{EI}\right)^{0.5} \quad (4\text{-}66)$$

Where:

E: modulus of elasticity,lb/ft^2

I: moment of inertia,ft^4

P_c: compressive load on drill collar,lb_f

The compressive load on the drill collar P_c can be determined by:

$$P_c = WOB - 0.5 W_c B_c L_T \cos(\alpha) \quad (4\text{-}67)$$

4.8.1.2. Single Stabilizer BHA:

Figure (4-6) shows BHA with one stabilizer. Jiazhi[40] present the following equation to calculate bit side force:

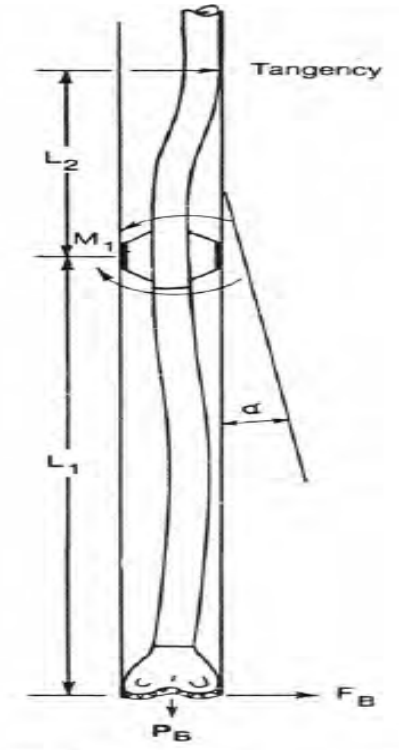

Figure 4-6: Single Stabilizer Bottom Hole Assembly [58].

$$F_B = -0.5 B_c W_c L_1 \sin(\alpha) + \frac{P_{c1}\ell_1}{L_1} - \frac{m}{L_1} \quad (4\text{-}68)$$

Where

L_1: distance from bit to stabilizer, ft.

m : bending moment, ft-lb.

P_{c1}: the compressive load of first section, lb_f.

ℓ_1: clearance of the stabilizer, ft.

ℓ_2: clearance of drill collar, ft.

The following equations are used to calculate the above parameters:

$$\ell_1 = 0.5(db - ds) \quad (4\text{-}69)$$

$$\ell_2 = 0.5(db - dc) \quad (4\text{-}70)$$

$$P_{c1} = WOB - \left[\frac{L_1 W_{c1} B_c \cos(\alpha)}{2}\right] \quad (4\text{-}71)$$

$$P_{c2} = WOB - \{[(W_{c1} B_c L_1) + (0.5 W_{c2} B_c L_2)]\cos(\alpha)\} \quad (4\text{-}72)$$

The tangency length is calculated from the following equation:

$$L_T^{\,4} = \frac{24 E I_2 (\ell_2 - \ell_1)}{q_2 x_2} - \frac{4 m_1 L_T^{\,2} W_2}{q_2 x_2} \quad (4\text{-}73)$$

The bending moment, m1 is calculated from the relationship:

$$2m_1\left(V_1 + \frac{L_2 I_1 V_2}{L_1 I_2}\right) = -\frac{q_1 L_1^{\,2} x_1}{4} - \frac{q_2 L_2^{\,3} I_1 x_2}{4 L_1 L_2} + \frac{6 E I_1 \ell_1}{L_1^{\,2}} + \frac{6 E I_1 (\ell_1 - \ell_2)}{L_1 L_2} \quad (4\text{-}74)$$

Where

$$q_1=W_{c1}B_cSin(\alpha) \quad (4\text{-}75)$$

$$q_2=W_{c2}B_cSin(\alpha) \quad (4\text{-}76)$$

Where

W_{c1} : the weight of drill collars from bit to stabilizers.

W_{c2} : the weight of drill collars from stabilizers to the point of tangency.

The coefficients W_i and V_i can be calculated from the following equations:

$$W_i = \frac{3}{u_i}\left(\frac{1}{\sin(2u_i)} - \frac{1}{2u_2}\right) \quad (4\text{-}77)$$

$$V_i = \frac{3}{2u_i}\left(\frac{1}{2u_i} - \frac{1}{\tan(2u_i)}\right) \quad (4\text{-}78)$$

Where i=1 or 2

The coefficients x_i and u_i are determined from the following equations:

$$x_i = \frac{3[\tan(u_i) - u_i]}{u^3{}_i} \quad (4\text{-}79)$$

$$u_i = \frac{L_i}{2}\left(\frac{P_{ci}}{EI_i}\right)^{0.5} \quad (4\text{-}80)$$

4.8.1.3. Two Stabilizers BHA:

Figure(4-7) depicts a typical two stabilizer building assembly where L_1 and L_2 are known lengths between the bit and first stabilizer

and between the first and second stabilizer. The distance L_3 between the second stabilizer and the point of tangency is unknown and must be estimated initially.

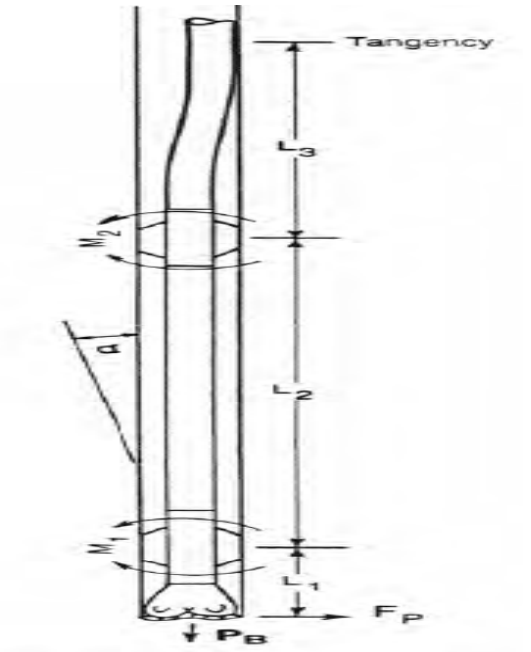

Figure 4-7: Two Stabilizer Bottom Hole Assembly [58].

The clearance between the stabilizers and the wellbore and the last collar and the wellbore are given by:

$$\ell_1 = 0.5(db - ds_1)/12 \tag{4-81}$$

$$\ell_2 = 0.5(db - ds_2)/12 \tag{4-82}$$

$$\ell_3 = 0.5(db - dc)/12 \tag{4-83}$$

The bit side force can be calculated from the following relationship:

$$F_B = -0.5W_c B_c L_1 \sin(\alpha) + P_{c1}\ell_1 / L_1 - m_1 / L_1 \quad (4\text{-}84)$$

The calculated tangency length is estimated from the below equation:

$$L_T{}^4 = \frac{24EI_3(\ell_3 - \ell_2)}{q_3 x_3} - \frac{4m_2 L_3{}^2 W_3}{q_3 x_3} \quad (4\text{-}85)$$

$$q_{ii} = W_c B_c \sin(\alpha) \quad (4\text{-}86)$$

Where i=1,2,or 3.

The above equation required the value of bending moment about the second stabilizer m_2 which can be found by assuming L_3 and calculating m_1 and m_2 from following equations:

$$2m_1\left(V_1 + \frac{L_2 I_1 V_2}{L_1 I_2}\right) + m_2 \frac{L_2 I_1 W_2}{L_1 I_2} = -\frac{q_1 L_1{}^2 x_1}{4} - \frac{q_2 L_2{}^3 I_1 x_2}{4 L_1 I_2} + \frac{6EI_1\ell_1}{L^2{}_1} + \frac{6EI_1(\ell_1 - \ell_2)}{L_1{}^2} \quad (4\text{-}87)$$

$$m_1 W_2 + 2m_2\left(V_2 + \frac{L_3 I_2 V_3}{L_2 I_3}\right) = -\frac{q_2 L_2{}^2 x_2}{4} - \frac{q_3 L_3{}^3 I_2}{4 L_2 I_3} - \frac{6EI_2(\ell_1 - \ell_2)}{L_2{}^2} - \frac{6EI_2(\ell_3 - \ell_2)}{L_2 L_3} \quad (4\text{-}88)$$

Where X_i,W_i, and V_i can be calculated from the following equations:

$$x_i = \frac{3[\tan(u_i) - (u)_i]}{u_i{}^3} \quad (4\text{-}89)$$

$$W_i = \frac{3}{u_i}\left[\frac{1}{\sin(2u_i)} - \frac{1}{(2u_i)}\right] \quad (4\text{-}90)$$

$$V_i = \frac{3}{2u_i}\left[\frac{1}{2u_i} - \frac{1}{\tan(2u_i)}\right] \quad (4\text{-}91)$$

$$u_i = \frac{L_i}{2}\left[\left(P_{ci} / EI_i\right)^{0.5}\right] \tag{4-92}$$

$$P_2 = WOB - \left\{\left[\left(W_{c1}B_cL_1\right) + 0.5W_{c2}L_2\right]\cos(\alpha)\right\} \tag{4-93}$$

$$P_3 = WOB - \left\{\left[\left(W_{c1}B_cL_1\right) + \left(W_{c2}B_cL_2\right) + \left(0.5W_{c3}L_3\right)\right]\cos(\alpha)\right\} \tag{4-94}$$

A computer program was written to calculate bit side force for these three types of bottom hole assemblies.

4.8.2.Finite Element Method:

For the displacement method of analysis, The potential energy (π) of finite –element system (BHA) is the system strain energy minus the work done by the concentrated forces and moments applied at the nodes. In matrix form this can be expressed as

$$\Pi\pi = \frac{1}{2}s^{\rightarrow T}\left\|K\right\|s^{\rightarrow} - s^{\rightarrow T}F^{\rightarrow} \tag{4-95}$$

Where

$s^{\rightarrow}$: nodal displacement vector.

$s^{\rightarrow T}$: transpose of nodal-displacement vector

$\|K\|$: stiffness matrix of finite element assembly

$F^{\rightarrow}$: applied nodal force vector

To guarantee equilibrium of the finite element BHA , it is necessary that:

$$\frac{\partial\pi}{\partial s^{\rightarrow}} = \mathbf{0} \tag{4-96}$$

Applying the equilibrium condition on Equation 1 will result in:

$$\|K\ \|s^{\rightarrow} - F = 0^{\rightarrow} \tag{4-97}$$

Or as

$$F^{\rightarrow} = \|K\ \|s^{\rightarrow} \tag{4-98}$$

Equation (4-95) is the force displacement relation of the system which is constructed from assembly of force displacement relationships for an element "e"of the form:

$$F^{\rightarrow e} = \|K^{e}\ \|s^{\rightarrow e} \tag{4-99}$$

The force displacement relation (Equation (4-99)) is generated for each element and the master stiffness matrix is assembled to formulate the mathematical relations for external forces acting at any node.

4.8.2.1. Stiffness Matrix of BHA-Three Dimensions:

Consider certain length of BHA composed of number of beam elements. Figure (4-8) depicts three dimension straight a BHA element of circular cross section with two end nodes. The x-axis (longitudinal axis) passes through the centeroid of the BHA cross section. The y and z axes are the principal axes for area moments of inertia of the cross section. Each node was loaded by six external forces which are axial, bending, shear, and three moment forces. The components of the applied nodal forces vector can be written as:

$$F^{\rightarrow T} = \lfloor F_x F_y F_z M_x M_y M_z \rfloor \tag{4-100}$$

Where

F_x,F_y,F_z: forces acting along x,y, and z axes .

M_x,M_y,M_z: moments about x,y, and z axes.

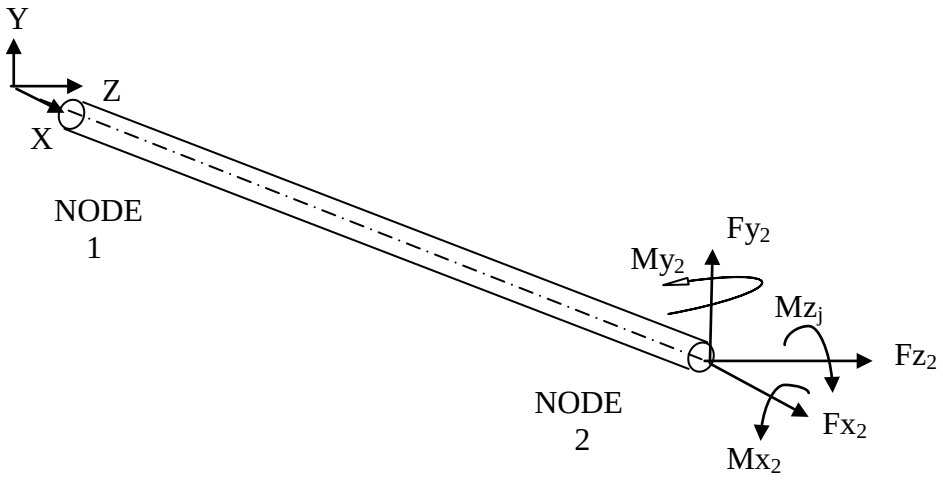

Figure 4-8: Nodal Force Components of BHA Element.

Owing to the applied external load vector, six components of nodal displacements (six degree of freedom) was possessed as shown in figure (4-9). The component of nodal displacements vector can be written as:

$$S^{\rightarrow T} = \left[\Delta_x \Delta_y \Delta_z \theta_x \theta_y \theta_z\right] \quad (4\text{-}101)$$

Where

Δ_x,Δ_y,Δ_z: Nodal displacements in x,y,and z axes.

Θ_x,θ_y,θ_z: Rotational displacements about x,y,and z axes.

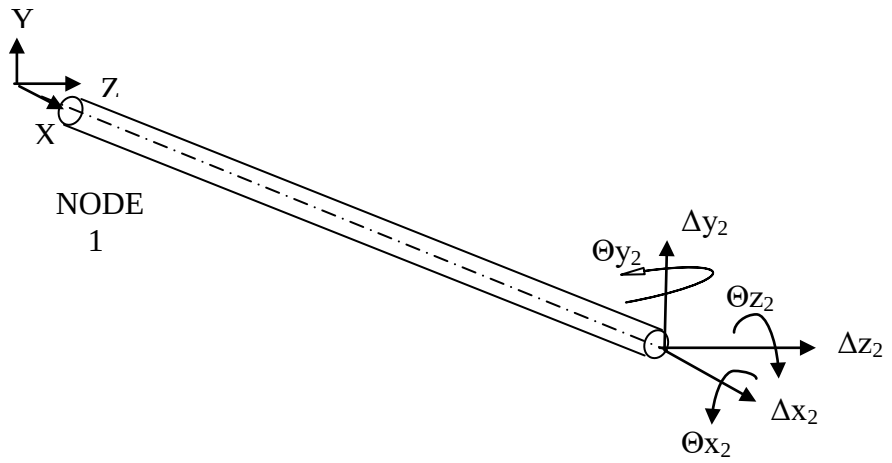

Figure 4-9: Nodal Displacements of BHA Element.

The stiffness matrix of BHA element in three dimension will be composed of stiffness matrix in x-y plane $[K_{bending}]_{xy}$,stiffness matrix in x-z plane$[K_{bending}]_{xz}$, axial matrix$[K_{axial}]$,and torsional matrix$[K_{torsional}]$. In matrix form this can be expressed as:

$$\|K^e\| = \begin{bmatrix} [k_{axial}] & [0] & [0] & [0] \\ [0] & [k_{bending}]_{xy} & [0] & [0] \\ [0] & [0] & [k_{bending}]_{xz} & [0] \\ [0] & [0] & [0] & [k_{torsion}] \end{bmatrix} \quad (4\text{-}102)$$

4.8.2.1.A. Bending Stiffness Matrix$[K_{bending}]_{xy}$:

In this case, the plane of bending is xy and the rotation will about z-axis. The BHA element is loaded at the two nodes by forces which transverse to the axis of element(x-direction) as shown in figure (4-10). These forces caused transverse displacements ν and rotational θ(slop) displacements at each node(two degree of freedom).

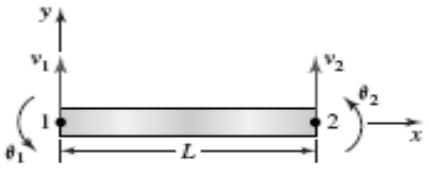

Figure 4-10: Nodal Displacements in xy Plane [62].

In this case the displacement function ν(x) is to be discretized such that

$$v(x) = f(v_1, v_2, \theta_1, \theta_2, x) \quad (4\text{-}103)$$

Subject to the boundary conditions

$$v(x = x_1) = v_1 \tag{4-104}$$

$$v(x = x_2) = v_2 \tag{4-105}$$

$$\left.\frac{dv}{dx}\right|_{x=x_1} = \theta_1 \tag{4-106}$$

$$\left.\frac{dv}{dx}\right|_{x=x_2} = \theta_2 \tag{4-107}$$

Considering the four boundary conditions and one dimensional problem, the displacement function will take the form:

$$v(x) = a_0 + a_1 x + a_2 x^2 + a_3 x^3 \tag{4-108}$$

Application of boundary conditions will yield:

$$v(x = 0) = v_1 = a_0 \tag{4-109}$$

$$v(x = L) = v_2 = a_0 + a_1 L + a_2 L^2 + a_3 L^3 \tag{4-110}$$

$$\left.\frac{dv}{dx}\right|_{x=0} = \theta_1 = a_1 \tag{4-111}$$

$$\left.\frac{dv}{dx}\right|_{x=L} = \theta_2 = a_1 + 2a_2 L + 3a_3 L^2 \tag{4-112}$$

Equations (4-106) to(4-109) are solved simultaneously to obtain the coefficients in terms of the nodal variables as:

$$a_0 = v_1 \tag{4-113}$$

$$a_1 = \theta_1 \tag{4-114}$$

$$a_2 = \frac{3}{L^2}(v_2 - v_1) - \frac{1}{L}(2\theta_1 + \theta_2) \tag{4-115}$$

$$a_3 = \frac{2}{L^3}(v_1 - v_2) + \frac{1}{L^2}(\theta_1 + \theta_2) \tag{4-116}$$

Substituting Equations (4-110)–(4-113) into Equation (4-105) and collecting the coefficients of the nodal variables results in the expression

$$v(x) = \left(1 - \frac{3x^2}{L^2} + \frac{2x^3}{L^3}\right)v_1 + \left(x - \frac{2x^2}{L} + \frac{x^3}{L^2}\right)\theta_1 + \left(\frac{3x^2}{L^2} - \frac{2x^3}{L^3}\right)v_2 + \left(\frac{x^3}{L^2} - \frac{x^2}{L}\right)\theta_2 \quad (4\text{-}117)$$

Which is the form

$$v(x) = N_1(x)v_1 + N_2(x)\theta_1 + N_3(x)v_2 + N_4(x)\theta_2 \quad (4\text{-}118)$$

Or in matrix notation,

$$v(x) = [N_1 \quad N_2 \quad N_3 \quad N_4]\begin{Bmatrix} v_1 \\ \theta_1 \\ v_2 \\ \theta_2 \end{Bmatrix} = [N]\{\delta\} \quad (4\text{-}119)$$

Where *N*1, *N*2, *N*3, and *N*4 are the interpolation functions that describe the distribution of displacement in terms of nodal values in the nodal displacement vector {_}.

The total strain energy is expressed as:

$$U_e = \frac{1}{2}\int_V \sigma_x \varepsilon_x \, dV \quad (4\text{-}120)$$

Where V is the total volume of the BHA element ,$\varepsilon_x$is the normal strain in direction x as result of bending, σ_x is the corresponding stress and they can express as:

$$\varepsilon_x = -y\frac{d^2v}{dx^2} \quad (4\text{-}121)$$

$$\sigma_x = E\varepsilon_x = -Ey\frac{d^2v}{dx^2} \quad (4\text{-}122)$$

Substituting the stress and strain equations into strain energy equation yield;

$$U_e = \frac{E}{2}\int_V y^2\left(\frac{d^2v}{dx^2}\right)^2 dV \qquad (4\text{-}123)$$

This can be written as

$$U_e = \frac{E}{2}\int_0^L \left(\frac{d^2v}{dx^2}\right)^2 \left(\int_A y^2\, dA\right) dx \qquad (4\text{-}124)$$

Since the area integral in above relation is the moment of inertia I_z about the centroidal axis perpendicular to the plane of bending, we have

$$U_e = \frac{EI_z}{2}\int_0^L \left(\frac{d^2v}{dx^2}\right)^2 dx \qquad (4\text{-}125)$$

For the strain energy of the finite element, substitute the discretized displacement relation of equation 4.27 to obtain

$$U_e = \frac{EI_z}{2}\int_0^L \left(\frac{d^2N_1}{dx^2}v_1 + \frac{d^2N_2}{dx^2}\theta_1 + \frac{d^2N_3}{dx^2}v_2 + \frac{d^2N_4}{dx^2}\theta_2\right)^2 dx \qquad (4\text{-}126)$$

Applying the first theorem of Castigliano to strain energy equation with respect to the nodal displacement v_1 gives the transverse force at node 1 as:

$$\frac{\partial U_e}{\partial v_1} = F_1 = EI_z\int_0^L \left(\frac{d^2N_1}{dx^2}v_1 + \frac{d^2N_2}{dx^2}\theta_1 + \frac{d^2N_3}{dx^2}v_2 + \frac{d^2N_4}{dx^2}\theta_2\right)\frac{d^2N_1}{dx^2}\, dx \qquad (4\text{-}127)$$

While application with respect to the rotational displacement give the moment as:

$$\frac{\partial U_e}{\partial \theta_1} = M_1 = EI_z \int_0^L \left(\frac{d^2N_1}{dx^2} v_1 + \frac{d^2N_2}{dx^2} \theta_1 + \frac{d^2N_3}{dx^2} v_2 + \frac{d^2N_4}{dx^2} \theta_2 \right) \frac{d^2N_2}{dx^2} dx \qquad (4\text{-}128)$$

For node 2, the result is:

$$\frac{\partial U_e}{\partial v_2} = F_2 = EI_z \int_0^L \left(\frac{d^2N_1}{dx^2} v_1 + \frac{d^2N_2}{dx^2} \theta_1 + \frac{d^2N_3}{dx^2} v_2 + \frac{d^2N_4}{dx^2} \theta_2 \right) \frac{d^2N_3}{dx^2} dx \qquad (4\text{-}129)$$

$$\frac{\partial U_e}{\partial \theta_2} = M_2 = EI_z \int_0^L \left(\frac{d^2N_1}{dx^2} v_1 + \frac{d^2N_2}{dx^2} \theta_1 + \frac{d^2N_3}{dx^2} v_2 + \frac{d^2N_4}{dx^2} \theta_2 \right) \frac{d^2N_4}{dx^2} dx \qquad (4\text{-}130)$$

The above four equations which related the nodal displacement values to applied nodal forces can be written in matrix form as:

$$\begin{bmatrix} k_{11} & k_{12} & k_{13} & k_{14} \\ k_{21} & k_{22} & k_{23} & k_{24} \\ k_{31} & k_{32} & k_{33} & k_{34} \\ k_{41} & k_{42} & k_{43} & k_{44} \end{bmatrix} \begin{Bmatrix} v_1 \\ \theta_1 \\ v_2 \\ \theta_2 \end{Bmatrix} = \begin{Bmatrix} F_1 \\ M_1 \\ F_2 \\ M_2 \end{Bmatrix} \qquad (4\text{-}131)$$

Where K_{mn},m,n=1,4 are the coefficient of the element stiffness matrix. By comparison of Equations 4.40–4.43 with the algebraic equations represented by matrix Equation 4.44, it is seen that

$$k_{mn} = k_{nm} = EI_z \int_0^L \frac{d^2N_m}{dx^2} \frac{d^2N_n}{dx^2} dx \qquad m, n = 1, 4 \qquad (4\text{-}132)$$

And the stiffness matrix is symmetric as expected for a linearly elastic element.

Converting the integration to the dimensionless length variable ξ=x/L by noting

$$\int_0^L f(x)\,\mathrm{d}x = \int_0^1 f(\xi)L\,\mathrm{d}\xi \tag{4-133}$$

$$\frac{\mathrm{d}}{\mathrm{d}x} = \frac{1}{L}\frac{\mathrm{d}}{\mathrm{d}\xi} \tag{4-134}$$

Thus the integration equation 4.45 become

$$k_{mn} = k_{nm} = EI_z \int_0^L \frac{\mathrm{d}^2N_m}{\mathrm{d}x^2}\frac{\mathrm{d}^2N_n}{\mathrm{d}x^2}\,\mathrm{d}x = \frac{EI_z}{L^3}\int_0^1 \frac{\mathrm{d}^2N_m}{\mathrm{d}\xi^2}\frac{\mathrm{d}^2N_n}{\mathrm{d}\xi^2}\,\mathrm{d}\xi \qquad m,n = 1,4 \tag{4-135}$$

The stiffness coefficients are evaluated as follows:

$$k_{11} = \frac{EI_z}{L^3}\int_0^1 (12\xi - 6)^2\,\mathrm{d}\xi = \frac{36EI_z}{L^3}\int_0^1 (4\xi^2 - 4\xi + 1)\,\mathrm{d}\xi$$

$$= \frac{36EI_z}{L^3}\left(\frac{4}{3} - 2 + 1\right) = \frac{12EI_z}{L^3}$$

$$k_{12} = k_{21} = \frac{EI_z}{L^3}\int_0^1 (12\xi - 6)(6\xi - 4)L\,\mathrm{d}\xi = \frac{6EI_z}{L^2}$$

$$k_{13} = k_{31} = \frac{EI_z}{L^3}\int_0^1 (12\xi - 6)(6 - 12\xi)\,\mathrm{d}\xi = -\frac{12EI_z}{L^3}$$

$$k_{14} = k_{41} = \frac{EI_z}{L^3}\int_0^1 (12\xi - 6)(6\xi - 2)L\,\mathrm{d}\xi = \frac{6EI_z}{L^2}$$

Continuing the direct integration gives the remaining stiffness coefficients as:

$$k_{22} = \frac{4EI_z}{L}$$

$$k_{23} = k_{32} = -\frac{6EI_z}{L^2}$$

$$k_{24} = k_{42} = \frac{2EI_z}{L}$$

$$k_{33} = \frac{12EI_z}{L^3}$$

$$k_{34} = k_{43} = -\frac{6EI_z}{L^3}$$

$$k_{44} = \frac{4EI_z}{L}$$

The complete stiffness matrix of the BHA element for plane of bending xy is written as:

$$[k_e] = \frac{EI_z}{L^3}\begin{bmatrix} 12 & 6L & -12 & 6L \\ 6L & 4L^2 & -6L & 2L^2 \\ -12 & -6L & 12 & -6L \\ 6L & 2L^2 & -6L & 4L^2 \end{bmatrix} \quad (4\text{-}136)$$

4.8.2.1.B. Axial Stiffness Matrix [K_{axial}] :

Suppose a BHA element subjected to transverse and axial loading at each two end nodes as depicted in the figure (4-11). At each node there are transverse, axial, and rotational displacement components (three degree of freedom), which means six displacement components for the BHA element.

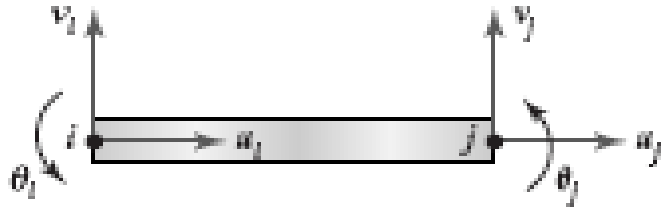

Figure 4-11: BHA Element with Transverse and Axial Displacements [62].

In this case of loading, stiffness matrix of BHA element will be combination of bar axial matrix and bending stiffness matrix. The bar axial matrix in one dimension can be written as follows:

$$[K_{axial}]= \frac{AE}{L}\begin{bmatrix} 1 & -1 \\ -1 & 1 \end{bmatrix} \qquad (4\text{-}137)$$

In two dimensions, the axial matrix can be written as:

$$[K_{axial}]=\begin{bmatrix} \frac{AE}{L} & -\frac{AE}{L} & 0 & 0 & 0 & 0 \\ -\frac{AE}{L} & \frac{AE}{L} & 0 & 0 & 0 & 0 \\ 0 & 0 & 0 & 0 & 0 & 0 \\ 0 & 0 & 0 & 0 & 0 & 0 \\ 0 & 0 & 0 & 0 & 0 & 0 \\ 0 & 0 & 0 & 0 & 0 & 0 \end{bmatrix} \qquad (4\text{-}138)$$

By addition the bar axial matrix to the bending stiffness matrix (plane xy) ,the stiffness matrix of BHA element with axial loading will be:

$$[k_e] = \begin{bmatrix} \frac{AE}{L} & \frac{-AE}{L} & 0 & 0 & 0 & 0 \\ \frac{-AE}{L} & \frac{AE}{L} & 0 & 0 & 0 & 0 \\ 0 & 0 & \frac{12EI_z}{L^3} & \frac{6EI_z}{L^2} & \frac{-12EI_z}{L^3} & \frac{6EI_z}{L^2} \\ 0 & 0 & \frac{6EI_z}{L^2} & \frac{4EI_z}{L} & \frac{-6EI_z}{L^2} & \frac{2EI_z}{L} \\ 0 & 0 & \frac{-12EI_z}{L^3} & \frac{-6EI_z}{L^2} & \frac{12EI_z}{L^3} & \frac{-6EI_z}{L^2} \\ 0 & 0 & \frac{6EI_z}{L^2} & \frac{2EI_z}{L} & \frac{-6EI_z}{L^2} & \frac{4EI_z}{L} \end{bmatrix} \quad (4\text{-}139)$$

Where Equation (4-139) represents the stiffness matrix of BHA element in two dimensions.

4.8.2.1.C.Bending Stiffness Matrix $[K_{bending}]_{xz}$:

In this case, the plane of bending is xz plane and the rotation will be about y axis. Nodal displacements in the z-direction are denoted w_1 and w_2 while nodal rotations are θ_{y1} and θ_{y2} as shown in figure (4-12).

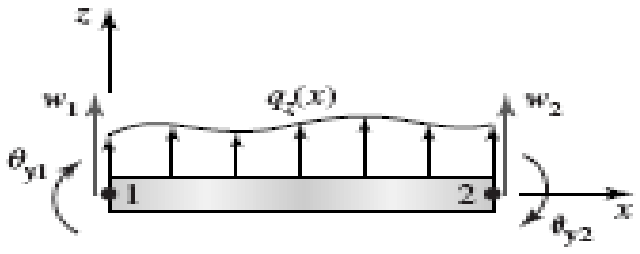

Figure 4-12: Nodal displacements in xz plane.

By following the same pervious steps of derivation, the BHA element stiffness matrix in xz plane will be:

$$[k_e]_{xz} = \frac{EI_y}{L^3} \begin{bmatrix} 12 & -6L & -12 & -6L \\ -6L & 4L^2 & 6L & 2L^2 \\ -12 & 6L & 12 & 6L \\ -6L & 2L^2 & 6L & 4L^2 \end{bmatrix} \quad (4\text{-}140)$$

By combining the bar element axial matrix, the xy plane stiffness matrix, and the xz plane stiffness matrix , the BHA element equilibrium equations for two-plane bending with axial stiffness are written in matrix form as:

$$\begin{bmatrix} [k_{\text{axial}}] & [0] & [0] \\ [0] & [k_{\text{bending}}]_{xy} & [0] \\ [0] & [0] & [k_{\text{bending}}]_{xz} \end{bmatrix} \begin{Bmatrix} u_1 \\ u_2 \\ v_1 \\ \theta_{z1} \\ v_2 \\ \theta_{z2} \\ w_1 \\ \theta_{y1} \\ w_2 \\ \theta_{y2} \end{Bmatrix} = \begin{Bmatrix} f_{x1} \\ f_{x2} \\ f_{y1} \\ M_{z1} \\ f_{y2} \\ M_{z2} \\ f_{z1} \\ M_{y1} \\ f_{z2} \\ M_{y2} \end{Bmatrix} \tag{4-141}$$

Where the 10× 10 BHA element stiffness matrix has been written in the shorthand form:

$$[k_e] = \begin{bmatrix} [k_{\text{axial}}] & [0] & [0] \\ [0] & [k_{\text{bending}}]_{xy} & [0] \\ [0] & [0] & [k_{\text{bending}}]_{xz} \end{bmatrix} \tag{4-142}$$

When the element coordinate (local coordinate) is oriented at an arbitrary angle (ψ) from the global coordinate as in figure (4.13), the nodal displacement must convert to global coordinate.

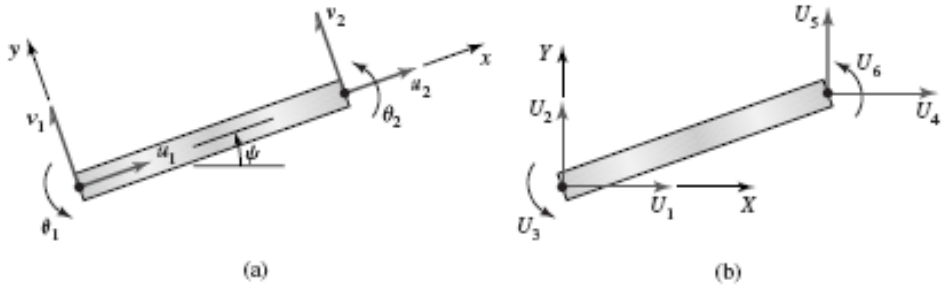

Figure 4-13: (a) Nodal displacements in the element coordinate system.(b)Nodal displacements in global coordinate system[62].

Using figure (4.13) the element displacements are written in terms of the global displacements as:

$$\begin{aligned} u_1 &= U_1\cos(\psi) + U_2\sin(\psi) \\ v_1 &= -U_1\sin(\psi) + U_2\cos(\psi) \\ \theta_1 &= U_3 \\ u_2 &= U_4\cos(\psi) + U_5\sin(\psi) \\ v_2 &= -U_4\sin(\psi) + U_5\cos(\psi) \\ \theta_2 &= U_6 \end{aligned} \tag{4-143}$$

Equations (4.143) can be written in matrix form as:

$$\begin{Bmatrix} u_1 \\ v_1 \\ \theta_1 \\ u_2 \\ v_2 \\ \theta_2 \end{Bmatrix} = \begin{bmatrix} \cos\psi & \sin\psi & 0 & 0 & 0 & 0 \\ -\sin\psi & \cos\psi & 0 & 0 & 0 & 0 \\ 0 & 0 & 1 & 0 & 0 & 0 \\ 0 & 0 & 0 & \cos\psi & \sin\psi & 0 \\ 0 & 0 & 0 & -\sin\psi & \cos\psi & 0 \\ 0 & 0 & 0 & 0 & 0 & 1 \end{bmatrix} \begin{Bmatrix} U_1 \\ U_2 \\ U_3 \\ U_4 \\ U_5 \\ U_6 \end{Bmatrix} = [R]\{U\} \tag{4-144}$$

Where [R] is the transformation matrix that related element displacements to global displacements. The 6*6 element stiffness in the global system is given by :

$$[K_e] = [R]^T[k_e][R] \tag{4-145}$$

4.7.2.1.D. Torsional Stiffness Matrix :

To add the torsion load to the general BHA element, consider figure (4.14a), which depicts a circular cylinder subjected to torsion via twisting moments applied at its ends. Figure (4-14b) shows torsional finite element where the nodes are 1and 2, the axis of the cylinder is the x-axis, and twisting moments are positive according to the right-hand rule. The angle of twist per unit length of a uniform, elastic circular cylinder subjected to torque T is given by:

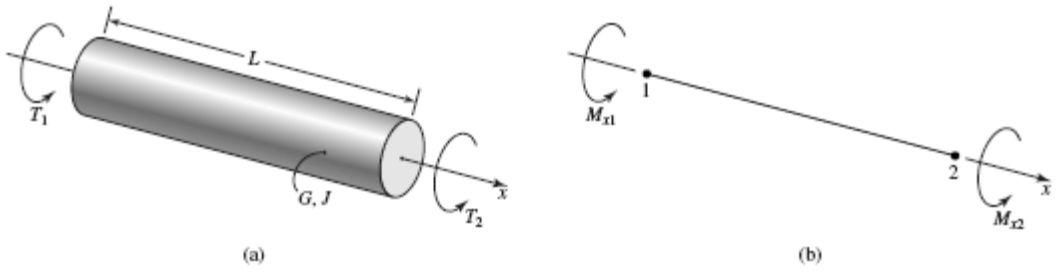

Figure 4-14: (a) Circular cylinder subjected to torsion.(b)Torsional finite element notation[62].

$$\phi = \frac{T}{JG} \tag{4-146}$$

Where

T:Torque

J: polar moment of inertia of the cross-section area

G: the shear modulus of the material.

As the angle of twist per unit length is constant, the total angle of twist of the element can be expressed in terms of the nodal rotations and twisting moments as:

$$\theta_{x2} - \theta_{x1} = \frac{TL}{JG} \tag{4-147}$$

Or

$$T = \frac{JG}{L}(\theta_{x2} - \theta_{x1}) = k_T(\theta_{x2} - \theta_{x1}) \qquad (4\text{-}148)$$

This can be written in term of element equilibrium equations as:

$$\frac{JG}{L}\begin{bmatrix} 1 & -1 \\ -1 & 1 \end{bmatrix}\begin{Bmatrix} \theta_{x1} \\ \theta_{x2} \end{Bmatrix} = \begin{Bmatrix} M_{x1} \\ M_{x2} \end{Bmatrix} \qquad (4\text{-}149)$$

So the torsional stiffness matrix is

$$[k_{\text{torsion}}] = \frac{JG}{L}\begin{bmatrix} 1 & -1 \\ -1 & 1 \end{bmatrix} \qquad (4\text{-}150)$$

A general three dimensional BHA element is capable of both axial and torsional deflections as well as two-plane bending. Adding the torsional stiffness matrix to the general BHA element (equation (4-142), the element equations become:

$$\begin{bmatrix} [k_{\text{axial}}] & [0] & [0] & [0] \\ [0] & [k_{\text{bending}}]_{xy} & [0] & [0] \\ [0] & [0] & [k_{\text{bending}}]_{xz} & [0] \\ [0] & [0] & [0] & [k_{\text{torsion}}] \end{bmatrix} \begin{Bmatrix} u_1 \\ u_2 \\ v_1 \\ \theta_{z1} \\ v_2 \\ \theta_{z2} \\ w_1 \\ \theta_{y1} \\ w_2 \\ \theta_{y2} \\ \theta_{x1} \\ \theta_{x2} \end{Bmatrix} = \begin{Bmatrix} f_{x1} \\ f_{x2} \\ f_{y1} \\ M_{z2} \\ f_{y2} \\ M_{z2} \\ f_{z1} \\ M_{y1} \\ f_{z2} \\ M_{y2} \\ M_{x1} \\ M_{x2} \end{Bmatrix} \qquad (4\text{-}151)$$

In expanded form, the 3-D BHA stiffness matrix can be written as follows:

$$[K_e]=\begin{bmatrix}
\frac{AE}{L} & 0 & 0 & 0 & 0 & 0 & \frac{-AE}{L} & 0 & 0 & 0 & 0 & 0 \\
0 & \frac{12EI_z}{L^3} & 0 & 0 & 0 & \frac{6EI_z}{L^2} & 0 & \frac{-12EI_z}{L^3} & 0 & 0 & 0 & \frac{6EI_z}{L^2} \\
0 & 0 & \frac{12EI_y}{L^3} & 0 & \frac{-6EI_y}{L^2} & 0 & 0 & 0 & \frac{-12EI_y}{L^3} & 0 & \frac{-6EI_y}{L^2} & 0 \\
0 & 0 & 0 & \frac{GJ}{L} & 0 & 0 & 0 & 0 & 0 & \frac{-GJ}{L} & 0 & 0 \\
0 & 0 & \frac{-6EI_y}{L^2} & 0 & \frac{4EI_y}{L} & 0 & 0 & 0 & \frac{6EI_y}{L^2} & 0 & \frac{2EI_y}{L} & 0 \\
0 & \frac{6EI_z}{L^2} & 0 & 0 & 0 & \frac{4EI_z}{L} & 0 & \frac{-6EI_z}{L^2} & 0 & 0 & 0 & \frac{2EI_z}{L} \\
\frac{-AE}{L} & 0 & 0 & 0 & 0 & 0 & \frac{AE}{L} & 0 & 0 & 0 & 0 & 0 \\
0 & \frac{-12EI_z}{L^3} & 0 & 0 & 0 & \frac{-6EI_z}{L^2} & 0 & \frac{12EI_z}{L^3} & 0 & 0 & 0 & \frac{-6EI_z}{L^2} \\
0 & 0 & \frac{-12EI_y}{L^3} & 0 & \frac{6EI_y}{L^2} & 0 & 0 & 0 & \frac{12EI_y}{L^3} & 0 & \frac{6EI_y}{L^2} & 0 \\
0 & 0 & 0 & \frac{-GJ}{L} & 0 & 0 & 0 & 0 & 0 & \frac{GJ}{L} & 0 & 0 \\
0 & 0 & \frac{-6EI_y}{L^2} & 0 & \frac{2EI_y}{L} & 0 & 0 & 0 & \frac{6EI_y}{L^2} & 0 & \frac{4EI_z}{L} & 0 \\
0 & \frac{6EI_z}{L^2} & 0 & 0 & 0 & \frac{2EI_z}{L} & 0 & \frac{-6EI_z}{L^2} & 0 & 0 & 0 & \frac{4EI_z}{L}
\end{bmatrix} \quad (4\text{-}152)$$

Which is 12× 12 symmetric matrix composed of the individual stiffness matrices representing axial loading, two-plane bending, and torsion.

4.7.2.2. Element Loaded Forces (F):

For BHA modeling ,The element loaded forces in Equation(4-99) will be summation of an equivalent force representing the portion of the BHA weight F_W ,and the boundary force representing the string normal forces due to contact of node with well wall F_b. In mathematical form this will be written as:

$$F = F_w + F_b \quad (4\text{-}153)$$

In addition to the loads specified by Equation (4-153), an axial force (x-direction) was applied at the uppermost node of the BHA finite element

model. This force was applied to account for the weight of the string above the BHA.

4.7.2.2.A.Weight Force(F_w):

The element weight force could be computed from the relation:

$$F_w=L_e W_n B_c \cos(\theta) \quad (4\text{-}154)$$

Where

L_e: element length,ft.

W_n: nominal weight of BHA lb/ft.

B_c:Bouyancy Factor,dimensionless.

4.7.2.2.B. Normal Contact Force(F_n):

It is the lateral force exerted by the drillstring on the wall of the hole due to dog-leg or inclination of the hole. If the pipe is within an inclined hole , the contact force is the product of its buoyed weight and the sine of the inclination angle of the hole ,or:

$$F_n= W_n B_c \sin(\theta) \quad (4\text{-}155)$$

If the pipe within a dog-leg,the normal force is computed with the equation:

$$F_n = 2T_d \sin\left[DLS \frac{L_j}{2} \right]$$

Where

T_d:tension in the drillpipe at dog-leg,lb.

L_j:joint length of one drill pipe,ft.

4.7.2.3. Computer Program:

A computer program in FORTRAN(90) language is written to analysis the bottom hole assembly in three dimension for static case. The program adopted matrix displacement method in the analyzing of BHA. The bottom hole assembly was considered as structure consists of beam-rod elastic elements that could sustained axial load, transverse load, and bending moment. The main program is connected to a number of subroutines which have a specific function.

Figure (4-15) depicts the procedure of program to solve bottom hole assembly configuration. The main program starts with definition of all variables and dynamic arrays that used in the program.

In section" input & initialization" ,data such as dimensions, material properties, lengths, number of stabilizers , distances ,and boundary conditions are entered. Other data like geometric coordinates of nodal points, element connectivity are generated. Using these data , element stiffness matrix relationships are generated with subroutine "rigiedjointed" and assembled into global matrix by subroutine "formKV". Then ,Gaussian elimination on the system equations is applied and back-substitution phase was performed by subroutine "BACSUB".The nodal displacements are then computed and printed. A final post-processing phase is a multiplication of element nodal displacements by element stiffness matrix to compute element actions. The element actions include the internal and reaction forces for each element.

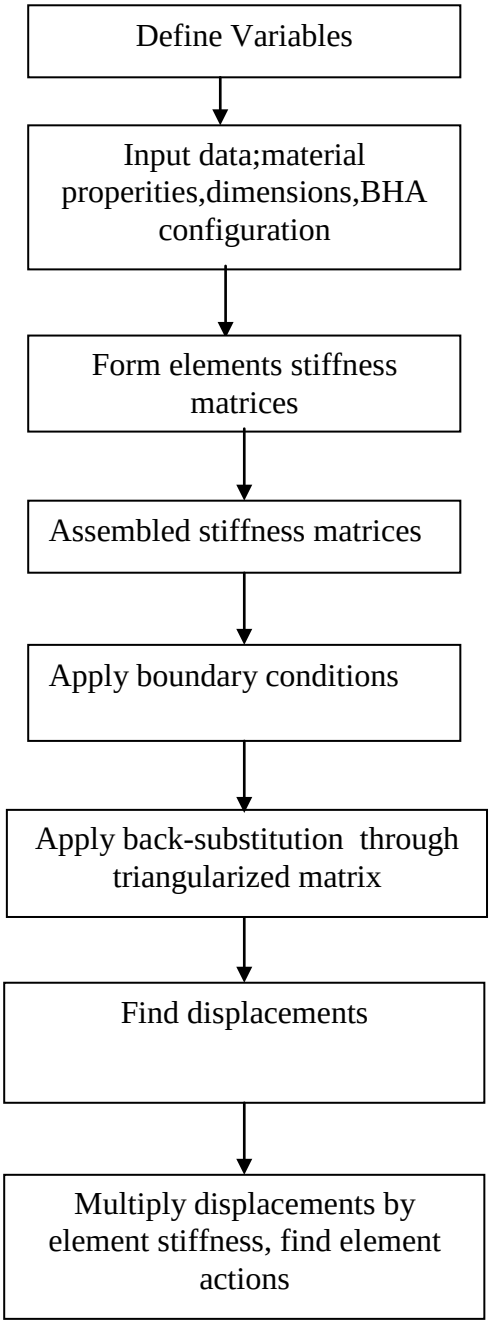

Figure 4-15: Solution Procedure For Bottom Hole Assembly.

Chapter Five
Results and Discussion

In this chapter, steps of design horizontal well will be discuses. Z14 oil field was selected as an example for this design. A number of programs were built, and each program was constructed to deal with a specific aspect of horizontal well design. The results of application of these programs will be presented.

5.1. Selection of Bit and Casing Sizes:

With the aid of Table (4-1) and Table (4-2), bit and casing sizes could be detected. HORWELL[8] study suggested hole size of about 8.5 in for horizontal well. If the production casing or liner size was chooses as 7 in, the sizes of bits to drill the whole well and casing sizes for casing the well would be as shown in Table (5-1).

Table 5-1: Bit and Casing Sizes for 7 in Production Casing.

Bit Size, in	Casing Size ,in
17 1/2	13 3/8
12 1/4	9 5/8
8 1/2	7

5.2. Casing Seat Depths and Drilling Fluid Densities:

Pore and fracture pressures data of the Z14 field were gathered from offset well reports (drilling reports).Table (5-2) shows these values of pressures at different depths. With these data, Casing setting depths and drilling fluid densities were determined. Since the depth of

Euphrates formation is nearly 2978 ft(setting depth of the production casing), Table(5-3) provides setting depths of other casing strings and required density for drilling these sections.

Table 5-2: Pore and Fracture Pressure Data

Depth(RTKB) ft	Pore pressure psi	Fracture pressure psi
2263	1519	2057
2407	1573	2212
2569	1490	2383
2750	1494	2637

Table 5-3: Setting Depths and Drilling Mud Densities.

Setting Depth ,ft	Mud Density, ppg
1443	8.919
2522	12.631
2978	11.769

5.3. Casing Grads:

Casing Grads and weights were determined for each section based on the density of drilling mud and formation pressures of the field. A worst conditions design were considered in computing of tension, burst, and collapse loads imposed on casing string. Also safety

factors with high values for each type of load were assumed. Table (5-4) gives the detailed information about the casing program.

Table 5-4: Casing Grads and Weights.

Hole Size in	Casing Size in	Grade	Weight Lb/ft	Setting Depth	Length ft
17.5	13 3/8	k-55	54.5	1443	1443
12.25	9 5/8	K-55	36	2522	2522
8.5	7	N-80	26	2978	2978

5.4. Construction of Well Profile:

A drillstring simulator was build to generated well profile and computed drillstring loads. Geological data such as true vertical depth, horizontal distance, and measured depth are needed to constructed well profile. Z14 oil field has many vertical wells with known depths. These vertical wells could be converted to short radius wells (reentry wells) by drilling building section with a high build rate of angle. Figure (5-1) depicts single build (constant build) horizontal well profile suggested for this field when the rate of build is 90 deg/100ft. Table (5-5) presents the dimensions of this profile (Short radius well profile).

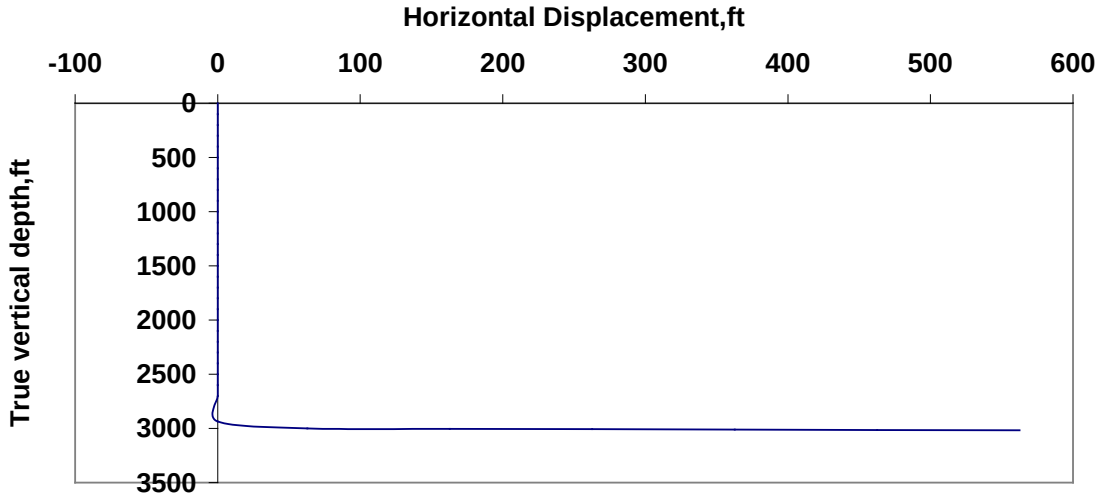

Figure 5-1: Horizontal Well Profile.

Table 5-5: Dimensions of Horizontal Well Profile.

Radius of Curvature, ft	65.195
Vertical Depth of Build Section, ft	65.069
Horizontal Length of Build Section, ft	62.839
Length of build Section, ft	100
Kick-off Point(KOP),ft	2933
Total Measured depth, ft	3533

5.5. Specifications of Short Radius Motor:

Usually, the build and lateral sections of short radius wells are drilled with PDM motor equipped with double tilt unit (DTU) housing. This unit have maximum bent angle of 1.5 deg. Table (5-6) provides the specifications of suggested PDM.

Table 5-6: Specifications of Short Radius Motor.

Motor Diameter, in	4.75
Motor Length, ft	8
Motor Weight,lb	650
Flow Rate,gpm	185-320
Operating Pressure, psi	75-720
Operating Torque, ft-lb	350-700
Motor Speed,rpm	150-260
Motor Horsepower,hp	34-85
L1+L2,ft	3.33

Since high build rate is required to convert the wellbore from vertical to horizontal within distance 63.658 ft, drillstring in build section must be articulated. The maximum length between two articulations must not exceed 15 ft.

5.6. Construction of Drillstring Loads Profile:

After generation of the well profile, drillstring design began with torque and drag modeling. Loads of six operating parameters (pick-up without rotation, slack-off without rotation, sliding, pick with rotation, slack-off with rotation, drilling with rotation) are computed. Also, buckling tendencies (sinusoidal and helical buckling) of drillstring are calculated for the well profile. Table (5-7) shows the required data for prediction loads of drillstring.

Table 5-7: Required Data for Calculation Drillstring Loads.

Hole Diameter, in	8.5
Drillpipe Diameter ,in	3.5
Drillpipe Weight, lb/ft	15.5
Mud Weight, ppg	11.77
Weight on Bit, lb	30000
Overpull at Bit ,lb	50000
Torque at Bit ,lb-ft	2000
Formation Friction Factor	0.4
Casing Friction Factor	0.24
Tensile Strength,lb	388000
Make-up Torque,lb-ft	25000
Horizontal Displacement,ft	500
BHA Torque,lb-ft	2000
BHA Drag,lb	2600

Figure (5-2) shows the loads analysis of inverted drillstring using drillpipe type(S-135) and drillcollar without rotation. While Figure (5-3) shows the string loads for rotating case. In both cases, a maximum surface tension of the string was recorded in pick-up condition. These values are smaller than the tensile strength of drillpipe(388000 lb),which provided reasonable safety margin. Also, maximum compressive load has been achieved when using steerable BHA(sliding mode). This mode of drilling could be used safely since the sinusoidal critical buckling of drillpipe (40000 lb) is larger than the

compressive load in the string. In addition, a sufficient surface slack-off load is noticed which provided adequate string weight to offset the axial friction effects while tripping in the hole.

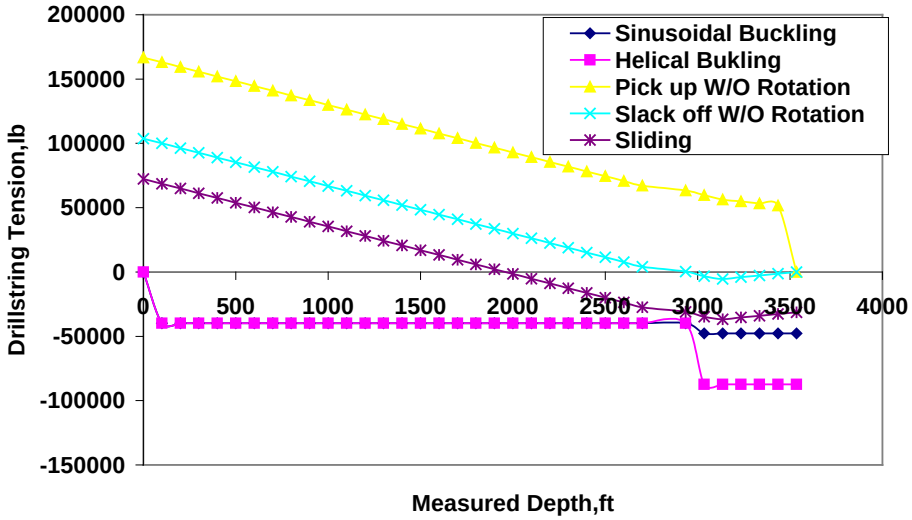

Figure 5-2: Drillstring Loads without Rotation.

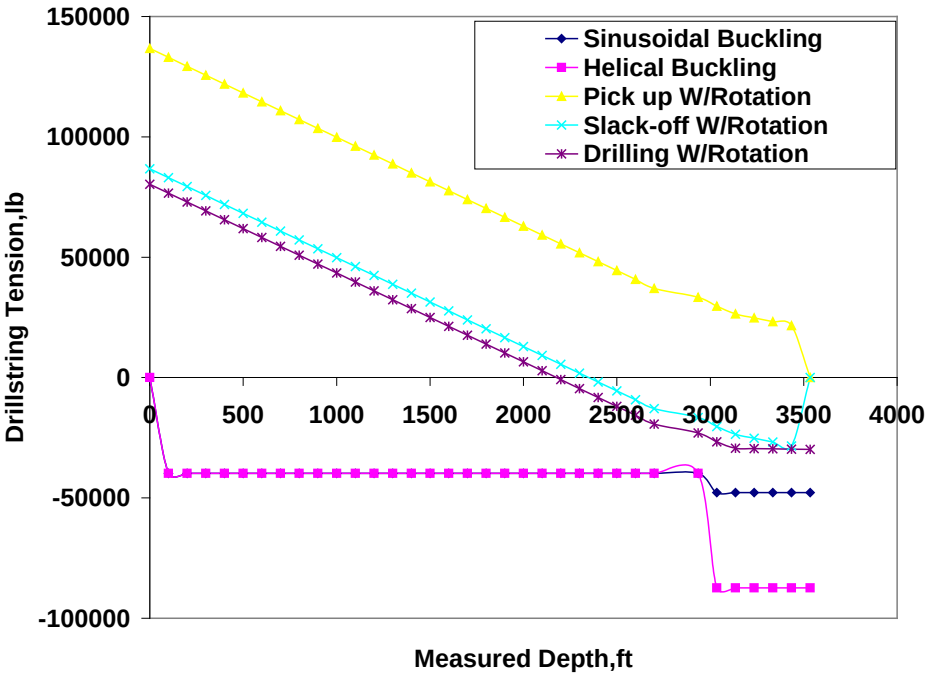

Figure 5-3: Drillstring Loads With Rotation.

As for torque load, drillstring torque for four cases which are encountered while drilling horizontal wells is computed. These cases

are Rotating-off bottom, pick-up with rotation, slack-off with rotation, and drilling with rotation. Figure (5-4) shows these torque loads. Ahighest value was recorded with drilling case(nearly 3600 lb-ft) which was smaller than the make –up torque of joint(25000 lb-ft).

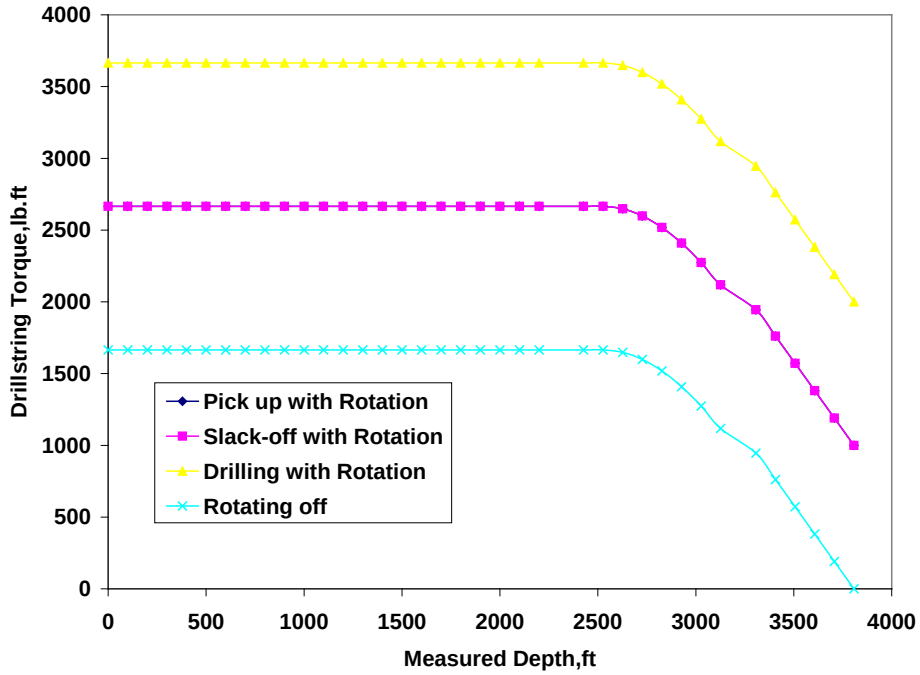

Figure 5-4: Torque loads of Drillstring.

5.7.Hydraulic Requirements:

The hydraulic program was designed to achieve adequate hole cleaning for each section of the hole. Table (5-8) provides the pressure losses in the circulation system for Bingham plastic fluid. Also nozzles size, jet velocity, hydraulic power at the bit (BHHP), and impact force of the bit (BIF) were calculated.

Table 5-8: Hydraulic Calculation of Circulation System.

Dh in	Q gpm	Ps psi	P_{string} psi	$P_{annulus}$ psi	P_{bit} psi	A_n In^2	V_n Ft/sec	D_n in	BHHB hp	BIF Lb_f
17.5	692	50	412	42	2525	0.39	562	13.1	1018	1789
12.25	510	38	403	73	2555	0.34	473	12.2	758	1577
8.5	310	22	250	94	2703	0.24	506	10.29	602	1179

The first and second section of the hole (17.5in, 12.25 in) are almost vertical, thus using Q_{max}(694 gpm) and (514 gpm) are sufficient for hole cleaning. The third section (8.5 in) of the hole will be build section. Angle hole between 40-60 deg present most problem because the cutting have a tendency to slide down. With Tarr's equation, A minimum annular velocity for no settling of cutting is almost 164 ft/m which give minimum flow rate equal to 314 gpm

5.8. Factors Affecting Torque and Drag:

In drilling horizontal wells, high friction forces between drillstring and hole wall are generated. This make the pipe movement in or out of well is difficult. Thus, the major limitations for drilling horizontal wells are torque and drag .With aid of "soft-string" model, a number of investigations were performed to examine factors that affects torque and drag. . In all cases of investigation, a single build up rate profile is considered.

5.8.1. Effect of Well Geometry (Build Rate):

Figure (5-5) shows well profiles of six build rates (2,4,6,8,10,12 deg/100ft).Note that when the rate of build increase, the location of Kick-off point will be deeper.

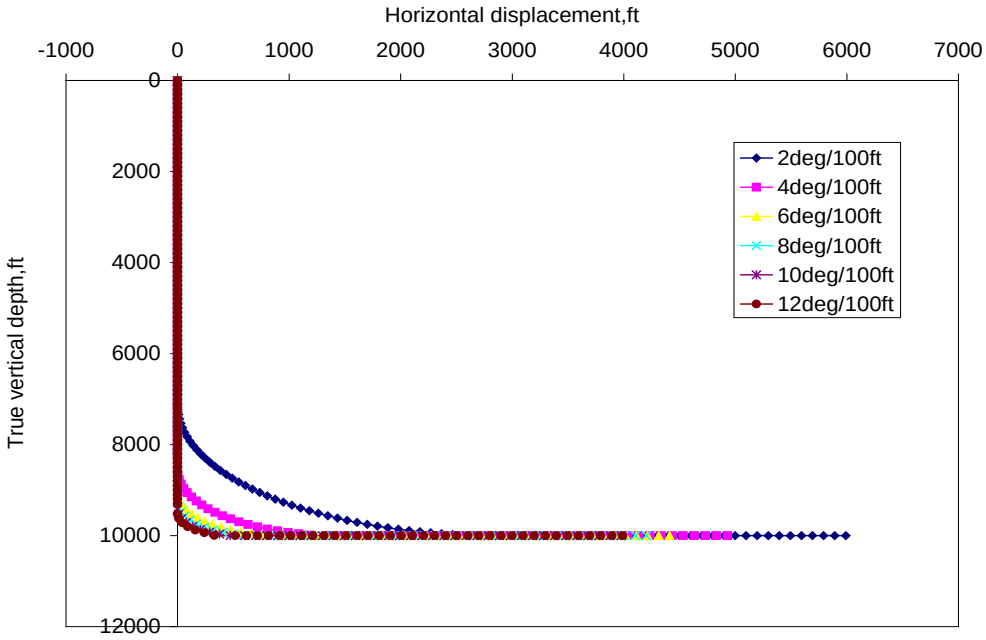

Figure 5-5: Single Build Horizontal Well Profile

Figures(5-6) through (5-8) shows the effect of variation of build rate and hole inclination on drillstring tension for cases of pick –up, slack-off, sliding, and drilling. Its observe from Fig(5-6) that the rate of build angle has an effect on pick-up load,i.e; drilling with high build rate recorded high surface tension to pull the string. This is attributed to increase of normal force with building rate which increase the drag force. On the other hand, increasing the final well angle will lower amount of surface pick-up load as result of decreasing of string weight component with the inclination. That indicated drilling to high inclination with low build rate will yield the least amount of drag. However, it should be noted that these differences in pick-up load is actually small.

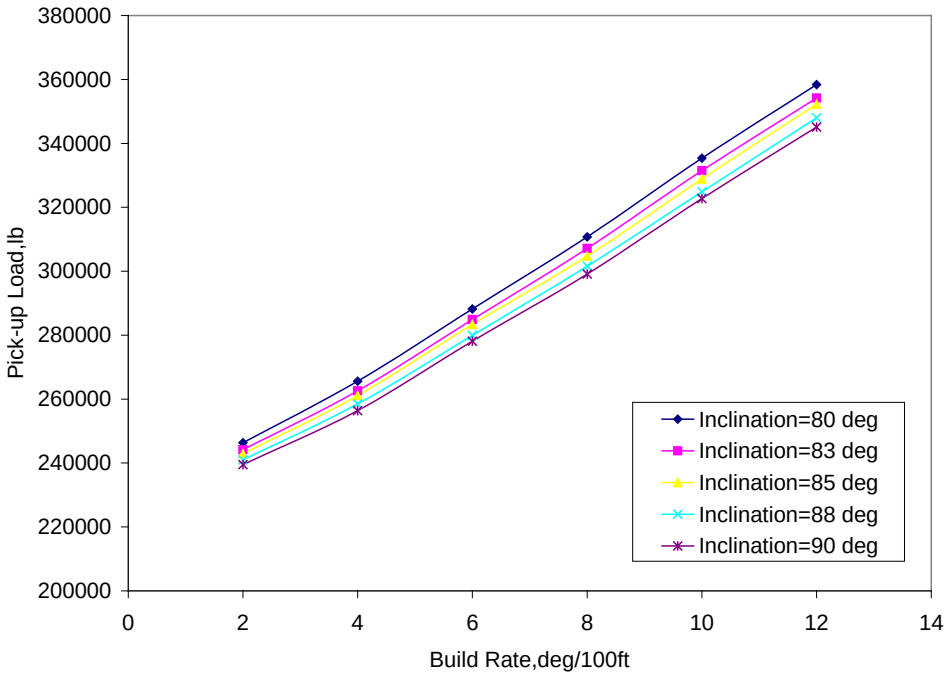

Figure 5-6: Effect of Build Rate on Pick Load.

As for slack-off case, figure (5-7), drilling of horizontal well with high build rate produce high slack-of load. High slack-off load means low resistance to sliding. Also, small difference in slack-off load is notice when changing inclination of well from80 deg to 90 deg. The same philosophy is applied for sliding case, figure (5-8) and drilling case, figure (5-9).

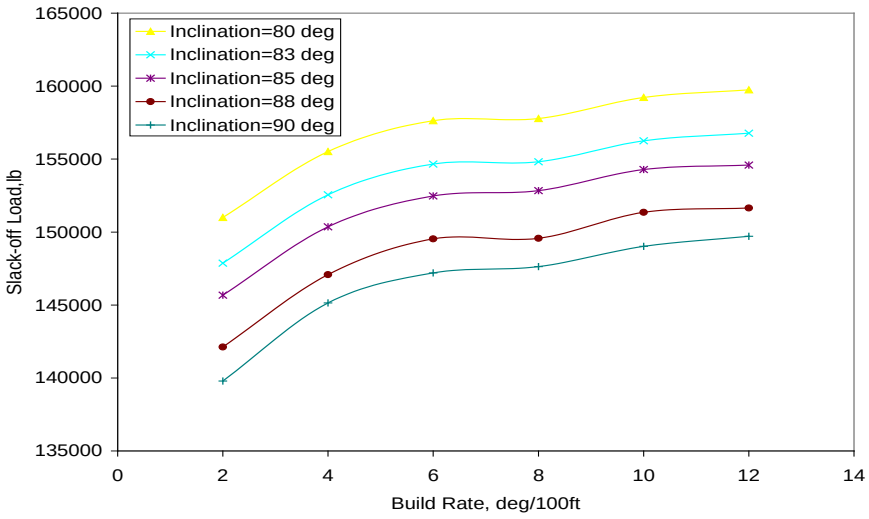

Figure 5-7: Effect of Build Rate on Slack-off Load.

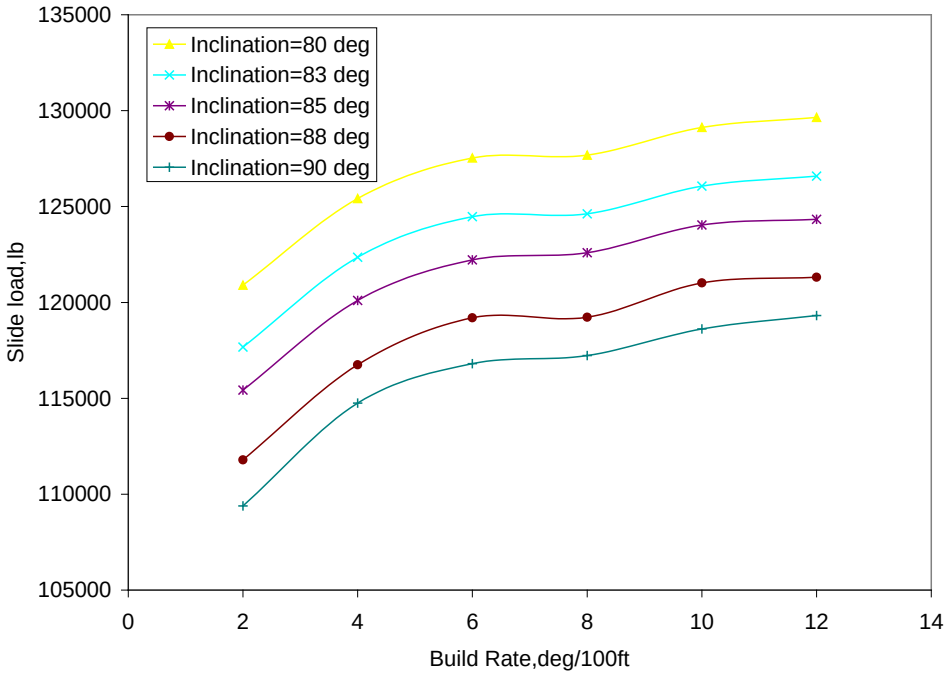

Figure 5-8: Effect of Build Rate on Slide Load.

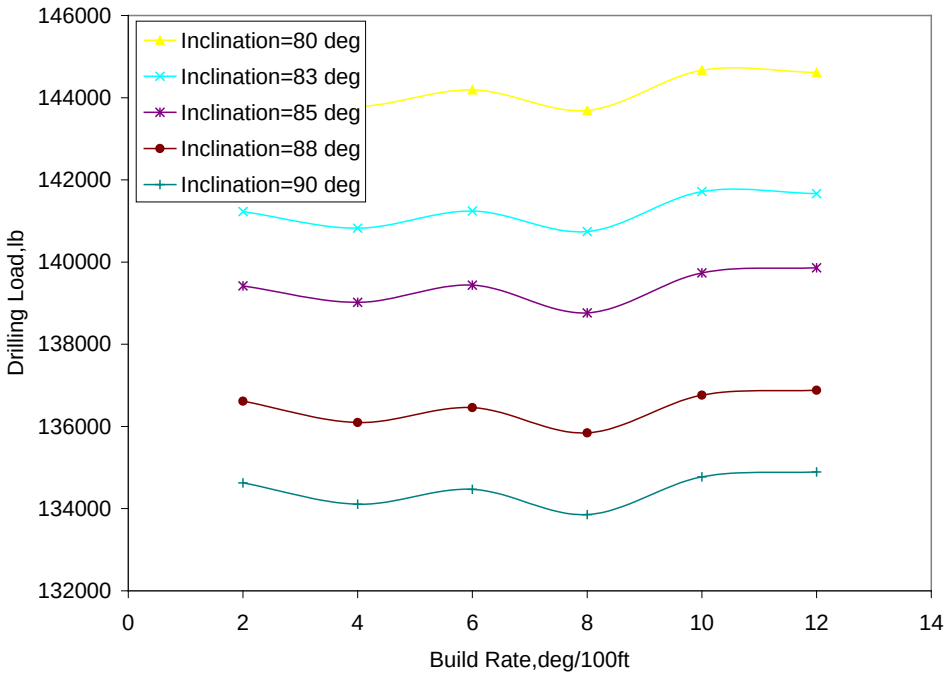

Figure 5-9: Effect of Build Rate on Drilling Load.

As for the torque required for rotating drillstring, Fig (5-10) shows strong influence of build rate and well inclination on the torque. This behavior may be attributed to increasing in wall contacts force with build rate which causes higher surface torsion.

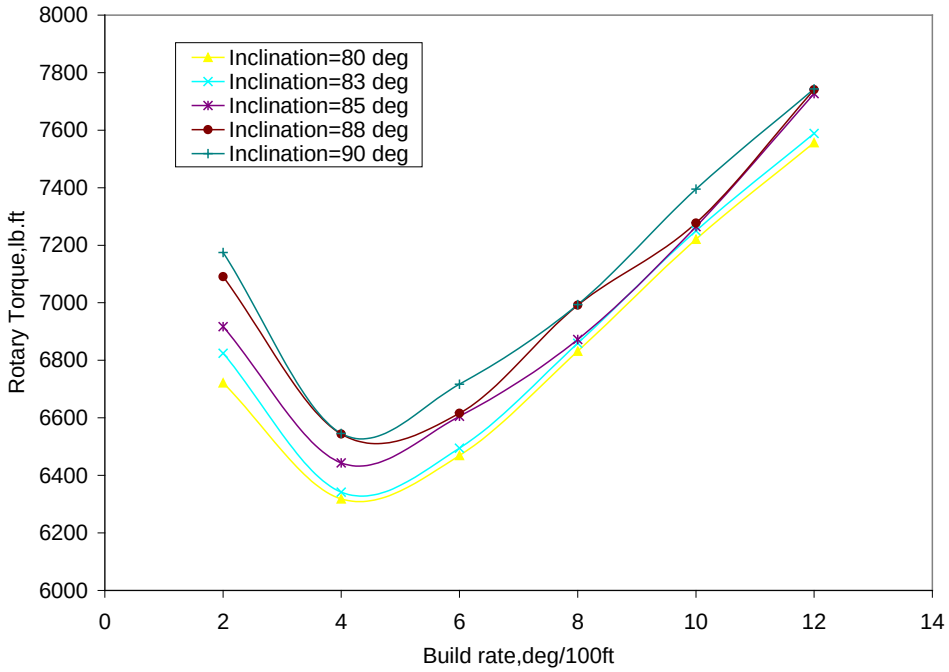

Figure 5-10: Effect of Build Rate on Torque Load.

5.8.2. Effect of Friction Factor:

In this investigation, different types of drilling fluids (wide range of friction factors) are tested to establish their effects on drillstring torque and drag loads in four cases of operating conditions.

For pick-up load, Fig (5-11) shows slight increasing in the load when changing friction factor from 0.17 to 0.4.its clear that oil base mud(0.17—0.25) has best lubrication property which lowering the drag compared to the water base mud . This may be attributed to the low solid content and formation of film around drillstring which help in reduction of friction. While for slack-off and sliding cases shows slight decreasing in surface loads when increasing friction factors as

shown in Fig (5-12) and Fig(5-13). Again, oil base mud in this case of operation exhibited high slack-off tendency compared to water base mud. This means that this type of mud exhibited less resistance to sliding of drillstring.

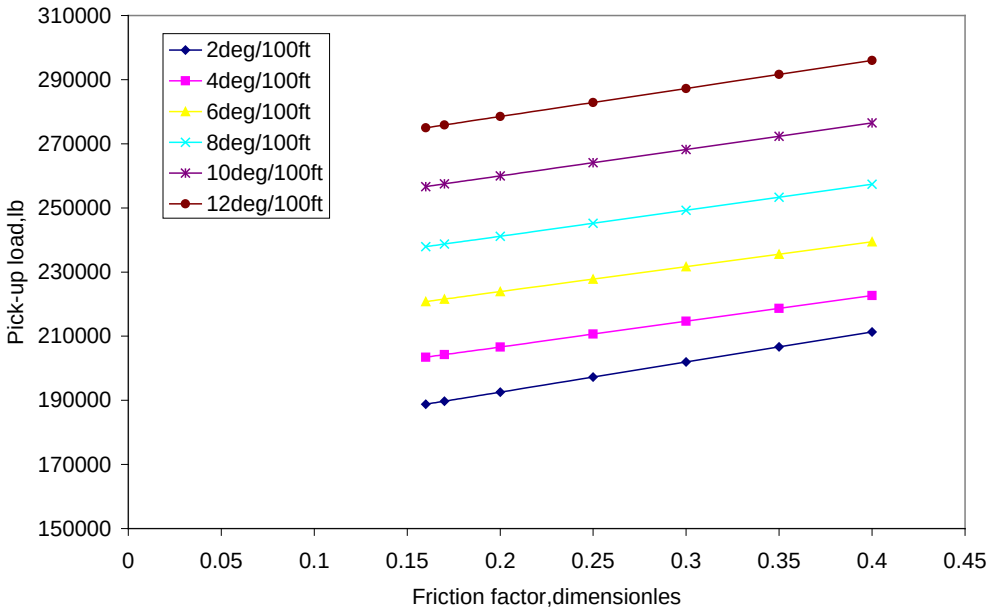

Figure 5-11: Effect of Friction Factor on Pick-up Load.

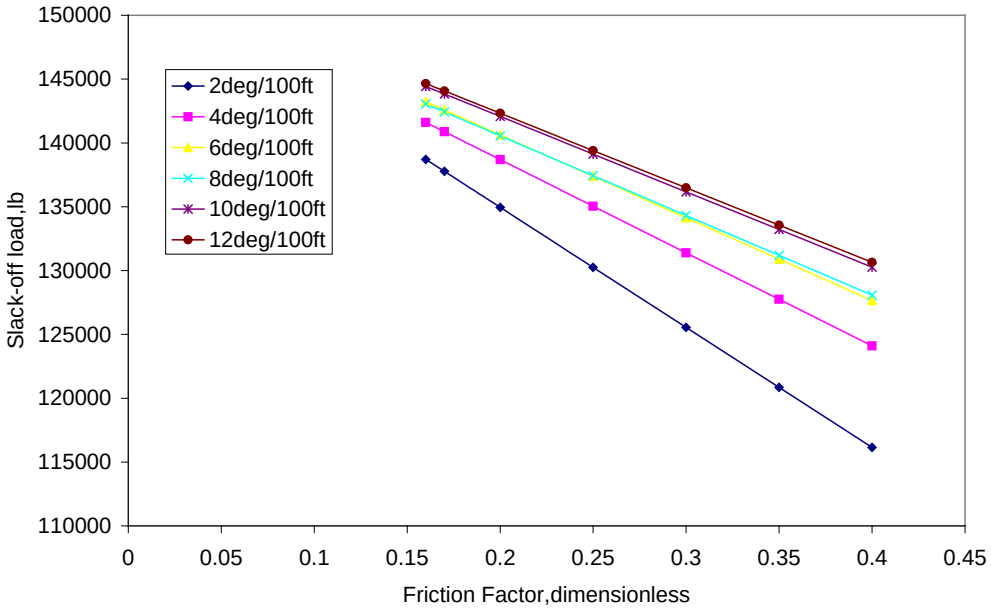

Figure 5-12 : Effect of Friction Factor on Slack-off Load.

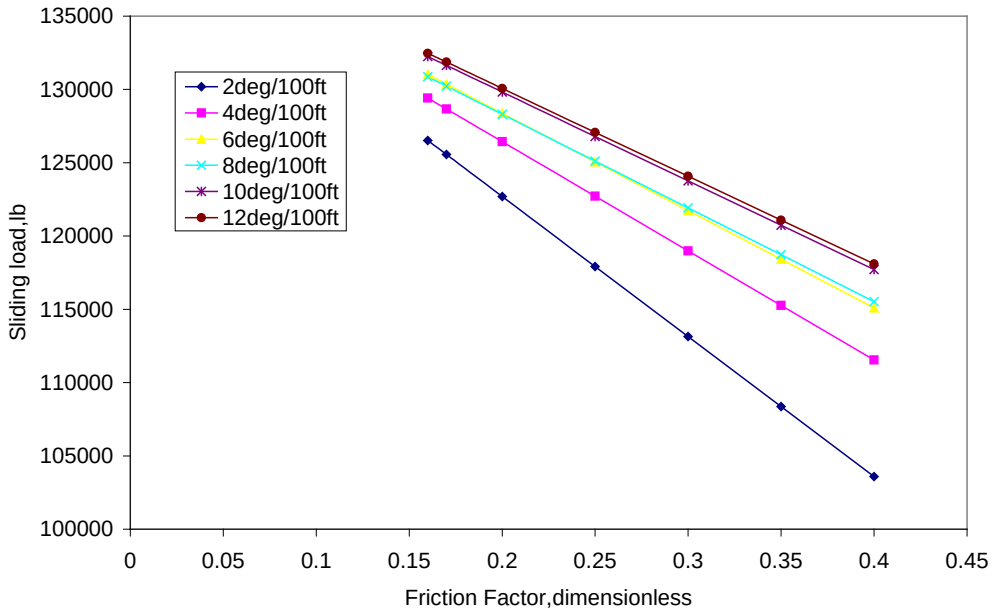

Figure 5-13: Effect of Friction Factor on Sliding Load.

As for torque, figure (5-14) shows how the rotation of drillstring could be affected strongly by the type of mud. As it seen from the

figure, the oil base mud has achieved the lowest value of torque required to rotate the drillstring.

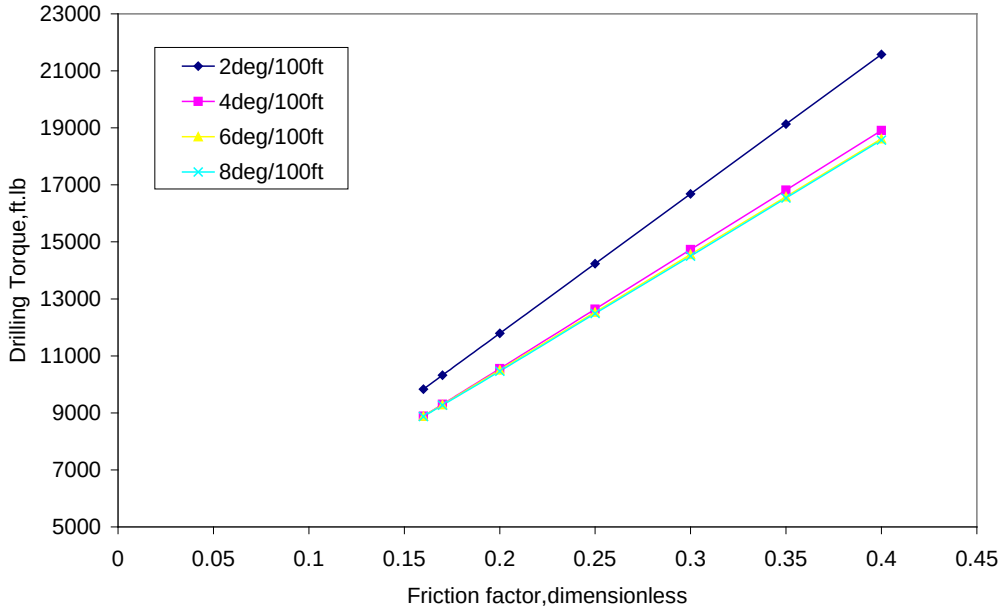

Figure 5-14: Effect of Friction Factor on Drilling Torque.

5.8.3. Effect of Pipe Weight:

The third parameter that affected on the calculation of torque and drag is nominal weight of pipe. Figure (5-15) through (5-18) presents the behavior of drilstring tension and torque of 5 in. drillpipe diameter for different nominal weights. As expected, increasing the pipe weight lead to increase in tension, which increase the normal force and cause high friction force.

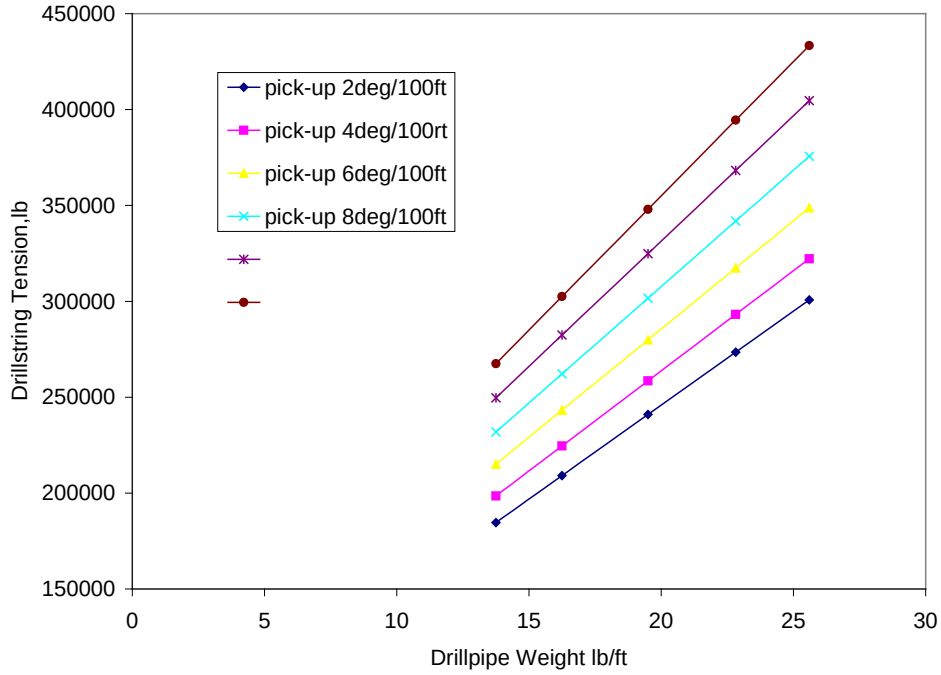

Figure 5-15: Effect of Drillpipe Weight on Pick-up Load.

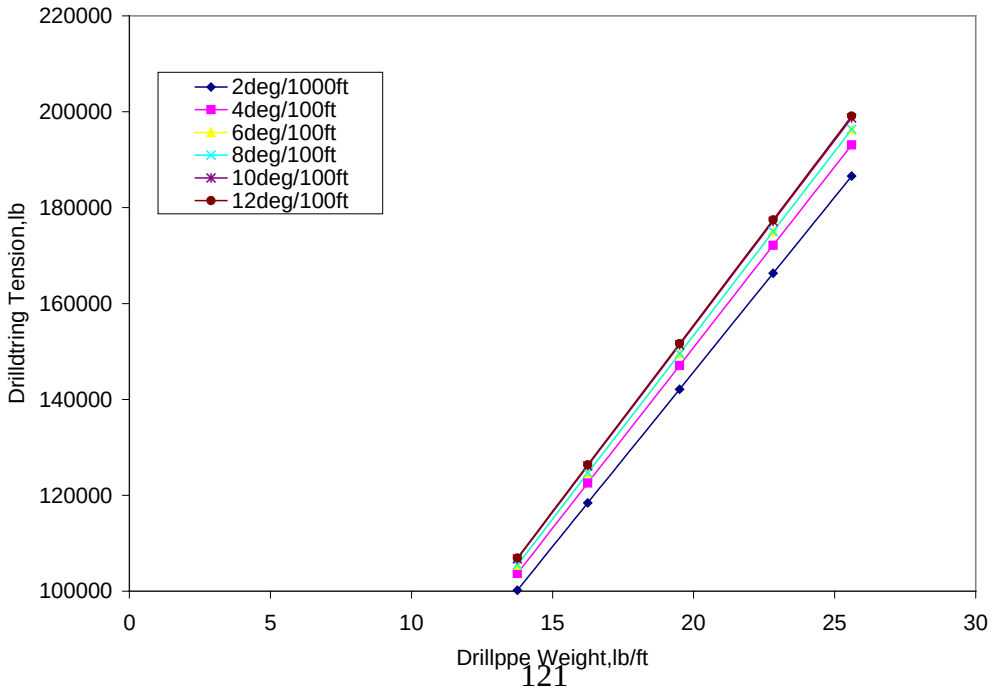

Figure 5-16: Effect of Pipe Weight on Slack-off Load.

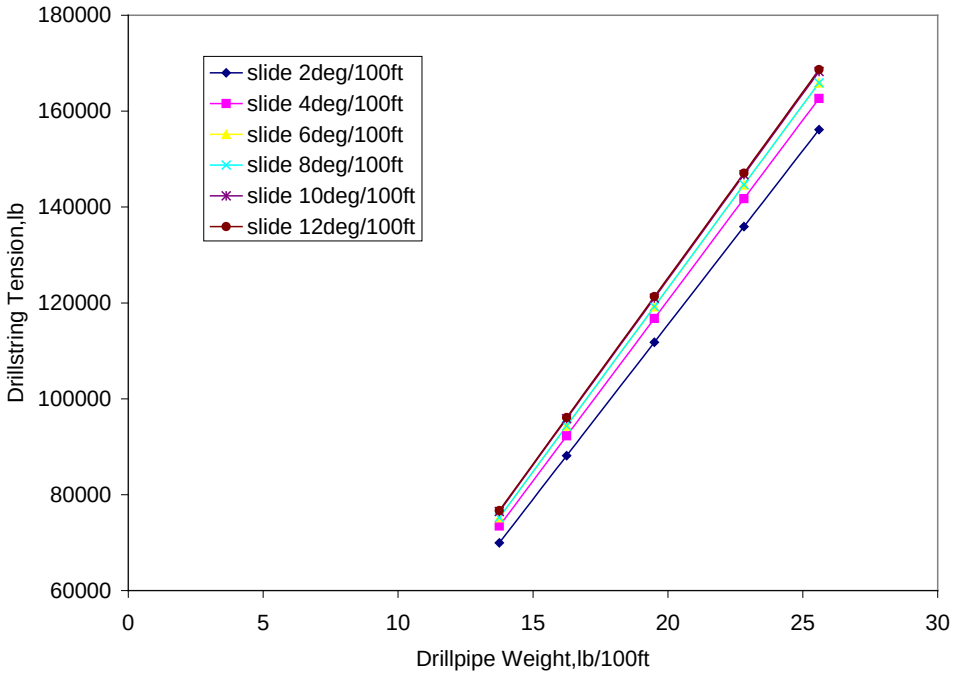

Figure 5-17: Effect of Pipe Weight on Slide Load.

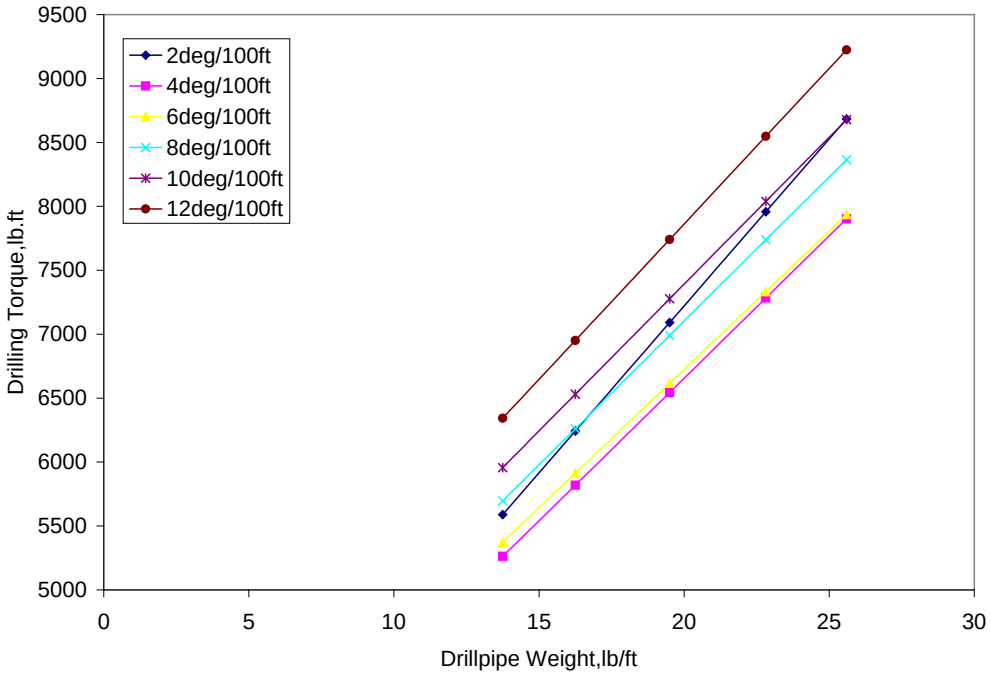

Figure 5-18: Effect of Pipe Weight on Drilling Torque.

5.9. Bottom Hole Assembly Analysis:

5.9.1. Validation of the Model:

The finite element model is first verified by comparing its results with analytical method, and Akgun[57] results (axisymmtric element) for two dimensions. Three types of rotary BHA are considered in comparisons which are slick, single stabilizer, and two stabilizers. The comparison will be based on calculated tangency length and bit side force as function of applied weight on bit.

Figure (5-19) presents the results of the three methods for slick BHA, where the tangency point will be first point where the pipe departs from the borehole wall above the bit. A good agreement between the methods is noticed for bit force, while the current model shows closer agreement for tangency length as shown in Fig(5-20).

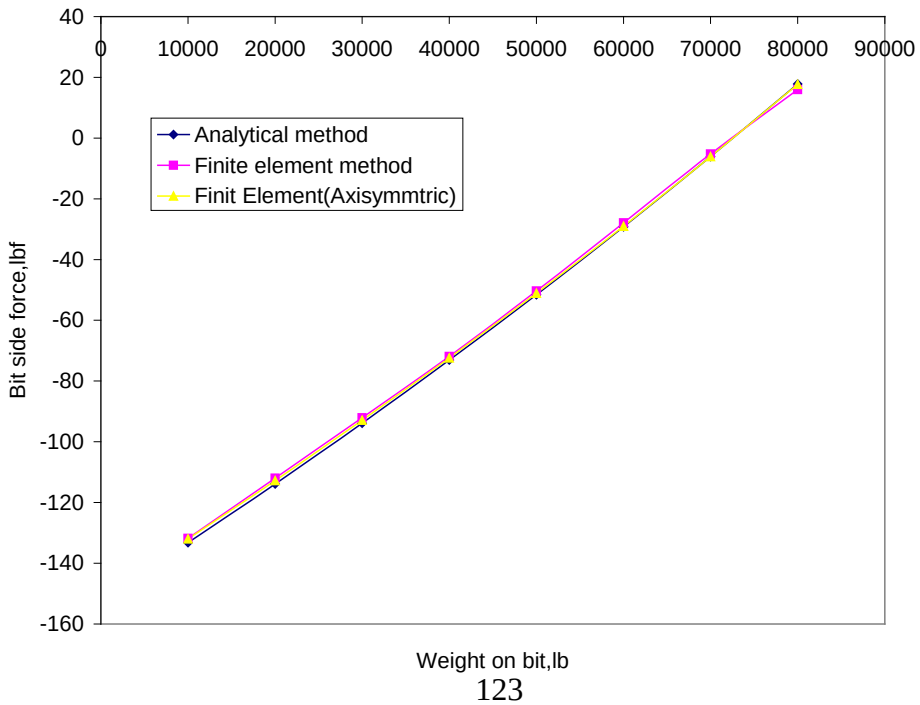

Figure 5-19: Bit Side Force From Analytical and Finite Element Methods, Slick BHA.

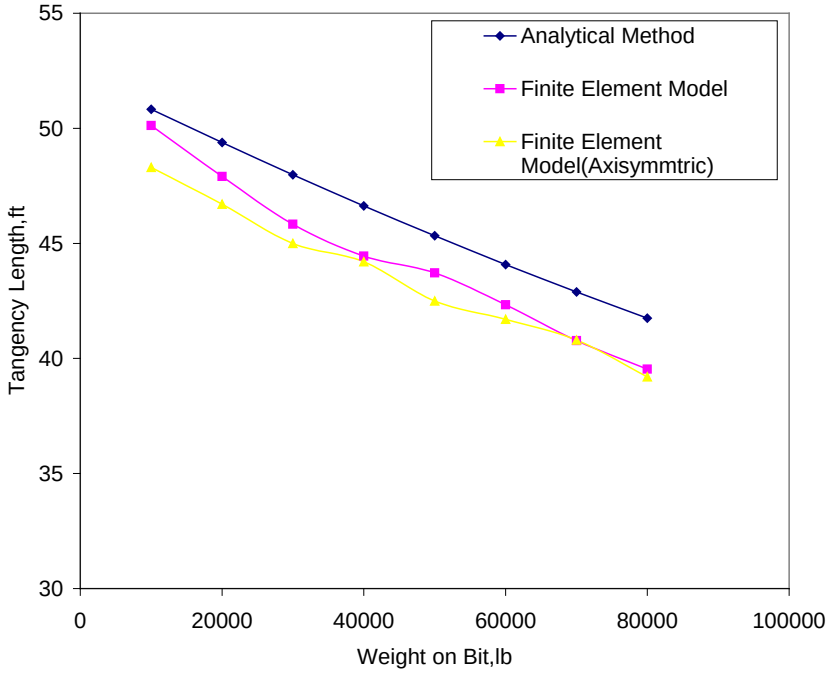

Figure 5-20:Tangency Length From Analytical and Finite Element Methods, Slick BHA.

Figure (5-21) through Figure (5-24) shows the results for single- and two- stabilizer BHA models respectively. These models were created from slick BHA model by adding x-direction displacement constrains on the corresponding nodes where stabilizers are to place. Again for most weights on bit, the current finite element model gave close results to the analytical method compared to Akgun results.. A clear difference has been noticed for two-stabilizer BHA at 70000 lb weight on bit. This difference may be attributed to additional pipe-hole contact below first stabilizer which is not considered in analytical solution.

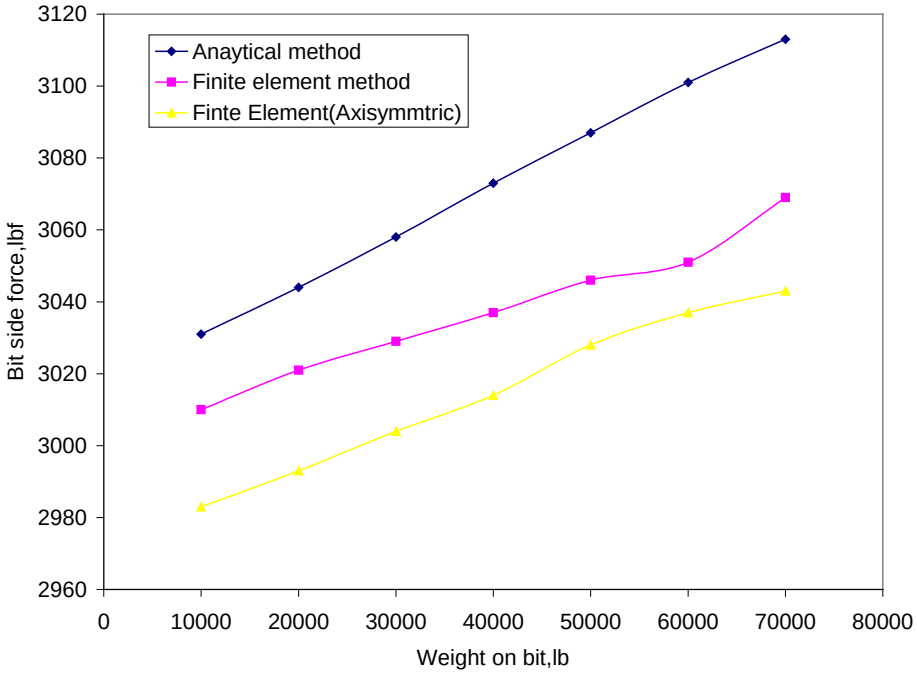

Figure 5-21: Bit Side Force From Analytical and Finite Element Methods, Single Stabilizer BHA.

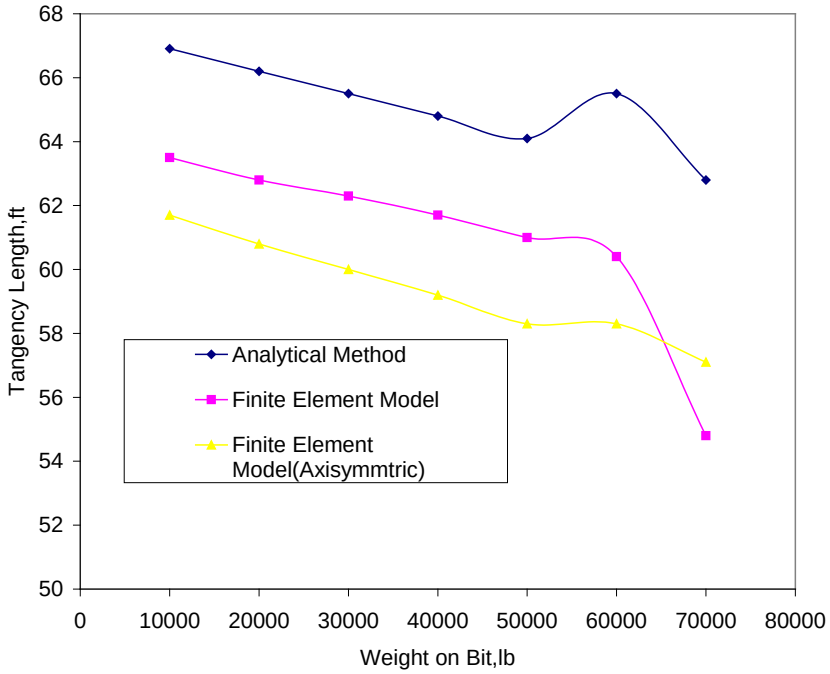

Figure 5-22: Tangency Length From Analytical and Finite Element Methods, Single Stabilizer BHA.

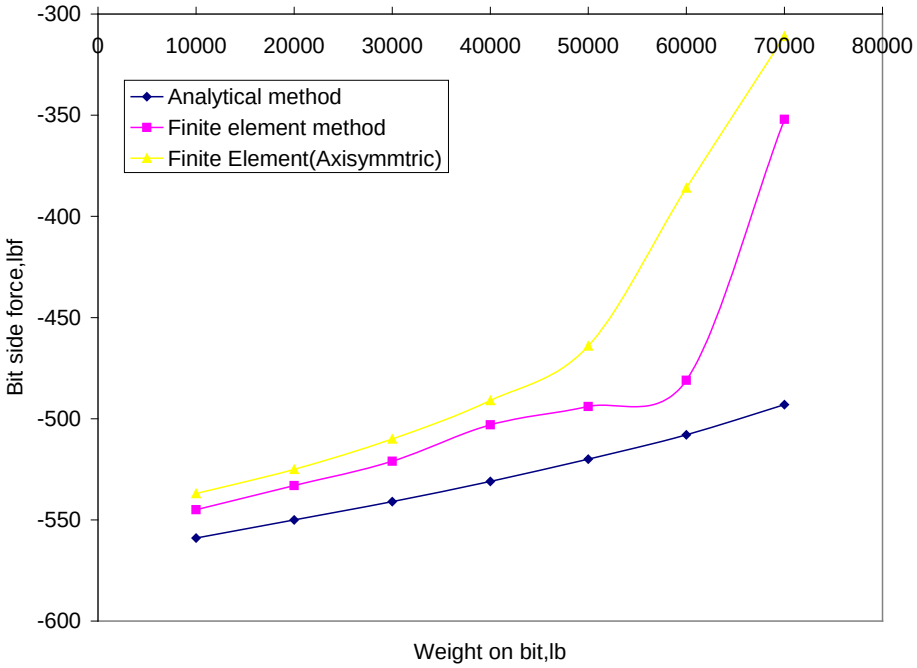

Figure 5-23: Bit Side Force Results From Analytical and Finite Element Methods, Two Stabilizers BHA.

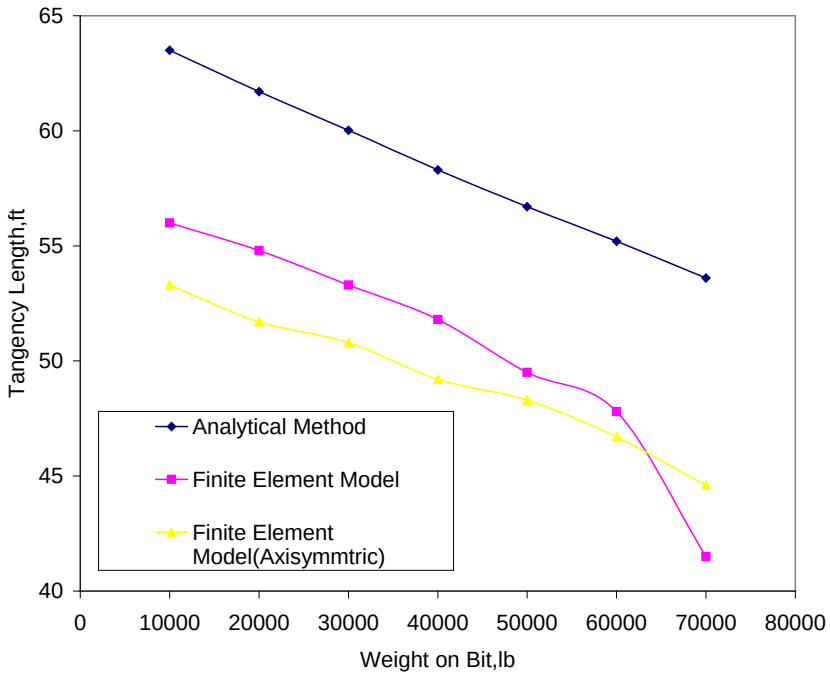

Figure 5-24: Tangency Length Results From Analytical and Finite Element Methods, Two Stabilizers BHA.

5.9.2. Factors Affecting Rotary BHA Performance:

With aid of finite element model, a number of investigations were performed to examine factors which have an effect on design of rotary BHA. The general inclination tendency of BHA will depend on sign of bit side force. If the sign of bit side force is negative, the BHA has dropping angle tendency, and when it positive sign, it has building tendency.

5.9.2.1. Effect of Weight on Bit:

Figure (5-25) shows the effect of applied WOB on the bit side force in term of hole inclination for single stabilizer BHA. At low hole angle, this BHA exhibited low response (increasing) building tendency with WOB due to increase of positive side force (building force). When the hole angle increase, the relationship is almost horizon. This behavior may be attributed to increasing of negative side force with inclination which opposite the effect of WOB and reduce its effect. Thus the effect of applied WOB in high angle wells on side force will be very small.

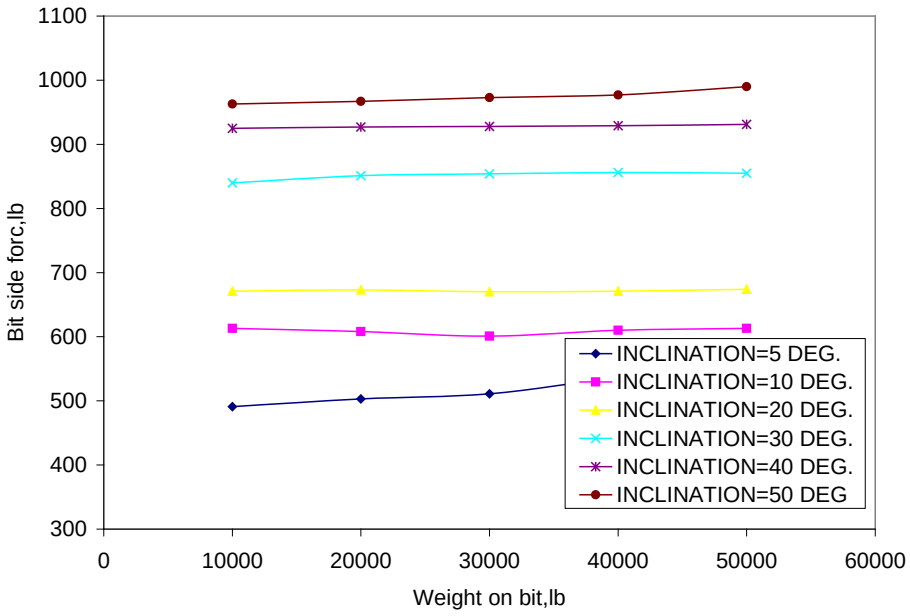

Figure 5-25: Effect of Weight on Bit on Side Force (Build Assembly).

5.9.2.2. Effect of Stabilizer Position:

Many BHA configurations contain stabilizer placed some where in drillstring. This practice represents easiest way to control the point of tangency. The mechanism of stabilizer could be explained by reviewing figure (5-26). As the plot indicated, placing stabilizer near the bit caused highest building or positive side force. As the stabilizer is moved away from the bit, the bit side force decreased and reach zero at particular distance. At this distance, the BHA has holding tendency. Beyond holding tendency, bit side force become negative and has dropping tendency (called pendulum BHA) and reached to maximum negative value. At this maximum negative value, the drill collar achieved tangency between the bit and the stabilizer. A continued increasing of the distance reduces the negative side force until it approaches the behavior of collar-only assembly.

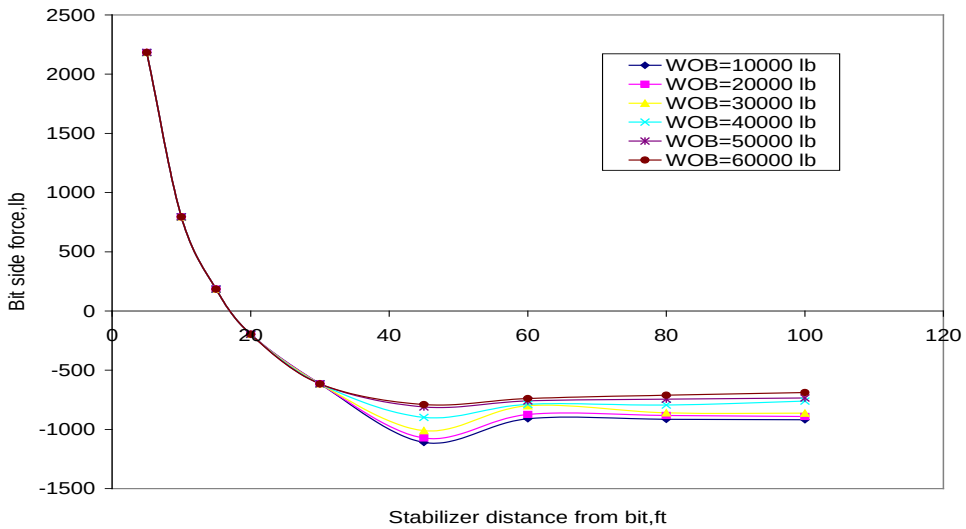

Figure 5-26: Effect of Stabilizer Position on Bit Side Force.

5.9.2.3.Effect of Collar Diameter:

Figure (5-27) shows the effect of changing collar diameter above the stabilizer on building force for building assembly. The first curve is for all diameters 6.75 in. The second and third curves for collar of diameter 6 in of different lengths (30 ft and 60 ft) beyond the stabilizer. The fourth and fifth curves are for big collar (8 in) for the same lengths (30 ft and 60 ft). A sizable effect on bit side force is noticed when adjusting diameter behind the stabilizer. A reduction in building force is noticed when using large size (8 in). Also lengthened the portion of changed collar diameter will caused some improvement in building force(bit side force).

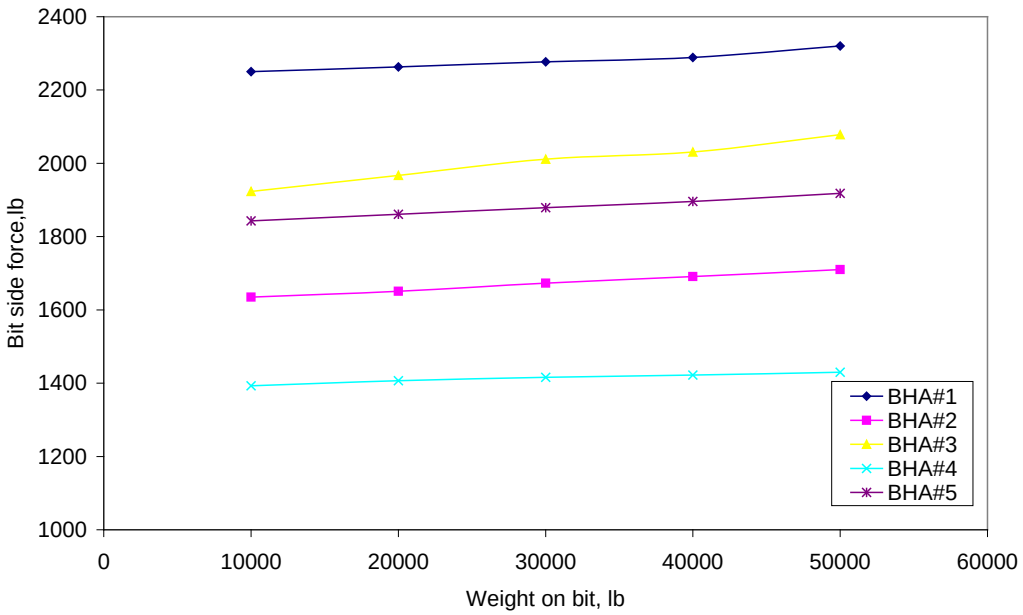

Figure 5-27: Effect of Collar Diameter on Bit Side Force

5.9.2.4.Effect Number of Stabilizers:

Figure (5-28) shows the performance of three pendulum bottom hole assemblies with different number of stabilizers. The first curve for single stabilizer, second curve for two stabilizers, and third curve for three stabilizers. As it shown, increasing number of stabilizers would strengthen the dropping tendency of BHA. This behavior may be attributed to reduction in positive bending force and increasing the negative side force.

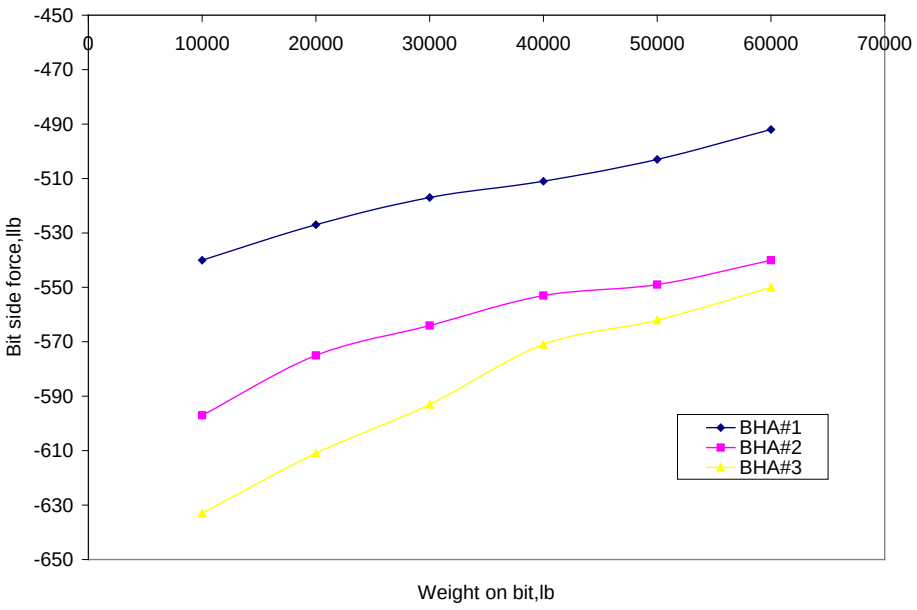

Figure 5-28: Effect Number of Stabilizers on Bit Side Force.

Chapter six

Conclusions & Recommendations

6.1. Conclusions:

This study is concerned with the design of horizontal well aspects. These included selection of bit and casing size, setting depths and drilling fluid densities, well profile, drillstring loads and casing. An oil field which is (Z14 field) is selected for application this design. In addition it's an attempt to predict the performance (inclination tendency) of rotary bottom hole assembly with the finite element method in three dimensions, static condition. Based on the obtained results, the following items have been drawn as the main conclusions for this study:

1- Drillstring simulator is adequate tool for either generation of well profile dimensions or estimation of drillstring loads for six operating conditions which could be encountered while drilling.
2- Short radius well is situated for horizontal drilling application in Z14 oil field, since there are many of drilled vertical wells which can be converted into reentry wells.
3- A single build profile with rate of build of about 90 deg/100ft could be implemented without exceeding the strength limit of the drillstring.
4- For single build horizontal well, torque and drag loads of drillstring could be limited by drilling with low build up rate, using oil base mud, and rotation of drillstring.
5- The finite element model of rotary BHA give closer results to analytical method for slick, single, and two stabilizers BHA more than axisymmtric model.

6- For single stabilizer building BHA, adjusting the weight on bit would cause small improving of building force at low angle. Increasing the inclination angle will limit this effect.

7- In single stabilizer BHA, placing stabilizer near the bit would cause building force. When the stabilizer moved away from the bit, the inclination tendency changed from building to dropping.

8- Reducing the diameter of drill collar behind the bit will affect the bit side force (increasing building force).

10- Using multistabilizer bottom hole assembly and lengthened distance between first and second stabilizer would increase the bit side force.

6.2. Recommendations:

Based on the obtained results and for future modification, the following recommendations are proposed:

1- Using the drillstring simulator during planning horizontal well for construction well profile and optimized drillstring loads (torque, drag, and buckling).

2- A realistic friction coefficient could be calculated from actual drilling data which included pickup weight, slack-off weight, and torque readings for directional or horizontal well.

3- Modification the bottom hole assembly modeling by considering other type of deflection tools such as bent sub, bent house, and adjusted stabilizer. Also, considering rotation of drillstring will give more accurate results.

4- If the field data are available, predictions of rotary BHA model could be compared with actual response which provides more support to the model.

REFERENCES

1. Economides, M.J., Watters, L.T., and Norman, S.D., "Petroleum Well Construction", John Willey& Sons Ltd, England, (1998).
2. Inglis, T.A., "Drictional Drilling", vol.2, Graham &Trotman Inc,(1987).
3. Rabia, H." Well Engineering & Constructions", (2005).
4. Szezuka. J.P., "Directional Drilling Enginerring", Edition3, Nov.(2005).
5. Carden, R.S., and Grace, R.D., "Directional Horizontal Drilling Manual", Petroskills, LLC. Tulsa, Oklahoma, (2008).
6. Sperry-Sun, "An Engineering Approach to Horizontal Drilling", (1995).

7. دراسة جيولوجية لحقل عجيل(1981)

8. Horwell, "Horizontal Drain Opportunties for Ajeel Field", December, (1996).
9. Dellinger, T.B., Gravley, W., and Tolle, S.C.," Directional Technology Will Extended Drilling Reach", OGJ., (Sept. 1980),153-169.
10. Johancsik, C.A., Friesen, D.B., and Dawson, R., "Torque and Drag in Directional Wells-Prediction and Measurement", JPT, (June 1984), 987-992.
11. Cobert, K.T., and Dawson, R., "Drillstring Design for Directional wells", OGJ. (Apr30, 1984), 61-66.
12. Sheppard, M.C., Wick, C. and Burgess, T.M., "Designing Well Paths to Reduce Drag and Torque", SPED15463, 1987.
13. Ho.H.S, "An Improved Modeling Program for Computing the Torque and Drag in Directional and Deep Wells", Paper

SPE18047, Presented at 63rd Annual Technical Conf., Houston, Oct.2-5,1986.

14. Wu, J., and Juvkam, W., "Drag and Torque Calculation in Horizontal and Extended Reach Wells", OGJ. (Apr.29, 1991),45-53.
15. Zifeng, T.H. ; Xisheng, G.H. and Zhang, S., "Steady Tension-Torque Model for Drillstring in Horizontal Wells', SPE27628, 1993.
16. Lubinski, A., and Woods, H.B., "Factors Affecting the Angle of Inclination and Doglegging in Rotary Boreholes", API Drill. and Prod.Prac.(1953),222.
17. Pasaly, P.R. and Bogy, D.B., "The Stability of a Circular Rod Laterally Constrained to be in Contact with an Inclined Circular Cylinder", J.Appl.Mec.(Dec.1964)31,605-10.
18. Dawson, R. and Pasaly, P.R., "Drillpipe Buckling in Inclined Holes", JPT, (Oct.1984), 1734-1738.
19. Cheatham, Jr., John, B. and Pattillo, P.D., "Helical Postbuckling Configuration of a weightless Column Under the Action of an Axial Load", SPEJ, (Feb. 1990).
20. Kown, Y.W., "Analysis of Helical Buckling ", IADC/SPE14729, 1986.
21. Mitchell, R.F., "New concepts for Helical Buckling", SPED15470, 1988.
22. Chen, Y.C.; Lin, Y.H., and Cheatham, J.B., "Tubing and Casing Buckling in Horizontal Well", JPT, (Feb. 1990).
23. Schuh, F.J., "The Critical Buckling Force and Stresses for Pipe in Inclined Curved Boreholes", Paper SPE/IADC21942 Presented At Drilling Conf., Amstrerdam, (March 11-14), 1991.

24. Mitchell, R.F., '"Effect of Well Deviation on Helical Buckling", SPE29462, 1995.
25. Stefan, M., and Cunha, J.C., "An Analysis of Helical Buckling of Tubulars Subjected to axial and Torsional Loading in Inclined wellbores", SPE 29460, 1995.
26. He, X., Halsey, G. and Kyllingstad, A., "Interaction Between Torque and Helical Buckling in Drilling", SPE.30521, 1995.
27. Mitcheel, R.f., "Buckling Analysis in Deviated wells: A Practical Method", SPE 36761, 1996.
28. Akgun,F., Gurakin, G., Mitcheel, B.J., Eustes, A. and Rahman, S., "Theoretical and Experimental Evaluation of Drillpipe Stability Conditions in Slim Holes",SPE37392,1996.
29. Jiang, Wu, "Torsional Load Effect on Drillstring Buckling", SPE 37477, 1997.
30. Lubinski, A., "Maximum Permissible Dog-Leg in Rotary Boreholes", JPT, (Feb. 1961), 175-194.
31. Hansford, J.E. and Lubinski, A., "Cumulative Fatigue Damage of Drillpipe in Dg-Legs", JPT, (Mar.1966), 359-363.
32. Pasaly, R., and Cennocky, E.P., "Bending Stress Magnification in Constant Curvature Doglegs with Impact on drillstring and Casing", SPE22547, 1991.
33. Jiang, Wu., "Drillpipe Bending and Fatigue in Rotary Drilling of Horizontal Wells",SPE37353,1996.
34. Woods, H.B., and Lubinski, A., "Use of Stabilizers in Drill-Collar String", OGJ. (Apr.4 1955).
35. Murphey, C.E., and Cheatham, J.B., "Hole Deviation and Drill String Behavior", SPE1259, 1965.
36. Walker, B.H., "Some Technical and Economic Aspects of Stabilizer Placement", JPT.,(June 1973),663-672.

37. Fischer, F.J., "Analysis of Drillstrings in Curved Boreholes", SPE.5071, 1974.
38. Millheim, K., "The Effect of Hole Curvature on the Trajectory Borehole", SPE.7779, 1977.
39. Millheim, K.and Apostal, M.C., "Bottom Hole Assembly Analysis Utilizing the Finite Element Method", JPT. (Feb.1978),265-273.
40. Cheatham, B. and Ho, C.Y, "A Theoretical Model for Directional Drilling Tendency of A Drill Bit in Anisotropic Rock", SPE10642, 1981.
41. Jiazhi, B., "Bottom Hole Assembly Problems Solved by Beam – Column Theory", SPE.10561, 1982.
42. Barid, J.A., Caskey, B.C., and Tinianow, M.A., "GEODYN: A Geological Formation/Drillstring Dynamics Computer Program", SPE13023, 1984.
43. Barid, J.A., Caskey, B.C., and Wormley, D.N.,"GEODYN2: A Bottom Hole Assembly –Geological Formation Dynamic Interaction Computer Program", SPE14328, 1985.
44. Birades, M., and Fenoul, R.,"ORPHEE 2D: A Microcomputer Program for Prediction of Bottom Hole Assembly", SPE15285, 1986.
45. Brett, J.F., Gray, J.A., Bell, R.K., and Dunbar, M.E.,"A Method of Modeling the Directional Behavior Assemblies Including Those with Bent Subs and Downhole Motors", SPE/IADC14767, 1986.
46. Rafie, S., Ho, H-S., and Chandra, U., "Applications of a BHA Analysis Program in Directional Drilling", SPE/IADC14765, 1986.

47. Birades, M.,"ORPHEE 3D: Static and Dynamic Tridimensional BHA Computer Models", SPE15466, 1986.
48. Ho, H-S., "General Formulation of Drillstring Under Large Deformation and its Use in BHA Analysis", SPE15562, 1986.
49. Lubinski, A., and Williamson, J.S., "Predicting Bottomhole Assembly Performance", SPE14764, 1987.
50. HO, H-S., "Prediction of Drilling Trajectory in Directional Wells Via a New Rock-Bit Interaction Model", SPE16658, 1987.
51. Williams, J.B., Apostal, M.C. and Haduch, G.A. "An Analysis of Predicted Wellbore Trajectory Using Three-Dimensional Model of a Bottomhole Assembly with Bent sub, Bent Housing, and Eccentric Contact Capabilities"SPE19545,1989.
52. Brakel, J.D., and Azar, J.J. "Prediction of Wellbore Trajectory Considering Bottom Hole Assmbly and Drilll-Bit Dynamics"SPE16172, 1989.
53. Zieng, L., Xingrui, M., Huang, W., and Xisheng, L., "A 3D analysis of a Bottom Hole Assembly Under Large Deflection", SPE28288, 1993.
54. Mamdouh, A., Rahman, S., and Maidla, E., "A New Approach to Selecting Optimum Bottom Hole Assembly Configuration for Any Given Well Trajectory", SPE28774, 1994.
55. Yinao, Su., Zhao, J., and Zhang, H.," Analysis and Design of Articulated Downhole Motor Assembly for Short Radius Horizontal Drilling", SPE29977,1995.
56. Mamdouh, A., Rahaman, S., and Maidla, E.,"BHA Design Algorithm for Extended Reach Wells", SPE35993, 1996.
57. Akgun, F.,"A Finite Element Model for Analyzing Horizontal Well BHA Behavior", JPSE, 2003.

58. Mitchell, B., "Advanced Oil Well Drilling Engineering Handbook & Computer program", 10th Edition,(1995).
59. Bourgoyne, A.Jr, Millheim, K., Chenevert, M., and Young, F. Jr., "Applied Drilling Engineering", 10th Edition, SPE, (2005).
60. Rabia, H., "Oil Well Drilling Engineering Principles & Practice", Graham & Trotman Limited, London, (1985).
61. Millheim, K., "Here are Basics of Bottom –Hole Assembly Mechnics", OGJ. DEC.(1978).
62. Butler, R., "Horizontal Wells for the Recovery of Oil, Gas and Bituman", the Petroleum Society of the Canadian Institute of Mining, Canda, (1994).
63. David, V.H., "Fundamentals of finite Element Analysis", McGraw-Hill, (2004).
64. Prezeminiecki, J.S., "Theory of Matrix Structural Analysis", McGraw-Hill, New York, (1968).
65. Rasmussen, B., Sorheim, E., Seiffert, O., Angeltvadt, O., and Giedrem, T.," World Record in Extended Reach drilling Well33/9-C10, Statfjord Field,Norway",SPE21984,(1991).

```
Sub BIT()
Dim CASING(13), BIT(13), TCASING(14), DRFIT(14), depth(8),
mudg(8), frag(8)
LD = Cells(27, 8).Value
 For i = 1 To 13
CASING(i) = Cells(9 + i, 5).Value: BIT(i) = Cells(9 + i, 10).Value
Next
For i = 1 To 14
TCASING(i) = Cells(9 + i, 16).Value: DRFIT(i) = Cells(9 + i, 18).Value
Next
15 K = K + 1
For i = 1 To 13
If LD = CASING(i) Then GoTo 10
Next
10 Cells(30 + K, 8).Value = LD
Cells(30 + K, 10).Value = BIT(i)
LD = BIT(i)
For i = 1 To 14
If DRFIT(i) >= LD Then GoTo 20
Next
20 LD = TCASING(i)
If K = 4 Then GoTo 30
GoTo 15
30 j = 1
For i = 1 To 8
depth(i) = Cells(43 + i, 6).Value: mudg(i) = Cells(43 + i, 16).Value:
frag(i) = Cells(43 + i, 19).Value
Next

MUDDENSITY = mudg(8): casingset = Cells(55, 9).Value
Cells(59, 5).Value = casingset: Cells(59, 7).Value = MUDDENSITY /
0.052
60 For i = 1 To 8
If frag(i) < MUDDENSITY Then GoTo 50
casingset = depth(i - 1) + ((depth(i) - depth(i - 1)) * (MUDDENSITY -
frag(i - 1))) / (frag(i) - frag(i - 1))
If casingset < 0 Then GoTo 70
MUDDENSITY = mudg(i - 1) + ((mudg(i) - mudg(i - 1)) / (depth(i) -
depth(i - 1))) * (casingset - depth(i - 1))
Cells(59 + j, 5).Value = casingset: Cells(59 + j, 7).Value =
MUDDENSITY / 0.052
j = j + 1
50 Next
```

```
If MUDDENSITY > frag(1) Then GoTo 60
70 lp = 0
End Sub
```

```
Sub CASING()
Dim GRADE(6), WEIGHT(6), PI(6), PC(6), FJ(6), YA(6)
For i = 1 To 6
GRADE(i) = Cells(6 + i, 9).Value: WEIGHT(i) = Cells(6 + i, 10).Value:
PI(i) = Cells(6 + i, 11).Value: PC(i) = Cells(6 + i, 12).Value: FJ(i) =
Cells(6 + i, 14).Value: YA(i) = Cells(6 + i, 13).Value
Next
MW = Cells(6, 5).Value: casingset = Cells(9, 5).Value: ni = Cells(10,
5).Value: nc = Cells(11, 5).Value: nj = Cells(12, 5).Value: mwf = Cells(7,
5).Value: poreg = Cells(8, 5).Value
PIC = (0.052 * casingset * (0.3 + mwf) - 220) * ni: pac = (0.052 * (0.3 +
mwf) * casingset - poreg * casingset) * ni
For i = 1 To 6
If PI(i) >= PIC Then GoTo 10
Next
10 L1 = ((PIC - PI(i - 1)) * casingset) / (PIC - pac): CC = i: tlength = L1:
tdepth = casingset
 pct = 0.052 * MW * casingset * nc
For i = 1 To 6
If PC(i) >= pct Then GoTo 20
Next
20 M = M + 1
 Cells(16 + M, 6).Value = GRADE(i): Cells(16 + M, 7).Value =
WEIGHT(i): Cells(16 + M, 8).Value = casingset: DD = i
For i = DD - 1 To 1 Step -1
LS = PC(i) / (0.052 * MW * nc)
30 w = W1 + WEIGHT(i + 1) * (casingset - LS)
A = (w / YA(i))
pcc = PC(i) * (Sqr(1 - 0.75 * A ^ 2) - 0.5 * A)
ls2 = pcc / (0.052 * MW * nc)
If (ls2 - LS) <= 5 Then GoTo 40
LS = ls2
GoTo 30
40 M = M + 1: G = casingset - ls2: tlength = tlength + G
wmax = FJ(i) / nj: length1 = (wmax - w) / WEIGHT(i)
If length1 < ls2 Then GoTo 50
Cells(16 + M, 6).Value = GRADE(i): Cells(16 + M, 7).Value =
WEIGHT(i): Cells(16 + M, 8).Value = ls2: Cells(16 + M - 1, 10).Value =
casingset - ls2
W1 = w: casingset = ls2
Next
50 tlength = tlength + length1
```

```
Cells(16 + M, 6).Value = GRADE(i): Cells(16 + M, 7).Value =
WEIGHT(i): Cells(16 + M, 8).Value = ls2: Cells(16 + M - 1, 10).Value =
length1: JJ = i
If tlength >= tdepth Then GoTo 60
For i = JJ + 1 To 6
ls1 = LS - length1
wmax = FJ(i) / nj
Length = (wmax - (W1 + LENGH1 * WEIGHT(i - 1))) / WEIGHT(i)
W1 = W1 + Length * WEIGHT(i): length1 = Length: M = M + 1
Cells(16 + M, 6).Value = GRADE(i): Cells(16 + M, 7).Value =
WEIGHT(i): Cells(16 + M, 8).Value = ls1: Cells(16 + M - 1, 10).Value =
Length
If Length > ls1 Then GoTo 60
LS = ls1
Next
60 M = M + 1
Cells(16 + M, 6).Value = GRADE(CC): Cells(16 + M, 7).Value =
WEIGHT(CC): Cells(16 + M, 8).Value = L1: Cells(16 + M, 10).Value =
L1
End Sub
```

```
Sub HYDRULIC()
IDP = Cells(11, 5).Value: ODP = Cells(12, 5).Value: depth = Cells(8,
5).Value: LDC = Cells(9, 5).Value: LDP = depth - LDC: DH = Cells(7,
5).Value
IDC = Cells(13, 5).Value: ODC = Cells(12, 5).Value: Q = Cells(29,
5).Value: MW = Cells(27, 5).Value: FAI300 = Cells(24, 4).Value:
FAI600 = Cells(25, 4).Value: PPUMP = Cells(18, 5).Value
PVI = FAI600 - FAI300: YP = FAI300 - PVI: n = 3.32 * Log(FAI300 /
FAI600): K = FAI300 / (511) ^ n: C = 8.91 * 10 ^ -5 * MW ^ 0.8 * Q ^
1.8 * PVI ^ 0.2
 TYP = Cells(32, 7).Value
 If TYP = 1 Then GoTo 5
 If TYP = 2 Then GoTo 6
 If TYP = 3 Then GoTo 7
 PS = 4.2 * 10 ^ -5 * MW ^ 0.8 * Q ^ 1.8 * PVI ^ 0.2
 GoTo 10
5  PS = 2.5 * 10 ^ -4 * MW ^ 0.8 * Q ^ 1.8 * PVI ^ 0.2
 GoTo 10
6  PS = 9.6 * 10 ^ -5 * MW ^ 0.8 * Q ^ 1.8 * PVI ^ 0.2
 GoTo 10
7  PS = 5.3 * 10 ^ -5 * MW ^ 0.8 * Q ^ 1.8 * PVI ^ 0.2
10  MODEL = Cells(33, 7).Value
  VA = (24.5 * Q) / IDP ^ 2
 P1 = (C * LDP) / IDP ^ 4.8
 VA = (24.5 * Q) / IDC ^ 2
 P2 = (C * LDC) / IDC ^ 4.8
 If MODEL = 2 Then GoTo 100
 VA = (24.5 * Q) / (DH ^ 2 - ODC ^ 2): DE = DH - ODC: VC = (97 *
PVI + (79 * Sqr(PVI * PVI + (6.2 * DE * YP)))) / (MW * DE)
 If VA < VC Then GoTo 60
 P3 = (C * LDC) / DE ^ 3 * (DH + ODC) ^ 1.8
 GoTo 65
60  P3 = (LDC * PVI * VA) / (60000 * DE ^ 2) + (LDC * YP) / (200 *
DE)
65 VA = (24.5 * Q) / (DH ^ 2 - ODP ^ 2): DE = DH - ODP
 VC = (97 * PVI + 97 * Sqr(PVI * PVI + 6.2 * DE * YP)) / (MW * DE)
 If VA < VC Then GoTo 70
 P4 = (C * LDP) / DE ^ 3 * (DH + ODP) ^ 1.8
 GoTo 80
70  P4 = (LDP * PVI * VA) / (60000 * DE ^ 2) + (LDP * YP) / (200 *
DE)
80  PC = PS + P1 + P2 + P3 + P4
 KP = PC / Q ^ 1.86
```

```
 PCBH = 0.35 * PPUMP: PCIF = 0.52 * PPUMP
 QBH = (PCBH / KP) ^ (1 / 1.86): QIF = (PCIF / KP) ^ (1 / 1.86)
 PBBH = PPUMP - PCBH: PBIF = PPUMP - PCIF
 TFABH = 0.0096 * QBH * Sqr(MW / PBBH): TFAIF = 0.0096 * QIF *
Sqr(MW / PBIF)
 DNBH = 32 * Sqr(4 * TFABH / 3 * 3.14159): DNIF = 32 * Sqr(4 *
TFAIF / 3 * 3.14159)
 t1 = Int(DNBH): t2 = Int(DNIF)
 Cells(3, 10).Value = t1 / 32: Cells(3, 11).Value = t1 / 32: Cells(3,
12).Value = (t1 + 1) / 32
 Cells(4, 10).Value = t2 / 32: Cells(4, 11).Value = t2 / 32: Cells(4,
12).Value = (t2 + 1) / 32

100 VA = (24.5 * Q) / (DH ^ 2 - ODC ^ 2): DE = DH - ODC: A = (2 * n
+ 1) / 3 * n: B = ((3.878 * 10 ^ 4 * K) / MW) ^ (1 / 2 - n)
VC = B * (2.4 * A / DE) ^ (n / 2 - n)
 If VC > VA Then GoTo 90
 P3 = (K * LDC) / (300 * DE) * (2.4 * VA * A / DE) ^ n
 GoTo 110
90  P3 = (C * LDC) / (DE ^ 3) * (DH + ODC) ^ 1.8
110 VA = (24.5 * Q) / (DH ^ 2 - ODP ^ 2): DE = DH - ODP
 VC = B * (2.4 * A / DE) ^ (n / 2 - n)
 If VC > VA Then GoTo 120
 P4 = (K * LDP) / (300 * DE) * (2.4 * VA * A / DE) ^ n
 GoTo 130
120  P4 = (C * LDP) / (DE ^ 3) * (DH + ODP) ^ 1.8
130 PC = PS + P1 + P2 + P3 + P4
KP = PC / Q ^ 1.86
PCBH = 0.35 * PPUMP: PCIF = 0.52 * PPUMP
QBH = (PCBH / KP) ^ (1 / 1.86): QIF = (PCIF / KP) ^ (1 / 1.86)
PBBH = PPUMP - PCBH: PBIF = PPUMP - PCIF
TFABH = 0.0096 * QBH * Sqr(MW / PBBH): TFAIF = 0.0096 * QIF *
Sqr(MW / PBIF)
DNBH = 32 * Sqr(4 * TFABH / 3 * 3.14159): DNIF = 32 * Sqr(4 *
TFAIF / 3 * 3.14159)
t1 = Int(DNBH): t2 = Int(DNIF)
Cells(7, 10).Value = t1 / 32: Cells(7, 11).Value = t1 / 32: Cells(7,
12).Value = (t1 + 1) / 32
Cells(8, 10).Value = t2 / 32: Cells(8, 11).Value = t2 / 32: Cells(8,
12).Value = (t2 + 1) / 32

   End Sub
```

```
Sub LIFTING()
Dim Q(10), VM(10), ANGLE(10), EFF(10), VS(10), VSC(10),
VCIR(10), QCIR(10)
PHI300 = Cells(12, 6).Value: PHI600 = Cells(13, 6).Value: MW =
Cells(7, 6).Value: DC = Cells(8, 6).Value: PD = Cells(9, 6).Value: DH =
Cells(10, 6).Value: DP = Cells(11, 6).Value
PVI = PHI600 - PHI300: YB = PHI300 - PVI: G = 32.2
n = 3.32 * Log(PHI600 / PHI300): K = PHI300 / (511) ^ n
DE = DH - DP: DES = DH ^ 2 - DP ^ 2: DD = (DC - MW) / MW
V2 = 44 * (DD * G ^ 3 * (DE / 12) ^ 3) ^ (1 / 6): S = 0: SS = 0
For i = 1 To 10
Q(i) = S + 150: VM(i) = (24.5 * Q(i)) / DES: ANGLE(i) = SS
S = S + 30: SS = SS + 10
Next
OPT = Cells(21, 6).Value: AA = (DC - MW) ^ 0.667: BB = (MW) ^
0.333
If OPT = 2 Then GoTo 100
For i = 1 To 10
EFF(i) = PVI + (300 * YB * DE) / (VM(i))
VS(i) = 1.8 * (175 * PD * AA) / (BB * (EFF(i)) ^ 0.333)
VSC(i) = VS(i) * Cos(ANGLE(i) * 3.14159 / 180)
VCIR(i) = VSC(i) + V2 * Sin((ANGLE(i)) * 3.14159 / 180)
QCIR(i) = (VCIR(i) * DES) / 24.5
Cells(25 + i, 4).Value = QCIR(i): Cells(25 + i, 6).Value = ANGLE(i)
Next
100 V = 1

End Sub
```

```
Sub Macro1()
Dim md(), vdc(), depc(), sinbuckl(), helbuckl(), rob(), trob(), pick(),
wpick(), tpick(), slacK(), wslack(), tslack(), SLIDING(), DRILLING(),
tdrilling(), INC(), az()
DH = Cells(50, 10).Value: MW = Cells(55, 10).Value: ODJ = Cells(54,
10).Value
ODP = Cells(51, 10).Value: IDP = Cells(52, 10).Value: LDP = Cells(56,
10).Value: wdp = Cells(53, 10).Value: YM = Cells(57, 7).Value: E =
Cells(58, 10).Value
ODC = Cells(52, 17).Value: IDC = Cells(53, 17).Value: WDC =
Cells(54, 17).Value: LDC = Cells(55, 17).Value
ODH = Cells(56, 17).Value: IDH = Cells(57, 17).Value: WDH =
Cells(59, 17).Value: LDH = Cells(58, 17).Value
FO = Cells(62, 10).Value: FC = Cells(63, 10).Value: MOP = Cells(61,
10).Value: WOB = Cells(59, 10): TOB = Cells(60, 10).Value:
BHADRAG = Cells(60, 17).Value: BHAT = Cells(61, 17).Value: BHAL
= Cells(62, 17).Value: BHAW = Cells(63, 17).Value
R = (DH - ODJ) / 2: I1 = 0.04909 * (ODP ^ 4 - IDP ^ 4): bf = 1 - (MW /
65.45): WB = bf * wdp: PI = 3.14159 / 180: CASSET = Cells(65,
10).Value
chioce = Cells(40, 8).Value
If chioce = 2 Then GoTo 100
tvd = Cells(5, 8).Value: dep = Cells(6, 8).Value: the = Cells(9, 8).Value:
REACH = Cells(8, 8).Value: BG = Cells(7, 8).Value
tvd1 = Cells(20, 8).Value: dep1 = Cells(21, 8).Value: MD1 = Cells(22,
8).Value: kop = Cells(23, 8).Value
RR = Cells(19, 8).Value
M = Int(kop / 100): n = Int(the / BG): l = Int(REACH / 100): K = M + n +
l
ReDim md(K), vdc(K), depc(K), sinbuckl(K), helbuckl(K), rob(K),
trob(K), pick(K), wpick(K), tpick(K), slacK(K), wslack(K), tslack(K),
SLIDING(K), DRILLING(K), tdrilling(K), INC(K), az(K)
DMD = 0: SSA = -2 * Sqr((E * I1 * WB * Sin(BG * 0.5 * PI)) / (12 * R))
For i = 1 To M
md(i) = DMD: vdc(i) = DMD: depc(i) = 0
sinbuckl(i) = SSA: helbuckl(i) = SSA: INC(i) = 0: DMD = DMD + 100
Next
md(M) = kop: vdc(M) = kop: depc(M) = 0: sinbuckl(1) = 0: helbuckl(1) =
0
j = 1
For i = M + 1 To M + n
```

```
md(i) = md(M) + j * 100
A = (md(i) - kop) * BG / 100
vdc(i) = kop + RR * Sin(A * PI)
X = (vdc(i) - kop) / RR
XX = Atn(X / Sqr(-X * X + 1))
depc(i) = RR * (1 - Cos(XX))
sinbuckl(i) = -2 * Sqr((E * I1 * WB * Sin(j * BG * PI)) / (12 * R))
helbuckl(i) = 1.83 * sinbuckl(i): INC(i) = j * BG
j = j + 1
Next
md(M + n) = kop + MD1: vdc(M + n) = kop + tvd1: depc(M + n) = dep1
SSB = -2 * Sqr((E * I1 * WB * Sin(the * PI)) / (12 * R)): j = 1
For i = M + n + 1 To K
md(i) = md(M + n) + j * 100
vdc(i) = vdc(M + n) + j * 100 * Cos(the * PI)
depc(i) = depc(M + n) + j * 100 * Sin(the * PI)
sinbuckl(i) = SSB: helbuckl(i) = SSB * 1.83: INC(i) = the
j = j + 1
Next
tdepth = kop + MD1 + REACH
GoTo 200
100 H = 1

tvd = Cells(5, 15).Value: dep = Cells(6, 15).Value: hold = Cells(11,
15).Value: BG1 = Cells(7, 15).Value: bg2 = Cells(8, 15).Value: THE1 =
Cells(9, 15).Value: THE3 = Cells(10, 15).Value: REACH = Cells(12,
15).Value

R1 = Cells(19, 15).Value: R2 = Cells(20, 15).Value: THE2 = THE3 -
THE1
tvd1 = Cells(24, 15).Value: dep1 = Cells(25, 15).Value: MD1 = Cells(26,
15).Value
tvd2 = Cells(28, 15).Value: DEP2 = Cells(29, 15).Value: MD2 =
Cells(30, 15).Value
TVD3 = Cells(32, 15).Value: DEP3 = Cells(33, 15).Value: MD3 =
Cells(34, 15).Value
kop = Cells(36, 15).Value
M = Int(kop / 100): n = Int(THE1 / BG1): l = Int(hold / 100): p =
Int(THE2 / bg2): Q = Int(REACH / 100): K = M + n + l + p + Q
ReDim md(K), vdc(K), depc(K), sinbuckl(K), helbuckl(K), rob(K),
trob(K), pick(K), wpick(K), tpick(K), slacK(K), wslack(K), tslack(K),
SLIDING(K), DRILLING(K), tdrilling(K), INC(K), az(K)
```

```
DMD = 0: SSA = -2 * Sqr((E * I1 * WB * Sin(BG1 * PI)) / (12 * R)):
sinbuckl(1) = 0: helbuckl(1) = 0
For i = 1 To M
md(i) = DMD: vdc(i) = DMD: depc(i) = 0: sinbuckl(i) = SSA: helbuckl(i)
= SSA: INC(i) = 0
DMD = DMD + 100
Next
sinbuckl(1) = 0: helbuckl(1) = 0: md(M) = kop: vdc(M) = kop: depc(M) =
0
j = 1
For i = M + 1 To M + n
md(i) = md(M) + j * 100
vdc(i) = kop + R1 * Sin((md(i) - kop) * PI * BG1 / 100)
X = (vdc(i) - kop) / R1
XX = Atn(X / Sqr(-X * X + 1))
depc(i) = R1 * (1 - Cos(XX))
sinbuckl(i) = -2 * Sqr((E * I1 * WB * Sin(j * BG1 * PI)) / (12 * R))
helbuckl(i) = 1.83 * sinbuckl(i): INC(i) = j * BG1
j = j + 1
Next
md(M + n) = md(M) + MD1: vdc(M + n) = kop + tvd1: depc(M + n) =
dep1
j = 1: SSB = -2 * Sqr((E * I1 * WB * Sin(THE1 * PI)) / (12 * R))
For i = M + n + 1 To M + n + l
md(i) = md(M + n) + j * 100
vdc(i) = vdc(M + n) + (md(i) - md(M + n)) * Cos(THE1 * PI)
depc(i) = dep1 + (vdc(i) - vdc(M + n)) * Tan(THE1 * PI)
sinbuckl(i) = SSB: helbuckl(i) = 1.83 * SSB: INC(i) = THE1
j = j + 1
Next
md(M + n + l) = md(M + n) + hold: vdc(M + n + l) = vdc(M + n) + tvd2:
depc(M + n + l) = dep1 + DEP2
j = 1
For i = M + n + l + 1 To M + n + l + p
md(i) = md(M + n + l) + j * 100
D = (md(i) - md(M + n + l)) * bg2 / 100
vdc(i) = vdc(M + n + l) + R2 * Sin(D * PI)
If vdc(i) > tvd Then vdc(i) = tvd
A = (vdc(i) - vdc(M + n + l)) / R2
AA = Atn(A / Sqr(-A * A + 1))
depc(i) = depc(M + n + l) + R2 * (1 - Cos(AA))
sinbuckl(i) = -2 * Sqr((E * I1 * WB * Sin((THE1 + j * bg2) * PI)) / (12 *
R))
```

```
helbuckl(i) = 1.83 * sinbuckl(i): INC(i) = THE1 + j * bg2
j = j + 1
Next
CC = M + n + l + p
md(CC) = md(M + n + l) + MD3: depc(CC) = dep1 + DEP2 + DEP3
j = 1: SSC = -2 * Sqr((E * I1 * WB * Sin(THE3 * PI)) / (12 * R))
For i = CC + 1 To K
md(i) = md(CC) + j * 100
vdc(i) = tvd
depc(i) = depc(CC)
sinbuckl(i) = SSC: helbuckl(i) = SSC * 1.83: INC(i) = THE3
j = j + 1
Next
tdepth = kop + MD1 + hold + MD2 + REACH
200 Length = BHAL: F = FO: W1 = bf * BHAL * BHAW: w = bf * wdp
* 100: MOP1 = MOP: MOP2 = MOP: TBHA1 = BHAT: TBHA2 =
BHAT
rob(K) = 0: trob(K) = 0: pick(K) = 0: wpick(K) = 0: tpick(K) = BHAT:
slacK(K) = 0: wslack(K) = 0: tslack(K) = BHAT: tdrilling(K) = TOB
For i = K To 1 Step -1
DETHE = INC(i) - INC(i - 1): THEAVG = (INC(i) + INC(i - 1)) / 2
If i = K Then w = W1
fn1 = w * Sin(THEAVG * PI)
F1 = (WOB * Sin(THEAVG * PI)) ^ 2: F2 = (WOB * DETHE + w *
Sin(THEAVG * PI)) ^ 2
fn2 = Sqr(F1 + F2)
depth = tdepth - Length: Length = Length + 100
If depth <= CASSET Then F = FC
If i = K Then GoTo 10
rob(i) = S1 + w * Cos(THEAVG * PI): S1 = rob(i)
trob(i) = S6 + (F * fn1 * ODP) / 24: S6 = trob(i)
pick(i) = MOP1 + w * Cos(THEAVG * PI) + (F * fn1): MOP1 = pick(i)
MOP22 = MOP2 + w * Cos(THEAVG * PI) + (F * fn1): MOP2 =
MOP22
wpick(i) = MOP22 - WOB
tpick(i) = TBHA1 + (F * fn1 * ODP) / 24: TBHA1 = tpick(i)
slacK(i) = S2 + w * Cos(THEAVG * PI) - (F * fn1): S2 = slacK(i)
ss3 = S3 + w * Cos(THEAVG * PI) + (F * fn1): S3 = ss3
wslack(i) = ss3 - WOB
tslack(i) = TBHA2 + (F * fn1 * ODP) / 24: TBHA2 = tslack(i)
tdrilling(i) = TOB + (F * fn1 * ODP) / 24: TOB = tdrilling(i)
10 ss4 = S4 + w * Cos(THEAVG * PI) - (F * fn1): S4 = ss4
 SLIDING(i) = ss4 - WOB
```

```
SS5 = S5 + w * Cos(THEAVG * PI): S5 = SS5
DRILLING(i) = SS5 - WOB

Next

For i = 1 To K
Cells(75 + i, 1).Value = md(i): Cells(75 + i, 2).Value = vdc(i): Cells(75 +
i, 3).Value = depc(i): Cells(75 + i, 4).Value = INC(i)

Cells(75 + i, 5).Value = sinbuckl(i): Cells(75 + i, 6).Value = helbuckl(i):
Cells(75 + i, 7).Value = rob(i)
Cells(75 + i, 8).Value = pick(i): Cells(75 + i, 9).Value = slacK(i):
Cells(75 + i, 10).Value = SLIDING(i)
Cells(75 + i, 11).Value = wpick(i): Cells(75 + i, 12).Value = wslack(i):
Cells(75 + i, 13).Value = DRILLING(i)
Cells(75 + i, 14).Value = trob(i): Cells(75 + i, 15).Value = tpick(i):
Cells(75 + i, 16).Value = tslack(i): Cells(75 + i, 17).Value = tdrilling(i)
Next
End Sub
```

```
module newlibrary
contains
!---------------------node freedom array---------------------------------
subroutine formnf(nf)
implicit none
integer,intent(in out)::nf(:,:)
integer::i,j,m
m=0
do j=1,ubound(nf,2)
do i=1,ubound(nf,1)
if(nf(i,j)/=0)then
m=m+1;nf(i,j)=m
end if
end do
end do
return
end subroutine formnf

 !-----------------------------streeing vector----------------------------------
 subroutine numtog(num,nf,g)
 implicit none
 integer,intent(in)::NUM(:),nf(:,:)
 integer,intent(out)::g(:)
 integer::i,k,nod,nodof;nod=ubound(num,1);nodof=ubound(nf,1)
 do i=1,nod
 k=i*nodof;g(k-nodof+1:k)=nf(:,num(i))
 end do
 return
 end subroutine numtog
 !---------------------------bandwidth-----------------------------------
 function bandwidth(g) result(nband)
 implicit none ;integer::nband
 integer,intent(in)::g(:)
 nband=maxval(g,1,g>0)-minval(g,1,g>0)
 end function bandwidth
 !---------------------------element matrix----------------------------
 subroutine rigidjointed(km,prop,gamma,etype,iel,coord)
 implicit none
 real,intent(in)::gamma(:),coord(:,:),prop(:,:)
 integer,intent(in)::etype(:),iel
 real,intent(out)::km(:,:)
 integer::ndim,i,j,k
```

```
  real::ell,x1,x2,y1,y2,z1,z2,c,s,e1,e2,e3,e4,pi,xl,yl,zl,cg,sg,den
  real::ea,ei,eiy,eiz,gj
  real::a1,a2,a3,a4,a5,a6,a7,a8,sum,gamrad,x
  real::t(12,12),tt(12,12),cc(12,12),ro(3,3)
  ndim=ubound(coord,2)
  select case(ndim)
  case(1)
  ei=prop(1,etype(iel));ell=coord(2,1)-coord(1,1)
  km(1,1)=12.*ei/(ell*ell*ell);km(3,3)=km(1,1)
  km(1,2)=6.*ei/(ell*ell);km(2,1)=km(1,2);km(1,4)=km(1,2)
  km(4,1)=km(1,4);km(1,3)=-km(1,1);km(3,1)=km(1,3);km(3,4)=-
km(1,2)
  km(4,3)=km(3,4);km(2,3)=km(3,4);km(3,2)=km(2,3);km(2,2)=4.*ei/ell
  km(4,4)=km(2,2);km(2,4)=2.*ei/ell;km(4,2)=km(2,4)
  case(2)
  ea=prop(1,etype(iel));ei=prop(2,etype(iel))
  x1=coord(1,1);y1=coord(1,2);x2=coord(2,1);y2=coord(2,2)
  ell=sqrt((y2-y1)**2+(x2-x1)**2)
  c=(x2-x1)/ell;s=(y2-y1)/ell
  e1=ea/ell;e2=12.*ei/(ell*ell*ell);e3=ei/ell;e4=6.*ei/(ell*ell)
  km(1,1)=c*c*e1+s*s*e2;km(4,4)=km(1,1);km(1,2)=s*c*(e1-e2)
  km(2,1)=km(1,2);km(4,5)=km(1,2);km(5,4)=km(4,5);km(1,3)=-s*e4
  km(3,1)=km(1,3);km(1,6)=km(1,3);km(6,1)=km(1,6);km(3,4)=s*e4
  km(4,3)=km(3,4);km(4,6)=km(3,4);km(6,4)=km(4,6);km(1,4)=-km(1,1)
  km(4,1)=km(1,4);km(1,5)=s*c*(-
e1+e2);km(5,1)=km(1,5);km(2,4)=km(1,5)
  km(4,2)=km(2,4);km(2,2)=s*s*e1+c*c*e2;km(5,5)=km(2,2);km(2,5)=-
km(2,2)
  km(5,2)=km(2,5);km(2,3)=c*e4;km(3,2)=km(2,3);km(2,6)=km(2,3)
  km(6,2)=km(2,6);km(3,3)=4.*e3;km(6,6)=km(3,3);km(3,5)=-c*e4
  km(5,3)=km(3,5);km(5,6)=km(3,5);km(6,5)=km(5,6);km(3,6)=2.*e3
  km(6,3)=km(3,6)
  case(3)

ea=prop(1,etype(iel));eiy=prop(2,etype(iel));eiz=prop(3,etype(iel));gj=pr
op(4,etype(iel))
  x1=coord(1,1);y1=coord(1,2);z1=coord(1,3)
  x2=coord(2,1);y2=coord(2,2);z2=coord(2,3)
  xl=x2-x1;yl=y2-y1;zl=z2-z1;ell=sqrt(xl*xl+yl*yl+zl*zl)
  km=0.0;t=0.0;tt=0.0
  a1=ea/ell;a2=12.*eiz/(ell*ell*ell);a3=12.*eiy/(ell*ell*ell)
  a4=6.*eiz/(ell*ell);a5=6.*eiy/(ell*ell);a6=4.*eiz/ell
  a7=4.*eiy/ell;a8=gj/ell
```

```
  km(1,1)=a1;km(7,7)=a1;km(1,7)=-a1;km(7,1)=-
a1;km(2,2)=a2;km(8,8)=a2
  km(2,8)=-a2;km(8,2)=-a2;km(3,3)=a3;km(9,9)=a3;km(3,9)=-
a3;km(9,3)=-a3
  km(4,4)=a8;km(10,10)=a8;km(4,10)=-a8;km(10,4)=-a8;km(5,5)=a7

km(11,11)=a7;km(5,11)=0.5*a7;km(11,5)=0.5*a7;km(6,6)=a6;km(12,12)
=a6

km(6,12)=0.5*a6;km(12,6)=0.5*a6;km(2,6)=a4;km(6,2)=a4;km(2,12)=a4
  km(12,2)=a4;km(6,8)=-a4;km(8,6)=-a4;km(8,12)=-a4;km(12,8)=-a4
  km(5,9)=a5;km(9,5)=a5;km(9,11)=a5;km(11,9)=a5;km(3,5)=-a5
  km(5,3)=-a5;km(3,11)=-a5;km(11,3)=-a5
  pi=acos(-
1.);gamrad=gamma(iel)*pi/180.;cg=cos(gamrad);sg=sin(gamrad)
  den=ell*sqrt(xl*xl+zl*zl)
  if (den/=0.0)then
  ro(1,1)=xl/ell;ro(1,2)=yl/ell;ro(1,3)=zl/ell
  ro(2,1)=(-xl*yl*cg-ell*zl*sg)/den;ro(2,2)=den*cg/(ell*ell)
  ro(2,3)=(-yl*zl*cg+ell*xl*sg)/den;ro(3,1)=(xl*yl*sg-ell*zl*cg)/den
  ro(3,2)=-den*sg/(ell*ell);ro(3,3)=(yl*zl*sg+ell*xl*cg)/den
  else
  ro(1,1)=0.;ro(1,3)=0.;ro(2,2)=0.;ro(3,2)=0.
  ro(1,2)=1.;ro(2,1)=-cg;ro(3,3)=cg;ro(2,3)=sg;ro(3,1)=sg
  end if
  do i=1,3;do j=1,3
  x=ro(i,j)
  do k=0,9,3;t(i+k,j+k)=x;tt(j+k,i+k)=x;end do
  end do;end do
  do i=1,12;do j=1,12
  sum=0.
  do k=1,12;sum=sum+km(i,k)*t(k,j);end do
  cc(i,j)=sum
  end do;end do
  do i=1,12;do j=1,12
  sum=0.
  do k=1,12;sum=sum+tt(i,k)*cc(k,j);end do
  km(i,j)=sum
  end do;end do
  end select
  return
  end subroutine rigidjointed
```

```
!-----------------globilization-----------------
subroutine formkv(bk,km,g,n)
implicit none
real,intent(in)::km(:,:);real,intent(out)::bk(:)
integer,intent(in)::g(:),n
integer::idof,i,j,icd,ival
idof=size(km,1)
do i=1,idof
if(g(i)/=0)then
do j=1,idof
if(g(j)/=0)then
icd=g(j)-g(I)+1
if(icd-1>=0)then
ival=n*(icd-1)+g(I)
BK(ival)=bk(ival)+km(i,j)
end if
end if
end do
end if
end do
return
end subroutine formkv
!-----------------------------------------gaussian factorization-----------------
subroutine banred(bk,n)
implicit none
real,intent(IN OUT)::bk(:);integer,intent(in)::n
integer::i,ill,kbl,j,ij,nkb,m,ni,nj,iw;real::sum
iw=ubound(bk,1)/n-1
do i=2,n
ill=i-1;kbl=ill+iw+1
if(kbl-n>0)kbl=n
do j=i,kbl
ij=(j-i)*n+i;sum=bk(ij);nkb=j-iw
if(nkb<=0)nkb=1
if(nkb-ill<=0)then
do m=nkb,ill
ni=(i-m)*n+m;nj=(j-m)*n+m
sum=sum-bk(ni)*bk(nj)/bk(m)
end do
end if
bk(ij)=sum
end do
end do
```

```
 return
 end subroutine banred
 !------------------------equation solution-----------------------
 subroutine bacsub(bk,loads)
 implicit none
 real,intent(in)::bk(:);real,intent(in out)::loads(0:)
 integer::nkb,k,i,jn,jj,il,n,iw;real::sum
 n=ubound(loads,1);iw=ubound(bk,1)/n-1
 loads(1)=LOADS(1)/BK(1)
 do i=2,n
 sum=loads(i);il=i-1;nkb=i-iw
 if(nkb<=0)nkb=1
 do k=nkb,il
 jn=(i-k)*n+k;sum=sum-bk(jn)*loads(k)
 end do
 loads(i)=sum/bk(i)
 end do
 do jj=2,n
 i=n-jj+1;sum=0.0;il=i+1;nkb=i+iw
 if(nkb-n>0)nkb=n
 do k=il,nkb
 jn=(k-i)*n+i;sum=sum+bk(jn)*loads(k)
 end do
 loads(i)=loads(i)-sum/bk(i)
 end do
 return
 end subroutine bacsub
 end module


  program p44
! ---------------main program-------------------------------------------------
-
 use newlibrary ;implicit none
integer
::nels,neq,nn,nband,nod=2,nodof,ndof,iel,i,k,ndim,fixednodes,nprops,npt
ypes,ldc,depth,wob,j,dd,ns,Ls,LS1,l1,ls2,l2,nve1,nve2,nve3,nvet,m,mn,m
m,nve4,ls3,l3
real::mw,inc,bc,wc,cweight,dh,idc,odc,the,aa,bb,e1,e2,g1,g2,j1,j2,v,tw1,t
w,area1,area2,moi1,moi2,R,diff,uf,wobc
!--------------------dynamic arrays-----------------------------------------
---------
```

```
REAL,ALLOCATABLE::Km(:,:),kaxial(:,:),eld(:),kv(:),LOADS(:),COO
Rd(:,:),action(:),gcoord(:,:),value(:),prop(:,:),gamma(:)

INTEGER,ALLOCATABLE::NF(:,:),G(:),NUM(:),GNUM(:,:),no(:),GG(
:,:),node(:),sense(:),etype(:)
!-------------------INPUT&INITILISATION----------------------------------
---------------------------------

  open (11,file='result.res',status='replace',action='write')
  dh=9.875;idc=2;odc=8;area1=3.14159*(odc*odc-
idc*idc)/(144*4);area2=1/144;moi1=0.049*(odc**4-
idc**4)/(12**4);moi2=1/(12**4);mw=10;the=10;depth=10000
 bb=0.9 ;aa=0.5*(dh-
odc)/12;E1=29.e6*144;e2=10*144;v=0.3;ldc=180;j1=2*moi1;j2=2*moi2
;g1=(e1*e1)/(e1+e1+2*v*e1);g2=(e2*e2)/(e2+e2+2*v*e2)
 inc=(the*3.14159)/180
 ndim=2;nprops=2;nptypes=2
 print*,"enter no. of stablizers,ns";read*,ns
 if(ns==0)then
 nvet=ldc/bb
 end if
 if(ns==1)then
 print*,"enter distance from bit to stabilizer, Ls"
 Ls=30;L1=1;nve1=Ls/L1;nve2=(ldc-Ls)/bb;nvet=nve1+nve2
 end if
 if(ns==2)then
 print*,"enter distances ls1,ls2"
 ls1=56;L1=7;ls2=52;l2=13;nve1=ls1/l1;nve2=ls2/l2;nve3=(ldc-
(ls1+ls2))/bb;nvet=nve1+nve2+nve3
 end if
 if(ns==3)then
 print*,"enter distances ls1,ls2,ls3"

ls1=10;l1=2;ls2=72;l2=8;ls3=26;l3=2;nve1=ls1/l1;nve2=ls2/l2;nve3=ls3/l
3;nve4=(ldc-(ls1+ls2+ls3))/bb;nvet=nve1+nve2+nve3+nve4
 end if
 nels=2*nvet+1;nn=2*nvet+2
 select case(ndim)
 case(1);nodof=2;case(2);nodof=3;case(3);nodof=6
 case default;write(11,'(a)')"wrong numberof dimensionsminput"
 end select
 NDOF=NOD*NODOF
```

```
ALLOCATE(NF(NODOF,NN),KM(NDOF,NDOF),COORD(NOD,NDI
M),GCOORd(NDIM,NN),eld(ndof),action(ndof),gnum(nod,nels),  &
              num(nod),g(ndof),
gamma(nels),gg(ndof,nels),prop(nprops,nptypes),etype(nels),Kaxial(ndof
,ndof))
  if(ndim==2)then

prop(1,1)=E1*area1;prop(2,1)=(E1*moi1);prop(1,2)=e2*area2;prop(2,2)
=(e2*moi2)
  end if
  if(ndim==3)then
  if(nptypes>1)then
  prop(1,1)=e1*area1;prop(1,2)=e2*area2
  prop(2,1)=e1*moi1   ;prop(2,2)=e2*moi2
  prop(3,1)=e1*moi1  ;prop(2,3)=e2*moi2
  prop(4,1)=g1*j1   ;prop(2,4)=g2*j2
  else

prop(1,1)=e1*area1;prop(2,1)=e1*moi1;prop(3,1)=e1*moi1;prop(4,1)=g
1*j1
  end if;end if
 kaxial(:,:)=0
 if(ndim==2)then
 kaxial(1,1)=(area2*e2)/aa;kaxial(1,4)=-(area2*e2)/aa; kaxial(4,1)=-
(area2*e2)/aa;kaxial(4,4)=(area2*e2)/aa
 end if
 if (ndim==3)then
 kaxial(1,1)=(area2*e2)/aa;kaxial(1,7)=-(area2*e2)/aa;kaxial(7,1)=-
(area2*e2)/aa;kaxial(7,7)=(area2*e2)/aa
 end if
  etype=1
 if(nptypes>1)then
 do i=1,nvet
 etype(i)=1;end do

 do i=nvet+1,nels
 etype(i)=2;end do
 end if
 if(ndim==3)then
 !print*,"enter element gamma"
 do i=1,nvet
 gamma(i)=90;end do
```

```
do i=nvet+1,nels
gamma(i)=0;end do
end if
!"enter g-coordinate x,y,z of node"
j=0
do k=1,nn-1,2
gcoord(1,k)=0;gcoord(2,k)=J*bb;gcoord(3,k)=0
j=j+1
end do
j=0
do k=2,nn,2
gcoord(1,k)=aa;gcoord(2,k)=j*bb;gcoord(3,k)=0
j=j+1
end do
!"enter gnum (1,k)&(2,k)"

do k=1,nvet
gnum(1,k)=2*k-1;gnum(2,k)=1+2*k;end do
j=1
do k=nvet+1,nels
gnum(1,k)=2*j-1;gnum(2,k)=2*j
j=j+1
end do
!" Enter no of restained nodes"
nf=1
if(ndim==2)then
!"restained nodes of bit"

 nf(1,1)=0;nf(2,1)=0;nf(3,1)=0
!restained nodes of one stabilizer
if(ns==1)then
!"restrined of upper nodes of 1st stabilizer"

nf(1,2*nve1+1)=0;nf(2,2*nve1+1)=0;nf(3,2*nve1+1)=0
end if
!restained nodes of two stabilizer
if(ns==2)then
!restained upper node of 1st stabilizer
nf(1,2*nve1+1)=0;nf(2,2*nve1+1)=0;nf(3,2*nve1+1)=0
!restanied upper node of 2nd stabilizer

nf(1,2*(nve1+nve2)+1)=0;nf(2,2*(nve1+nve2)+1)=0;nf(3,2*(nve1+nve2)
+1)=0
```

```
 end if
 !restained nodes of three stabilizer
 if(ns==3)then
 nf(1,2*nve1+1)=0;nf(2,2*nve1+1)=0;nf(3,2*nve1+1)=0

nf(1,2*(nve1+nve2)+1)=0;nf(2,2*(nve1+nve2)+1)=0;nf(3,2*(nve1+nve2)
+1)=0

nf(1,2*(nve1+nve2+nve3)+1)=0;nf(2,2*(nve1+nve2+nve3)+1)=0;nf(3,2*
(nve1+nve2+nve3)+1)=0
 end if
 end if
 if(ndim==3)then
 nf(1,1)=0;nf(2,1)=0;nf(3,1)=0;nf(4,1)=0;nf(5,1)=0;nf(6,1)=0
 if(ns==1)then

nf(1,2*nve1+1)=0;nf(2,2*nve1+1)=0;nf(3,2*nve1+1)=0;nf(4,2*nve1+1)=
0;nf(5,2*nve1+1)=0;nf(6,2*nve1+1)=0
 end if
 if(ns==2)then

nf(1,2*nve1+1)=0;nf(2,2*nve1+1)=0;nf(3,2*nve1+1)=0;nf(4,2*nve1+1)=
0;nf(5,2*nve1+1)=0;nf(6,2*nve1+1)=0

nf(1,2*(nve1+nve2)+1)=0;nf(2,2*(nve1+nve2)+1)=0;nf(3,2*(nve1+nve2)
+1)=0;nf(4,2*(nve1+nve2)+1)=0;nf(5,2*(nve1+nve2)+1)=0;nf(6,2*(nve1
+nve2)+1)=0
 end if
 if(ns==3)then

nf(1,2*nve1+1)=0;nf(2,2*nve1+1)=0;nf(3,2*nve1+1)=0;nf(4,2*nve1+1)=
0;nf(5,2*nve1+1)=0;nf(6,2*nve1+1)=0

nf(1,2*(nve1+nve2)+1)=0;nf(2,2*(nve1+nve2)+1)=0;nf(3,2*(nve1+nve2)
+1)=0;nf(4,2*(nve1+nve2)+1)=0;nf(5,2*(nve1+nve2)+1)=0;nf(6,2*(nve1
+nve2)+1)=0

nf(1,2*(nve1+nve2+nve3)+1)=0;nf(2,2*(nve1+nve2+nve3)+1)=0;nf(3,2*
(nve1+nve2+nve3)+1)=0;nf(4,2*(nve1+nve2+nve3)+1)=0;nf(5,2*(nve1+
nve2+nve3)+1)=0;nf(6,2*(nve1+nve2+nve3)+1)=0
 end if
 end if
 if(ndim==2)then
```

```
 do k=2,nn,2
 nf(1,k)=0;nf(2,k)=0;nf(3,k)=0
  end do
  end if
  if(ndim==3)then
  do k=2,nn,2
  nf(1,k)=0;nf(2,k)=0;nf(3,k)=0;nf(4,k)=0;nf(5,k)=0;nf(6,k)=0
  end do
  end if

  call formnf(nf);neq=maxval(nf)

  !-----------------------------------loop the elements to find global array
sizes------------------------------
  nband=0

 do iel=1,nels
 num=gnum(:,iel);call numtog(num,nf,g)
 gg(:,iel)=g;if(nband<bandwidth(g))nband=bandwidth(g)
 end do

 allocate(kv(neq*(nband+1)),loads(0:neq));kv=0.0
  write(11,'(a)')"global coordinates"
 do k=1,nn
 write(11,'(a,i5,a,3e12.4)')"node   ",k,"       ",gcoord(:,k);end do
 write(11,'(a)')"global node numbers"
 do k=1,nels
 write(11,'(a,i5,a,27i3)')"element",k,"         ",gnum(:,k);end do
 write(11,'(2(a,i5),/)')"there are ",neq,"equations and the half-bandwdith
is",nband

 !--------------------------global stifness matrix assembly----------------------
---------------

  do iel=1,nels
  num=gnum(:,iel)
  coord=transpose(gcoord(:,num))
  call rigidjointed(km,prop,gamma,etype,iel,coord)
  if(iel>nvet)then
  km=kaxial
  end if
  g=gg(:,iel)
  call formkv(kv,km,g,neq)
```

```
  end do
  loads=0.0
  !" enter loads of node
load(1,k),loads(2,k),loads(3,k),loads(4,k)loads(5,k),loads(6,k),loads(6,k)"
   fixednodes=0.
   if(fixednodes/=0)then

allocate(node(fixednodes),no(fixednodes),sense(fixednodes),value(fixedn
odes))
   do i=1,fixednodes
   read*,node(i),sense(i),value(i);end do
   do i=1,fixednodes;no(i)=nf(sense(I),node(i));end do
   kv(no)=kv(no)+1.e20;loads(no)=kv(no)*value
   end if
   bc=(1-mw/65.45);wc=(3.14159*489*(odc*odc-
idc*idc))/(4*144);print*,bc,wc
   wob=15000;tw1=0;j=0
   wobc=bc*wob
   do k=3,nn-3,2
   if(ns==0)then
   cweight=wc*bc*bb*cos(inc)
   j=j+1;tw=tw1+cweight;tw1=tw
   end if
   if(ns==1)then
   if(k<2*nve1+1)then
   cweight=wc*bc*l1*cos(inc);j=j+1;tw=tw1+cweight;tw1=tw
   else
   cweight=wc*bc*bb*cos(inc);j=j+1;tw=tw1+cweight;tw1=tw
   end if;end if
   if(ns==2)then
   if(k<2*nve1+1)then
   cweight=wc*bc*l1*cos(inc);j=j+1;tw=tw1+cweight;tw1=tw
   else
   if(k<2*(nve1+nve2)+1)then
   cweight=wc*bc*l2*cos(inc);j=j+1;tw=tw1+cweight;tw1=tw
   end if;end if
   cweight=wc*bc*bb*cos(inc);j=j+1;tw=tw1+cweight;tw1=tw
         end if
         if(ns==3)then
         if(k<2*nve1+1)then
         cweight=wc*bc*l1*cos(inc);j=j+1;tw=tw1+cweight;tw1=tw
         else
         if(k<2*(nve1+nve2)+1)then
```

```
        cweight=wc*bc*l2*cos(inc);j=j+1;tw=tw1+cweight;tw1=tw
        else
        if(k<2*(nve1+nve2+nve3)+1)then
        cweight=wc*bc*l3*cos(inc);j=j+1;tw=tw1+cweight;tw1=tw
        end if;end if;end if
        cweight=wc*bc*bb*cos(inc);j=j+1;tw=tw1+cweight;tw1=tw
        end if
  if(tw>wobc)exit
  if(ndim==2)then
  loads(nf(1,k))=wc*bc*bb*sin(inc);loads(nf(2,k))=-
j*cweight;loads(nf(3,k))=0
  end if
  if(ndim==3)then
  loads(nf(1,k))=wc*bc*bb*sin(inc);loads(nf(2,k))=-
j*cweight;loads(nf(3,k))=0;loads(nf(4,k))=0;loads(nf(5,k))=0;loads(nf(6,
k))=0
  end if

  write(11,'(a)')   "node       weight"
  write(11,'(i5,e12.4)')k,tw
  enddo
  ! loads of topest node
  if(ndim==2)then
  loads(nf(1,nn-3))=wc*bc*bb*sin(inc);loads(nf(2,nn-3))=-
22600;loads(nf(3,nn-3))=0
  end if
  if(ndim==3)then
  loads(nf(1,nn-3))=wc*bc*bb*sin(inc);loads(nf(2,nn-3))=-
22600;loads(nf(3,nn-3))=0;loads(nf(4,nn-3))=0;loads(nf(5,nn-
3))=0;loads(nf(6,nn-3))=0
  end if
  if(tw<wobc)then
  uf=wob-tw
  loads(nf(2,nn-3))=-(uf+22600)
        end if
 !---------------------------------equation solution-----------------------------
------------------
 call banred(kv,neq)
 call bacsub(kv,loads)
 write(11,'(a)')"       node displacement are:"
 if(ndim==2)then
 write(11,'(a)')" node      Dx      Dy       Rotation"
 end if
```

```
 if(ndim==3)then
 write(11,'(a)')" node      Dx       Dy       Dz      Rotationx   Rotationy
Rotationz"
 end if
 do k=1,nn
 diff=loads(nf(1,k))-aa
 if(diff>0)then
 loads(nf(1,k))=aa;end if
 loads(nf(:,k))=1*loads(nf(:,k))
 write(11,'(i5,6e12.4)')k,loads(nf(:,k))
 end do
 write(11,'(a,i5,a,1e12.4,a,1e12.4)')"wob=",wob,"aa=",aa,"the=",the
 write(11,'(a)')" node     distance frombit      displacement"
 j=0;m=1;mn=1;mm=1
 do k=1,nn-1,2
 if(ns==0)then
 dd=j*bb;end if
 if(ns==1)then
 dd=j*l1
 if(k>2*nve1+1)then
 dd=ls+m*bb;m=m+1
 end if
 end if
 if(ns==2)then
 dd=j*l1
 if(k>2*nve1+1)then
 dd=ls1+m*l2;m=m+1;end if
 if(k>2*(nve1+nve2)+1)then
 dd=ls1+ls2+mn*bb;mn=mn+1
 end if
 end if
 if(ns==3)then
 dd=j*l1
 if(k>2*nve1+1)then
 dd=ls1+m*l2;m=m+1;end if
 if(k>2*(nve1+nve2)+1)then
 dd=ls1+ls2+mn*l3;mn=mn+1;end if
 if(k>2*(nve1+nve2+nve3)+1)then
 dd=ls1+ls2+ls3+mm*bb;mm=mm+1
 end if
 end if
 write(11,'(i5,i5,1e12.2)')k,    dd,       loads(nf(1,k))
 j=j+1
```

```
  end do
  !-------------------------------------retrieve elementand action---------------
-----------------
  write(11,'(a)')"        The Elements  actions are"
  if(ndim==2)then
  write(11,'(a)')"          Fx         Fy        moment        Fx          Fy
moment       REACTION"
  end if
  if(ndim==3)then
  write(11,'(a)')"          fx          fy        fz          mx         my         mz    "
  end if
  do iel=1,nels
  num=gnum(:,iel); coord =transpose(gcoord(:,num))
  g=gg(:,iel);eld=loads(g)
  call rigidjointed(km,prop,gamma,etype,iel,coord)
  action=matmul(km,eld)
   if(iel==1)then
   if(ndim==2)then
   action=action(1)
   else
   action=action(1)+24*action(4)/odc
   end if
   end if
  R=action(4)
  if(iel>nvet)then
  R=action(4)
  end if
  if(ndim<3)then
  write(11,'(i5,6e12.4,1e12.4)')iel,action,R
  else
  R=action(1)+ 24*action(4)/odc
  write(11,'(i5,6e12.4)')iel,  action(1:6:1)
   write(11,'(a,6e12.4)')"      ",action(7:12:1)
  end if
  end do
  end program
```